

DELFT UNIVERSITY OF TECHNOLOGY

LASER SWARM

MID TERM REVIEW

DESIGN SYNTHESIS EXERCISE

Authors:

S. BILLEMONT
L.S. BOERSMA
B. BUYENS
S.R. FINCK
J.P. FLORIJN
T.C. GOOSSENS
N.S. OBORIN
A.J. VOROBIEV
G.J. VAN DER WEL
Z. ZHOU

Tutor:

BEN GORTE

Coaches:

PREM SUNDARAMOORTHY
MATHIEU WILLAERT

May 17, 2010

Abstract

In February 2010 the ICESat mission ended after 7 years of measuring ice sheet mass balance, cloud and aerosol heights, as well as land topography and vegetation characteristics using a space based Light Detection And Ranging (LiDAR) system. ICESat used only one of the possible approaches for LiDAR, namely the use of a high energy laser and a large receiver telescope. The other approach is using a high frequency, low energy laser and a single photon detector. The advantage of the latter approach is that it has a much lower mass, but it is uncertain if even a single photon per pulse reaches the receiver. One possible solution could be to use a swarm of satellites around the emitter, each equipped with a single photon detector. However, the technical feasibility of this concept has not yet been proven.

This report briefly highlights different ways in which such a mission could be accomplished, and then decides what way will be the most likely to succeed.

Preface

The first month of this project has already passed, and this mid term report indicates an important milestone. We're not there yet, but we are getting on with it.

We did not, however, do everything by ourselves, and this is a good place to thank those who have been so kind as to give us some of their precious time.

First I want to mention professor Edoardo Charbon, who kindly explained and showed us the workings of his Single Photon Avalanche Diode (SPAD)¹: without his help we would be hopelessly in the dark on these fascinating devices. From this place I also thank professor Kourosh Khoshelham for helping us to some valuable material on remote sensing. I also want to thank Jasper Bouwmeester, who provided us with some helpful information on solar panel pricing.

And finally I thank our tutor, professor Ben Gorte, who was very generous to us with his time and has been very supportive of the entire project.

I hope you will have as much fun reading this report, as we had in making it!

Yours sincerely,

Co Florijn,
Chairman

¹See [Niclass(2008), 98-105], [M. Gersbach and Charbon(2009)] and [David Stoppa and Charbon(2009)]

Contents

Preface	1
1 Introduction	4
2 Technical Design Development	5
2.1 Project Approach Description	5
2.1.1 Group Procedures	5
2.1.2 Reporting	5
2.1.3 Project Outline	6
2.2 Work Flow Diagram	6
2.3 Work Breakdown Structure	6
2.4 Gantt chart	11
3 Risk Management	12
3.1 Market Analysis	12
3.2 Technical Resource Contingencies	12
3.3 Technical Risk Assessment	15
3.3.1 Ground Segment	15
3.3.2 During Mission	16
3.3.3 Measurement Protocol	19
3.3.4 Post-Mission	21
3.3.5 Risk Control	21
4 Design Options	23

<i>Group 13</i>	<i>Laser Swarm</i>	3
4.1	Attitude Determination and Control Subsystem	23
4.1.1	Attitude Determination	23
4.1.2	Attitude Control	23
4.1.3	Note on Receiver Pointing	24
4.2	Optical Emitting Payload	24
4.2.1	Introduction	24
4.2.2	Laser Characteristics	24
4.2.3	Laser Types	25
4.3	Electrical Power System	25
4.3.1	The Power Source	26
4.3.2	Power Storage	26
4.3.3	Power Regulation and Control	27
4.3.4	Power Distribution	28
4.4	Communications	28
4.4.1	Tracking	28
4.4.2	Swarm Satellites Crosslink Frequency	29
4.4.3	D/L and U/L Frequency	29
4.4.4	Antenna Configuration	30
4.4.5	Data Storage	30
4.4.6	Communications Architecture	30
4.5	Orbit Architecture	31
4.5.1	Common Orbits	31
4.5.2	Low Earth Orbit	32
4.5.3	Medium Earth Orbit	32
4.5.4	Geosynchronous Orbit	32
4.5.5	High Earth Orbit	32
4.5.5.1	Highly Elliptical Orbit	32
5	N^2 Chart	33
6	Tradeoff	35

6.1	Attitude and Orbit Determination and Control Subsystem (AODCS)	35
6.1.1	Pruning the ADCS design option tree	35
6.1.2	Attitude Determination Subsystem (ADS)	35
6.1.2.1	Trade method	37
6.1.2.2	Trade criteria	37
6.1.2.3	Weight factors	37
6.1.2.4	Trade-off	37
6.1.3	Attitude Control Subsystem (ACS)	38
6.1.3.1	Trade method	39
6.1.3.2	Trade criteria	39
6.1.3.3	Weight factors	39
6.1.3.4	Trade-off	39
6.1.4	Orbit Determination Subsystem (ODS)	40
6.1.5	Orbit Control Subsystem (OCS)	40
6.2	Trade-off for the electrical power system	41
6.2.1	Pruning of the EPS design option structure	41
6.2.1.1	Power Source	41
6.2.1.2	Power Storage	43
6.2.1.3	Power Distribution, Regulation and Control	43
6.2.2	Trade method rationale and organization	43
6.2.2.1	Multijunction solar cells	45
6.2.2.2	Thin film solar cells	45
6.2.2.3	Trade off method and rationale	46
6.2.3	Trade-off summary	46
6.3	Orbit Altitude	47
6.3.1	Earth Oblateness	47
6.3.2	Perturbations due to Other Celestial Bodies	48
6.3.3	Solar Radiation Pressure	48
6.3.4	Atmospheric Drag	48
6.3.5	Exposure to Particle Radiation	50

6.3.6 Conclusion	51
7 Operations and Logistics	66
8 Stability & Control	68
8.1 Stability	68
8.2 Control	69
9 Sustainable Development Strategy	71
9.1 Production and Logistics	71
9.2 Operations	71
9.3 End of Life	72
10 Simulation	73
10.1 Introduction	73
10.2 Simulation	73
10.2.1 Orbit	73
10.2.2 Earth Model	74
10.2.2.1 Digital Elevation Model	74
10.2.2.2 Scattering Model	74
10.2.3 Signal Path	75
10.2.4 Noise	76
10.3 Data Analysis	77
10.3.1 Altitude Determination	77
10.3.2 Bidirectional Reflection Density Function Determination	77
10.4 Simulations	78
10.4.1 Variation of Photon Density with Altitude	78
10.4.2 Solar Photons Fraction	79
A Design Option Diagrams	82
B Gantt Chart	94

List of Acronyms

ACS	Attitude Control Subsystem
ADCS	Attitude Determination and Control Subsystem
ADS	Attitude Determination Subsystem
AODCS	Attitude and Orbit Determination and Control Subsystem
ASTER	Advanced Spaceborne Thermal Emission and Reflection Radiometer
BRDF	Bidirectional Reflection Density Function
CMG	Control Moment Gyro
COTS	Components Of The Shelf
DEM	Digital Elevation Model
ECEF	Earth-Centered, Earth-Fixed
EOL	End-of-Life
EPS	Electrical Power System
FOV	Field Of View
GDEM	Global Digital Elevation Model
GEO	Geosynchronous Earth Orbit
GLAS	Geoscience Laser Altimeter System
GPS	Global Positioning System
HEIO	Highly Elliptical Orbit
HEO	High Earth Orbit
ISIS	Innovative Solutions In Space
JAT	Java Astrodynamics Toolkit
laser	Light Amplification by Stimulated Emission of Radiation
LEO	Low Earth Orbit
LiDAR	Light Detection And Ranging
MANS	Microcosm Autonomous Navigation System
MEO	Medium Earth Orbit
MTR	Mid Term Review
OCS	Orbit Control Subsystem
ODS	Orbit Determination Subsystem
OEP	Optical Emitting Payload
ORP	Optical Receiving Payload
PDS	Power Distribution System
SPAD	Single Photon Avalanche Diode
TDRS	Tracking and Data Relay Satellite

TOD True Of Date

WBS Work Breakdown Structure

WFD Work Flow Diagram

WGS84 World Geodetic System 1984

Chapter 1

Introduction

In February 2010 the ICESat mission ended after 7 years of measuring ice sheet mass balance, cloud and aerosol heights, as well as land topography and vegetation characteristics. To do all this, ICESat had only one instrument on board: a space based LiDAR system (Geoscience Laser Altimeter System (GLAS)), allowing for an unprecedented 3D view of the Earth's surface and atmosphere. The laser lifetimes, however, were severely limited because of manufacturing errors in one of the laser components.

ICESat followed only one of the possible approaches for LiDAR, namely the use of a high energy laser and a large receiver telescope. The other approach is using a high frequency low energy laser and a single photon detector. The advantage of the latter approach is that it has a much lower mass, but it is uncertain if even a single photon per pulse reaches the receiver. One possible solution could be the use of a swarm of satellites around the emitter, each equipped with a single photon detector. However the technical feasibility of this concept has not yet been proven.

In this mid term review some options for this concept are proposed and traded off so as to find the best fit for the mission. This tradeoff is what the bulk of this report is about. Also described are the workings and results from the simulator, as well as the project and risk management. Chapters on operation and logistics, stability and control and sustainability are included too.

Chapter 2

Technical Design Development

In this chapter an update is given on the Technical Design Development as given in the Project Plan. All charts and documents have been updated. First the project approach description is updated in section 2.1. Work Flow Diagrams and Work Breakdown Structures are updated in sections 2.2 and 2.3, whereas the Gantt chart is revisited in section 2.4.

2.1 Project Approach Description

2.1.1 Group Procedures

The DSE project is approached by first establishing specific roles for the group members, so that every group member is assigned a clearly defined managerial and technical function. After this the group operational procedures are defined. They are as follows:

1. The Chairman will lead a 'scrum' meeting every morning upon arrival of all members to establish what everyone has done the day before and what they will be doing the day of the meeting. This is done in order to keep all members up-to-date with all aspects of the project. The meeting concludes with updates on any external communications (with organizations and teaching staff) as well as any other points relevant at that time.
2. When done, groups responsible for certain design tasks will present their results to the rest of the team.
3. The team meets with tutor and coaches at least weekly.
4. Everyone is present at The Fellowship between 09:00 and 17:00 every workday, except for a 45 minute lunch break.
5. Upon completion of a deliverable, a meeting is conducted to establish a plan for the next deliverable.

2.1.2 Reporting

The reporting is done in L^AT_EX. There is a main report file which contains the layout of the report and the references to other files that contain the chapters, sections, figures, tables and other documents required for the report. When the file is compiled and printed it will show the entire report.

This has the advantage that work can be easily divided among group members, and any change made to a file will not influence the rest of the report. The file sharing is performed using Subversion (SVN). SVN not only allows file sharing, but it automatically assigns versions to a document and keeps track of changes. The repository is hosted with GoogleTMCode.

2.1.3 Project Outline

The official start of the DSE project is the establishment of the Mission Need Statement. At this point all members should be aware of the main goal of the assignment.

The design process is started by defining the tasks in the project plan, then finding the requirements and functions. From the requirements, a set of design options will be created for the Mid Term Review (MTR). In the MTR a trade-off will be made based on an extensive functional and risk assessment. After the MTR, work on the detailed design can begin. At this stage all subsystems will be given a careful consideration in terms of cost, mass and power budgets. Final decisions on detailed parameters and variables will be made. Leading up to the Final Review (FR), the feasibility study can be concluded.

Parallel to the design phase, the simulator software will be developed by a team of 3 to 4 people, depending on workload and time available. This software should be able to perform calculations accurate enough to aid the trade-off scheduled before the MTR. In this chapter the project planning will be revised. More specifically the Work Flow Diagrams (WFDs) and Work Breakdown Structures (WBSs) of the midterm and final reports and the Gantt chart. These have been updated because now it is more clear as to which tasks have to be performed for the remainder of the project. Also, the work flow for the simulator has been added to the charts. In sections 2.2 the revised Work Flow Diagram will be shown. This is followed by section 2.3, which shows the updated Work Flow Diagram. The final section gives the Gantt chart, our timeline for this project.

2.2 Work Flow Diagram

The tasks to be done on the simulator have been updated and presented in more detail. Some tasks have also been changed in the WFDs: they now start earlier or later so as to better describe the work flow of the project. The tasks in the green and blue boxes respectively describe the simulator design finalization and tradeoff execution in more detail. Red boxes are tasks which are explicitly needed for the Mid Term Review (MTR). The updated WFD of the MTR is given in figure 2.1, page 7.

The WFDs of the final report have also been updated. In retrospect, a very important part if the final report was not present in the WFDs: perfecting the design and the feasibility determination. Now these tasks have been added to the diagram to make it complete. As with the WFD of the MTR, all boxes in red are explicitly required for the final report. The diagram can be seen in figure 2.4, page 10.

2.3 Work Breakdown Structure

The WBSs have been updated like the work flow diagrams. Some extra and other more detailed tasks defined in the WFDs have also been added to these structures. Also, the layout has been changed somewhat to improve readability and correctness. The updated WBSs can be seen in figures 2.3 and 2.4, starting on page 9.

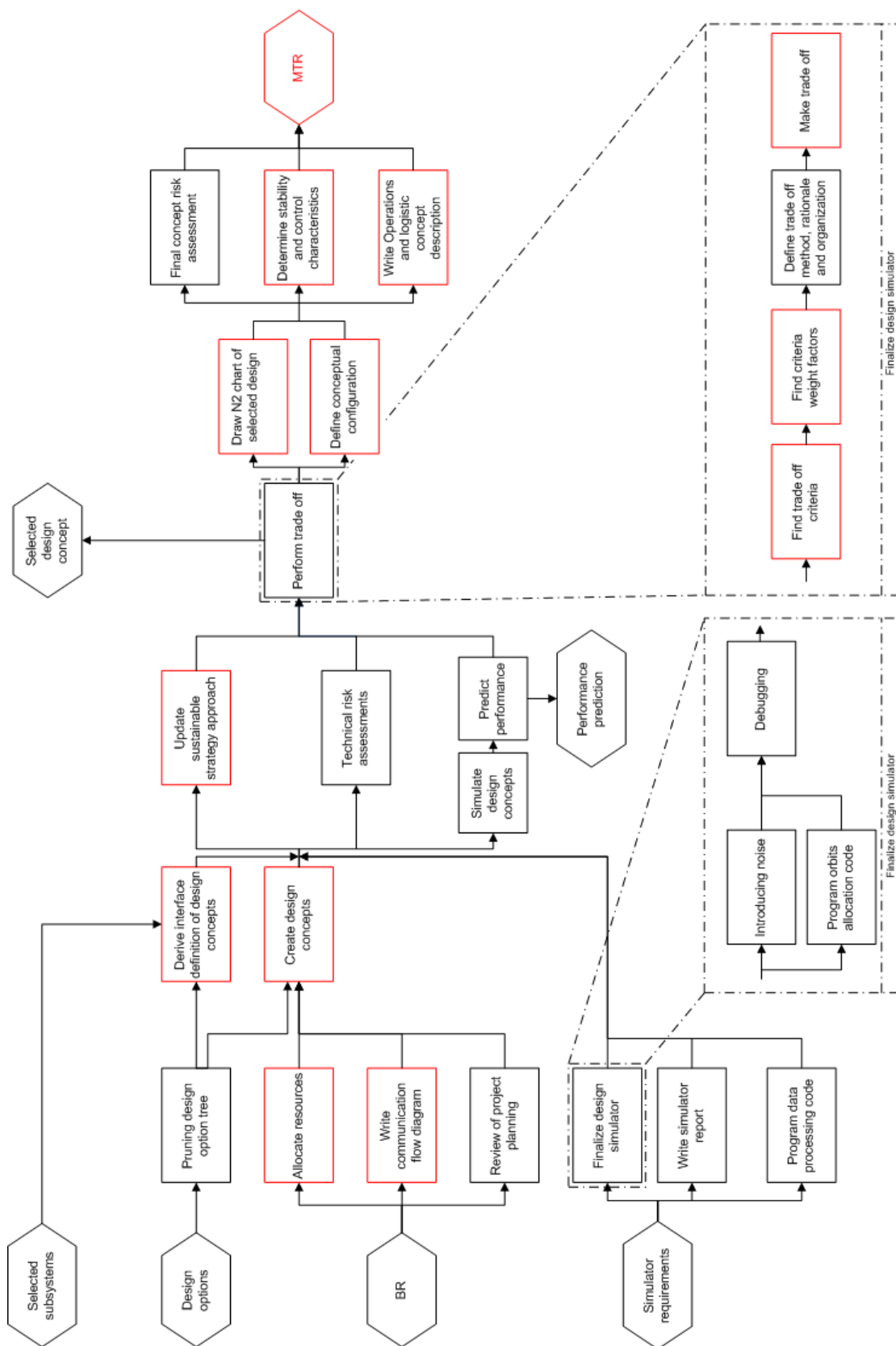


Figure 2.1: Updated work flow diagram for the mid-term report

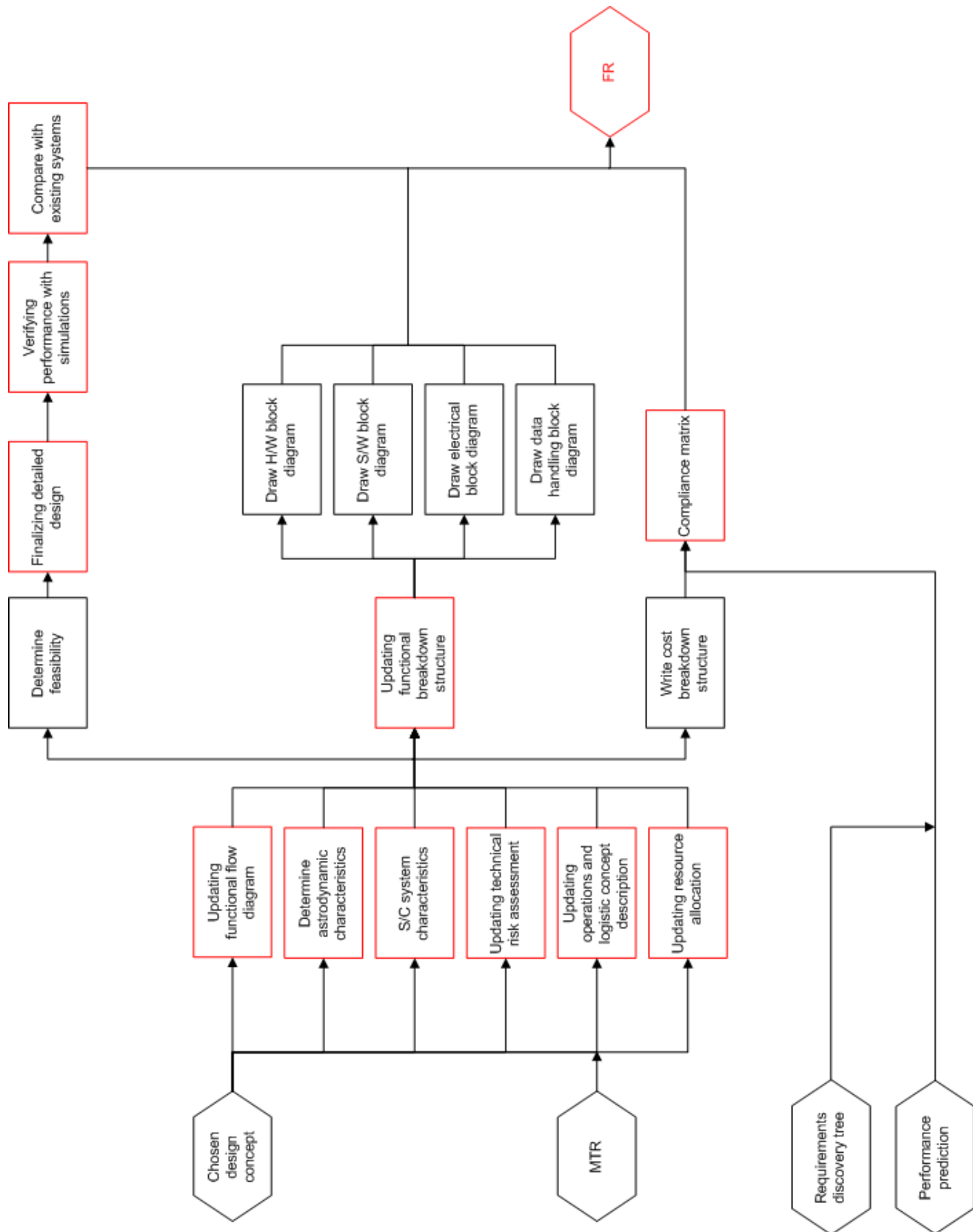


Figure 2.2: Updated work flow diagram for the final report

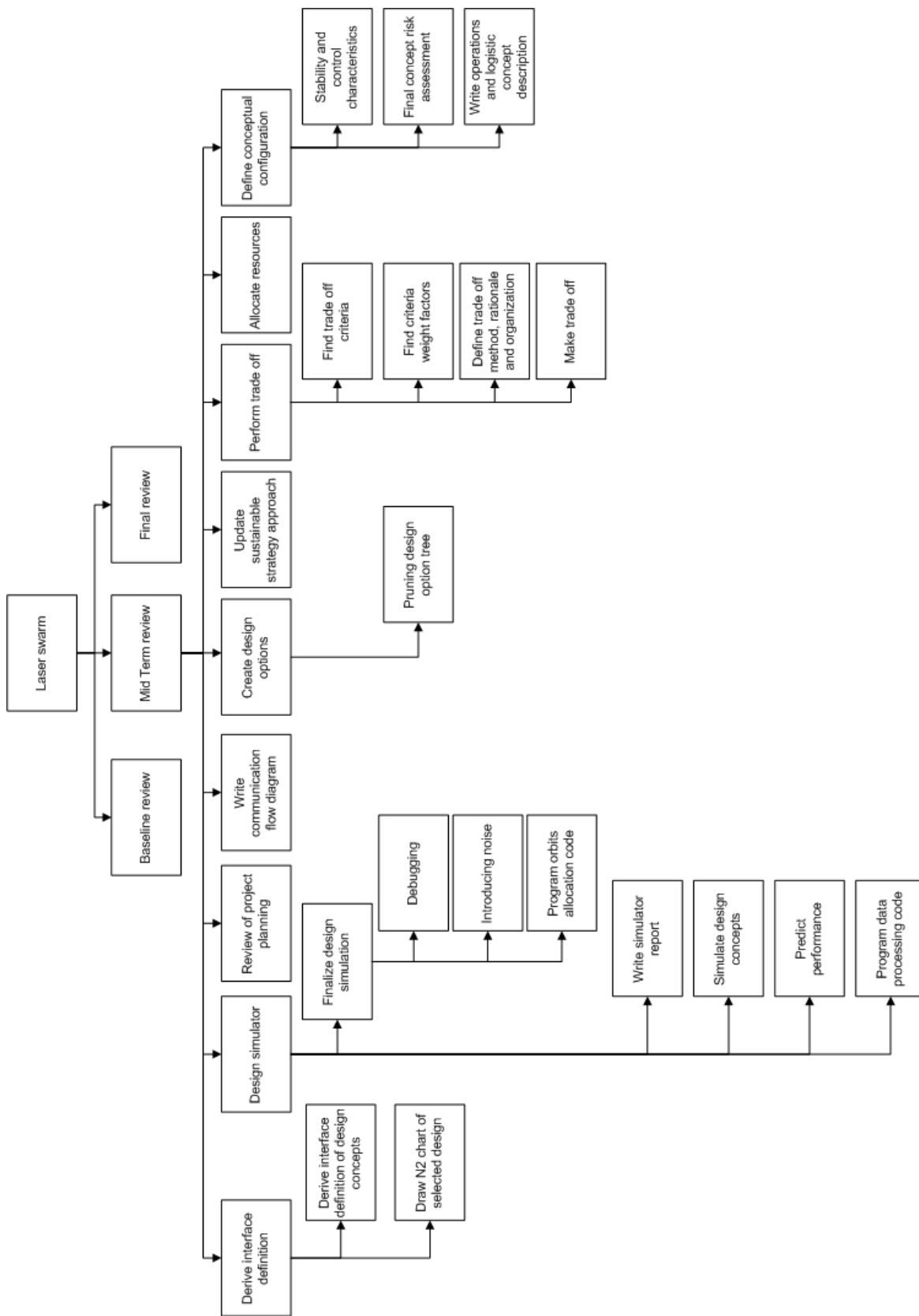


Figure 2.3: Updated work break-down structure for the mid-term report

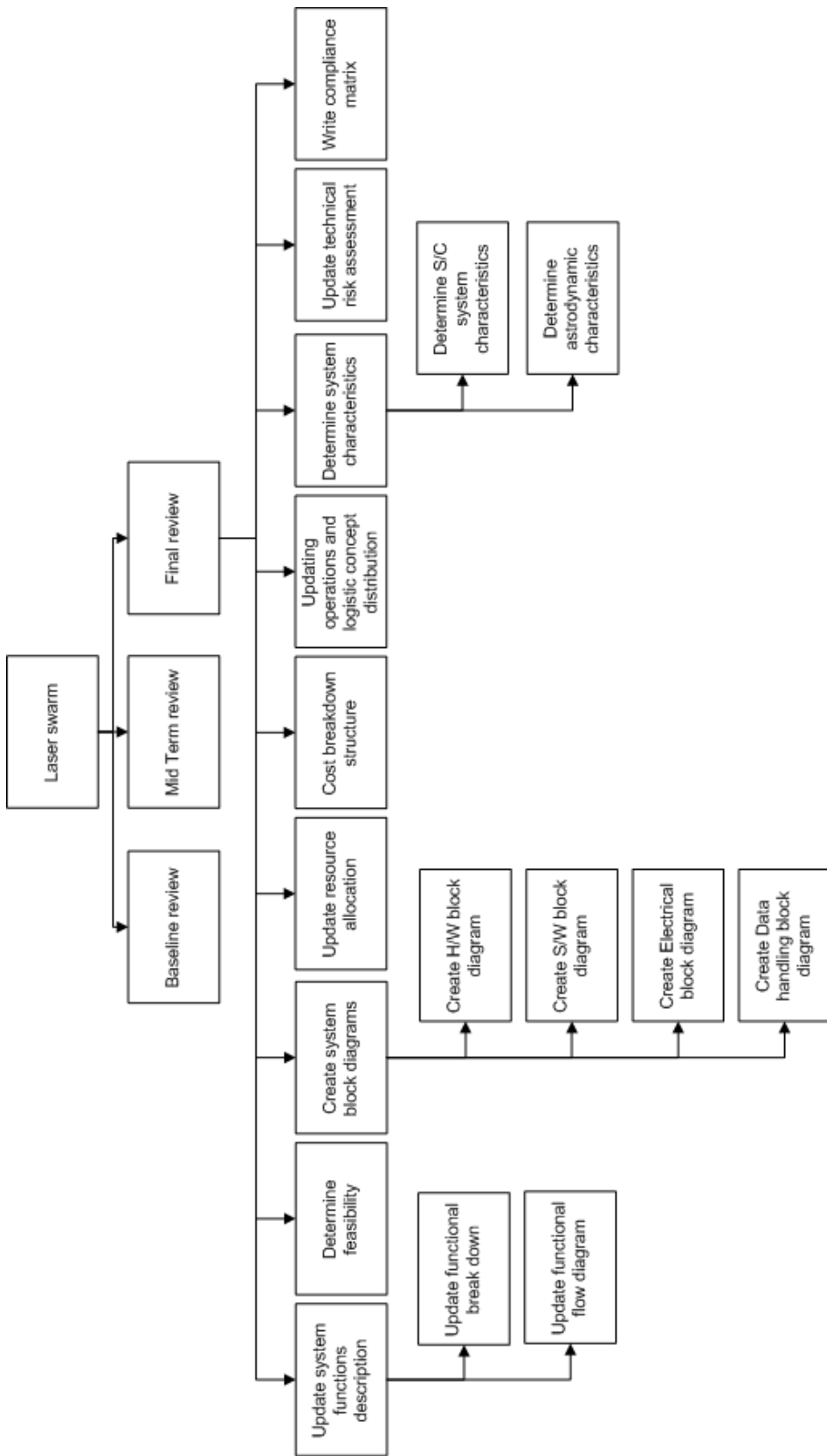


Figure 2.4: Updated work break-down structure for the final report

2.4 Gantt chart

As the WFDs and the WBSs have been updated, so the Gantt chart has also been updated. Now that we are further along in the project, it is easier to estimate which tasks need to be done for the mid-term and final reports. The estimated duration of these tasks also was much easier to estimate. The Gantt chart has been updated to contain all tasks set in the WFDs. Special care was taken to make sure the Gantt chart is consistent with the WFDs and the WBSs. This time the simulator tasks were not separated from the rest of the project because the simulator is more involved with the rest of the project for the mid-term and final reports. The updated Gantt chart can be found in appendix B, page 94.

Chapter 3

Risk Management

All projects, whether big or small, innovative or mundane, are bound to fail under certain circumstances. It is, therefore, in the interest of the team to foresee possible causes of failure and to try to account for them. This is why the risk analysis is performed - it aids in determining and evaluating the gravity of potential failures and helps minimize the damage.

First and foremost is the risk of technical failure which will render the system inoperational or malfunctioning. This risk accounts for the failure of one of the subsystems and is addressed in the 3.3.5 subsection.

Another risk is that the system will not meet market demands by either being too expensive or having a very narrow range of application. This risk is addressed in the 3.1 subsection.

In order to distribute the risks associated with the design process, contingency is introduced. This is discussed in the 3.2 subsection.

3.1 Market Analysis

Market analysis determines the main potential users and is mainly dependent on the quality and quantity of the obtained data. There are four types of the measurement data sets and it is convenient to analyze them separately. Figure 3.1 on page 13 gives the market diagram with the different data sets.

In the Market Breakdown Diagram, each data type has both science and commercial potential users. For example, in the science field the oceanographic data can be used for climate research. Scientists can study the evolution of weather patterns from the ocean system by modeling changes in the heat distribution of the ocean. On the other hand, in the commercial field maps of currents, eddies and vector winds are used in commercial shipping and recreational yachting to optimize routes. All the blocks in the diagram could be potential return on investment on short or long term.

3.2 Technical Resource Contingencies

When starting the design of a new system the technical resource budgets, like power or mass of the system, are not known yet. They must be estimated based on the information of previous missions, general guidelines and educated estimations. During the design process, the actual budgets will differ from these initial estimations. For example the mass of a satellite will change during the design process because of unexpected

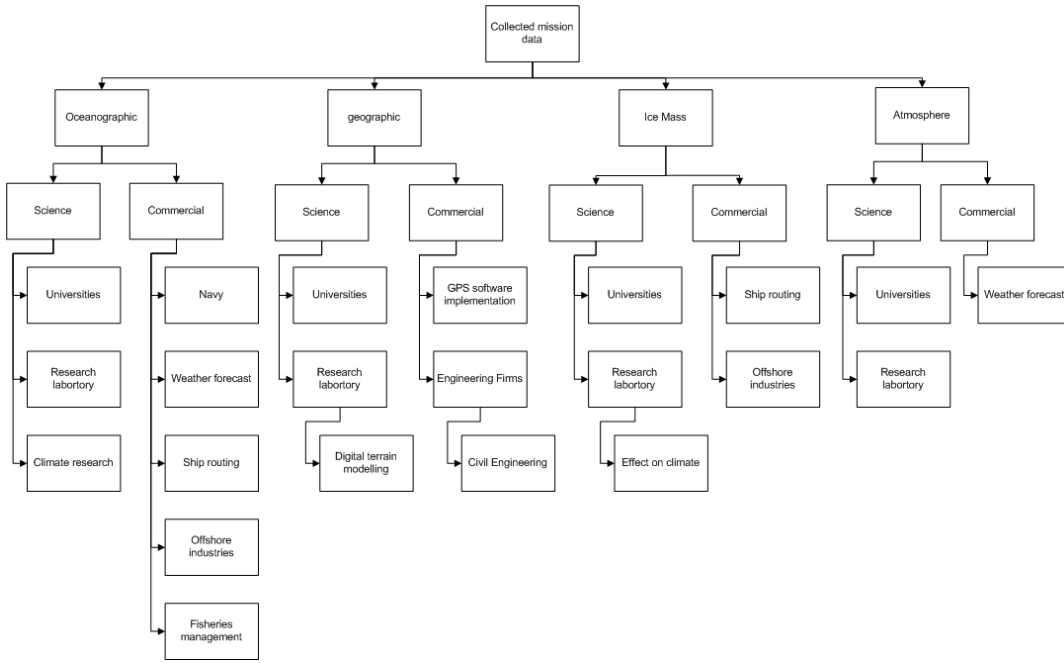


Figure 3.1: Market Breakdown Diagram with different data sets [Mar(2008)]

problems, changes in the design, etc. To ensure that a product will achieve the required performance while not overspending the budgets, Technical Performance Measurement (TPM) is used. This technique shows the difference between the actual and required performance. For example a contingency of 20% for the mass budget means that the actual mass can differ up to 20% of the required mass. TPM establishes contingencies for each technical parameter. This contingency is managed to provide a reserve to spend as the design difficulties are discovered. The contingency is reduced as the project matures and disappears at the product delivery.

Fortunately, some guidelines exist for contingencies of aerospace vehicles. The main technical resource budgets for our project are mass and power. Mass and power contingencies are given in tables 3.1 and 3.2 on page 14.

Design maturity	Contingencies [%]						
	Propulsion	ADCS	C&DH	Thermal	Power	Structures & Mechanisms	Payload
Conceptual estimate	20	20	25	20	15	20	20
Layout calculation	15	15	20	15	10	15	15
Pre-released drawings	5	5	10	10	5	5	5
Released drawings	3	3	5	5	5	3	3
Specifications (vendor/subcontractor)	5	5	5	5	5	5	5
Actual measurement qualification hardware	1	1	1	1	1	1	1
Actual measurement flight hardware	0	0	0	0	0	0	0

Table 3.1: The mass contingency allowance

Design maturity	Contingencies [%]			
	ADCS	C&DH	Power	Payload
Conceptual estimate	20	20	15	30
Layout calculation	15	15	10	20
Pre-released drawings	5	5	5	10
Released drawings	3	3	5	5
Specifications (vendor/subcontractor)	5	5	5	5
Actual measurement qualification hardware	1	1	1	1
Actual measurement flight hardware	0	0	0	0

Table 3.2: The power contingency allowance

3.3 Technical Risk Assessment

The main objective of the technical risk assessment is to determine the reliability compared to the possible (functional or financial) consequences per specific event. To be able to determine any of these reliabilities, a definition of reliability should be stated. In this case, reliability is formulated as:

The probability that a specific (part of a) subsystem will function without endangering the top level requirements over the expected lifetime.

Next to formulating the definition of reliability, it should be noted that the determined reliabilities in this section are relative reliabilities, i.e. the probability that a particular subsystem outperforms another subsystem with the same core function in terms of reliability. Hence, no absolute values of reliability are determined in this section. The relative reliabilities allow for comparison material during the trade-off between multiple design options. The risk assessment analysis is divided into four main sections:

- I Ground segment (before vehicle leaves Earth's atmosphere)
- II During mission
- III Measurement protocol
- IV Post-mission

The possible events, with their respective reliability, are outlined in these sections and after that the expected consequences are shortly explained.

3.3.1 Ground Segment

A *Financial*

A1. Insufficient funds or low market-demand

The approximate costs are determined in the cost budget. The mission data and the final results can be very interesting for a vast number of commercial parties and research or educational facilities. Every space mission is created for at least one specific (user-demanded) requirement set by a user. This third party is responsible for covering the cost. Since the space mission is developed after this request is set, the probability that there will be insufficient funds is low (especially when more than one company can be considered as the user). However, the consequence can be severe if the funds are not enough to start or continue the development.

B *Technological readiness*

B1. Technology for level zero requirements are not available

If the technology for measuring, detecting or processing the level zero requirements is not available at present, the requirements cannot be met and alternatives should be devised, or the mission should be terminated. In our case, the technical readiness level of the payload is relatively high and hence has a high reliability. If, however, the specific payload would have a low technical readiness level, the mission should be terminated or delayed. Therefore, it has important consequences to the mission.

C *Launch*

C1. Total launch failure

Total failure indicates complete failure of the launch vehicle and all laser swarm constellation components. Needless to say, the reliability is relatively low; however, the consequences of this event are catastrophic.

C2. Partial launch failure

Partial launch failure indicates non-complete failure of laser swarm constellation components, i.e. some of the satellites (more receivers and one emitter) can still perform core tasks. Considering historical launch data, the reliability that no partial failure will occur during launch is relatively high. The consequence can be very different, depending on which part (or what fraction) of the constellation cannot perform its core task. If one of the receivers will be destroyed, the level zero requirements might still be achievable. However, if the emitter is (partially) destroyed, the mission will surely be endangered.

C3. Delayed vehicle launch

Delaying the vehicle launch is not particularly a problem from the technological side of the mission; however, it will affect the financial situation. Next to the fact that the data and results are delayed, extra costs will be imposed due to an increase in launch vehicle pad costs, extra personnel costs and others. The reliability of this event is actual not that high, since it is dependent on a lot of criteria like third-party companies, the weather, and atmospheric properties. The consequences are mainly financial.

3.3.2 During Mission

D *Orbit accuracy*

D1. One or more satellites are in a wrong orbit.

After launch and orbit initializing, it is possible one or more of the satellites are in a wrong orbit. If this deviation from the desired orbit is relatively small, the ADCS subsystem should be able to cope with this minor error and adjust the orbit. If the altitude error is large, major altitude changes should be imposed. Assuming a low to moderate error, the consequence is not really severe if the ADCS system is working properly. The chance of actually putting a satellite in the wrong orbit is also relatively small.

In the next section, the reliability of the ADCS subsystems is compared. Assuming a non-hybrid spacecraft, i.e. a spacecraft which uses one of the ADCS subsystems considered in the design option tree, the consequences of failure are equal for all subsystems and thus shall not be inspected individually. The consequences are severe considering not only the loss of pointing accuracy, but also a decrease in vehicle stability and the total failure of controllable altitude control.

E *Altitude and control determination*

E1. *Passive systems*

E1a. Gravity-gradient.

The gravity gradient technique is only dependent on gravity fluctuation in nadir direction, which makes it relatively reliable.

E1b. Passive magnetic.

The passive magnetic technique is only dependent on magnetic fluctuation near a celestial body. Since this is the only dependency, the technique is really reliable.

E1c. Zero momentum.

The zero-momentum technique uses a momentum-bias wheel, initially with no angular velocity. Like with all mechanical systems, the presence of (angular) motion will decrease the reliability (due to possible mechanical failure like static failure, fatigue etc.). The reliability however is pretty high, but lower relative to passive magnetic and gravity gradient.

E1d. Momentum-bias wheel.

The momentum-bias wheel technique uses, like the name already predicts, momentum wheels to dump and correct torques. In that sense it has the same reliability as the zero-momentum subsystem. However, since these momentum wheels are constantly spinning, the reliability is slightly lower than the previous mentioned subsystem.

E1e. Spin stabilization.

Spin stabilization can be achieved using rotation about one principal axis (single-spin) or two principal axes (dual-spin). Next to the fact that due to external torques (debris collision, aerodynamic drag) the spacecraft can become unstable, i.e. this subsystem has more dependencies, making it relatively unreliable.

Figure 3.2 demonstrates relative reliabilities of different passive Attitude Determination and Control Subsystem (ADCS) systems.

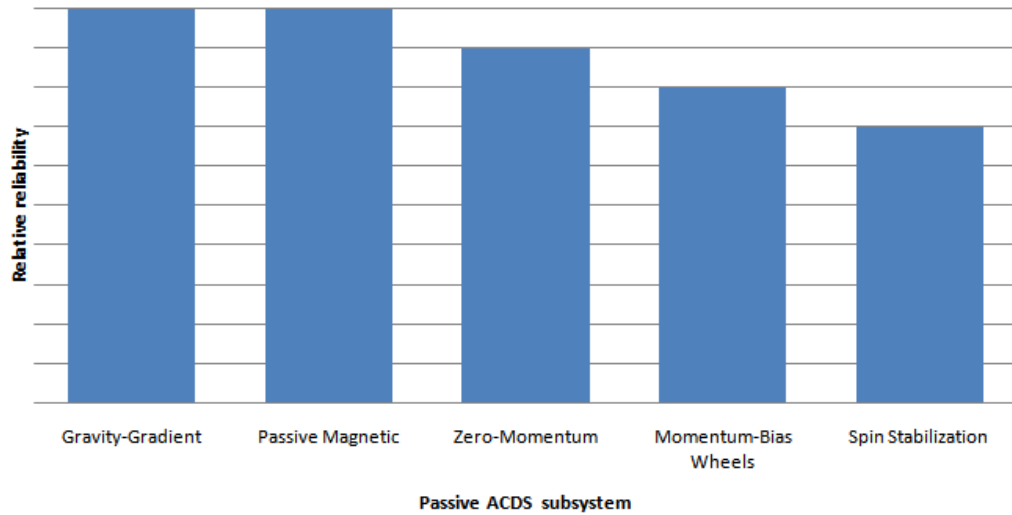


Figure 3.2: Relative reliability of passive ADCS subsystems.

F Active systems

F1. Actuator

F1a. Thrusters (hot and cold gas).

Multiple-axes thruster systems are very efficient ways for controlling attitude and stability. The system is dependent on fuel consumption, combustion and mechanical properties. Each of these dependencies decreases the reliability.

F1b. Reaction and momentum wheels.

Mechanical reliability is an import aspect for using active reaction and momentum wheels.

F1c. Control Moment gyros.

A control-moment-gyro system consists of a spinning rotor and one or more motorized gimbals that tilt the rotor's angular momentum. Mechanical reliability is an important aspect for using this. Since it is also dependent on the motorized gimbals, the reliability is slightly lower than the reaction and momentum wheels.

F1d. Magnetic torquers

The magnetic torquers interact with the Earth's magnetic field, creating compensating torques to induce stability. Reliability is high due to the fact that the magnetic field is known and the system is dependent on a low number of parameters.

F2. Sensors

Assuming a high technical readiness level of the sensors, the reliability is considered high. Also, the consequences of failure are high as the continuation of the mission may be impaired.

Figure 3.3 demonstrates relative reliabilities of different active ADCS systems.

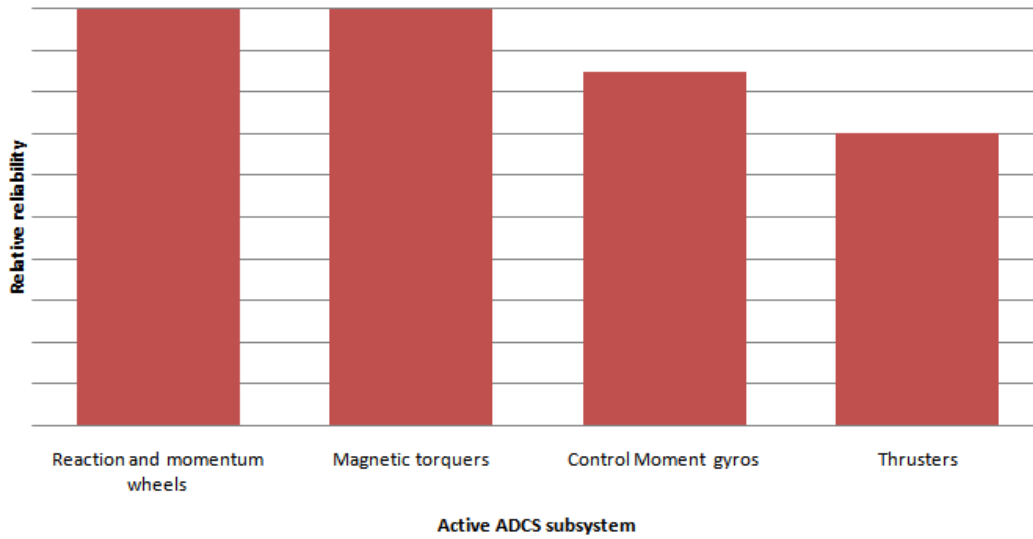


Figure 3.3: Relative reliability of active ADCS subsystems.

G *Electric Power System (EPS)*

G1. *Solar Panels*

G1a. Solar panel deflection error or mechanical failure.

During launch, the solar panels are retracted to achieve the lowest volume possible. During the initializing of the mission (assuming the spacecraft is in the right orbit), the solar panels need to be deployed. Errors can occur due to mechanical reasons or external disturbances. The probability of this is pretty low. The consequence can be however that the effective solar panel is decreased and hence a decrease in available electrical power will occur. This makes the consequences pretty severe. Any other mechanical failure (broken joints, internal PN-junction failure, or a loss of an entire solar panel) will have severe consequences as well.

G1b. Solar panel characteristics reliability (degradation).

Degradation of solar panels should always be considered during mission development. Since this (should be) known upfront, the consequences are relatively low. The probability of this actually happening is nearly 100%.

G1c. Severe degradation (due to external phenomenon)

Atomic oxygen, hazardous radiation, debris collision and other external factors can influence the performance of the solar panels. Since these are not known from the start, it is difficult to cope with them. The probability of this happening is pretty small, but will have pretty severe consequences.

G2. *Batteries*

G2a. Initial internal failure

Considering a high level of technical readiness level, the internal reliability is high. The consequences do

alter the functional capacity of the mission, since no energy can be stored if the energy capacity system would completely fail, meaning that during eclipse no energy can be used.

G2b. Decrease in capacity

Considering a high level of technical readiness level, the reliability is high. Consequences are low, because they are known and should be part of the mission analysis.

3.3.3 Measurement Protocol

Since actual measurements are an important level zero requirement, the consequence of the items in the measurement protocol are all really severe. Unless stated otherwise, the consequences in the following section can thus be stated in this way.

Measurement

H Emitter

H1. Laser pulses cannot be sent/ no photon generation

Considering a high level of technical readiness level, the reliability is high.

H2. Pointing towards nadir

This is dependent on ADCS risks.

H3. Laser notifies receiver (time adjustment)

Considering a high level of technical readiness level, the reliability is high.

H4. Laser degradation

Laser degradation is dependent on multiple parameters: thermal properties, input power interval, external factors and internal mechanical errors (manufacturing or design errors). However, due to extensive research and development concerning laser technology, the probability of severe laser degradation within the lifetime is relatively low.

I Receiver

I1. Point towards target

This is dependent on ADCS risks.

I2. Receive and detect photons

Considering multiple satellite receivers, the probability of total failure to receive and detect photons using advanced single photon receiving devices (like SILAT, GLAS or photon-receiving modules) is negligible.

I3. Turn photon into electrical signal

Considering a high level of technical readiness level, the reliability is high.

Communication

J Inter satellite communication

J1. Determine relative position receiver and emitter

Considering a high technical readiness level, the reliability is high.

J2. Time differences

Considering a high technical readiness level, the reliability is high.

K Data handling

K1. Store data/ make data package

Considering a high level of technical readiness level, the reliability is high.

K2. Transmit package

Considering a high level of technical readiness level and relative low-tech technology, the reliability is high.

K3. Interpreted results

Historical data comparisons for the interpretation of altimetry missions are sufficient, but not elaborate. However, the reliability is still pretty high.

K4. Reproduce terrain model

Historical data comparisons for the interpretation of altimetry missions are sufficient, but not elaborate. However, the reliability is still pretty high.

L Housekeeping/ Ground communication*L1. Housekeeping data from ground station to satellite*

Considering a high level of technical readiness level, the reliability is high.

L2. Adjusting space segment characteristics

Considering a high level of technical readiness level, the reliability is high.

M Structural*M1. Joints*

Considering a high level of technical readiness level, the reliability is high.

M2. Connection points

Considering a high level of technical readiness level, the reliability is high.

M3. Thermal limits

Thermal limits will alter the characteristics of pretty much all subsystems. However, thermal will be excluded in this analysis, because this is not a part of the project.

M4. Fatigue

High-cycle loading is usually not present (except for momentum wheels) and should therefore only play a minor role. The probability is low. The consequences are medium to high if high-cycle loading will lead to fatigue and hence partial failure.

M5. Electrical overlay failure

This event is dependent on the reliability of the EPS.

M6. Launch loads

Due to large forces and vibrations during launch the structure of the satellite can fail. Since the launch loads are well known the reliability is low, the consequences can be severe.

N External*N1. Debris collision*

Unknown external phenomenon. The probability of this event causing total failure, which is a function of multiple parameters like orbit and celestial position, is low to medium.

N2. Dangerous radiation

Unknown external phenomenon. The probability of this event causing total failure, which is a function of multiple parameters like orbit and celestial position, is low to medium.

N3. Charged particles collision

Unknown external phenomenon. The probability of this event causing total failure, which is a function of multiple parameters like orbit and celestial position, is low to medium.

N5. Politics or international influence

Political decisions or international influences can alter the space mission considerably. With altimetry missions, the probability of these external influences causing a delayed or complete stop of the mission is negligible. The consequences, however, could be very severe.

N6. Classified information (military)

Some parts of the measurement are considered classified information, for example military ground stations or governmental classified areas. The government and/ or military can pressure the vehicle engineers to keep certain information classified. However, if this is the case, most of the measurements still can be taken and analyzed. So where the probability is medium, the consequences are very low.

3.3.4 Post-Mission

O *Satellite decommission*

O1. *Decommission LEO*

At the end of life the satellites have to be decommissioned to allow new mission to take their place. To decommission satellites in Low Earth Orbit (LEO) one could just wait a couple of years and air drag will cause the satellites orbit to degrade to the point when they can burn up in the atmosphere, so the consequences are low. However, it is desirable to have the satellites burn up faster, so as to remove the risks of satellite collision. The probability to no longer be able to eject the satellite from orbit depends on whether or not its propulsion system is still working; as such this probability is low.

O2. *Decommission GEO*

Satellites in GEO can not be placed in an orbit that will cause them to burn up in the atmosphere because they will cross paths with too many other satellites. Because risk is so high these satellites are instead decommissioned by ejecting them from orbit further into space. This way, new GEO satellites can take the place of the swarm. If this is not done, then the dead satellites will continue orbiting the Earth, wasting space that can be used by other satellites, as a result the consequence of failure is high. Being able to reposition a satellite depends on the ADCS systems; as such the probability of this event is low.

3.3.5 Risk Control

Sometimes it is possible to decrease the failure probability. For example, A1, F1a and H4 could be the top 3 risk segment. Failure probability of A1 can be pulled down by doing detailed market analysis. In case of F1a, safe combustion performance as well as fuel consumption can be tested and modified in a laboratory environment to increase the thrusters' reliability. Laser degradation (H4) is crucial in the system, and reliable energy source should be used to prevent failure. Meanwhile, thermal control can be performed to achieve high reliability of the laser emitter.

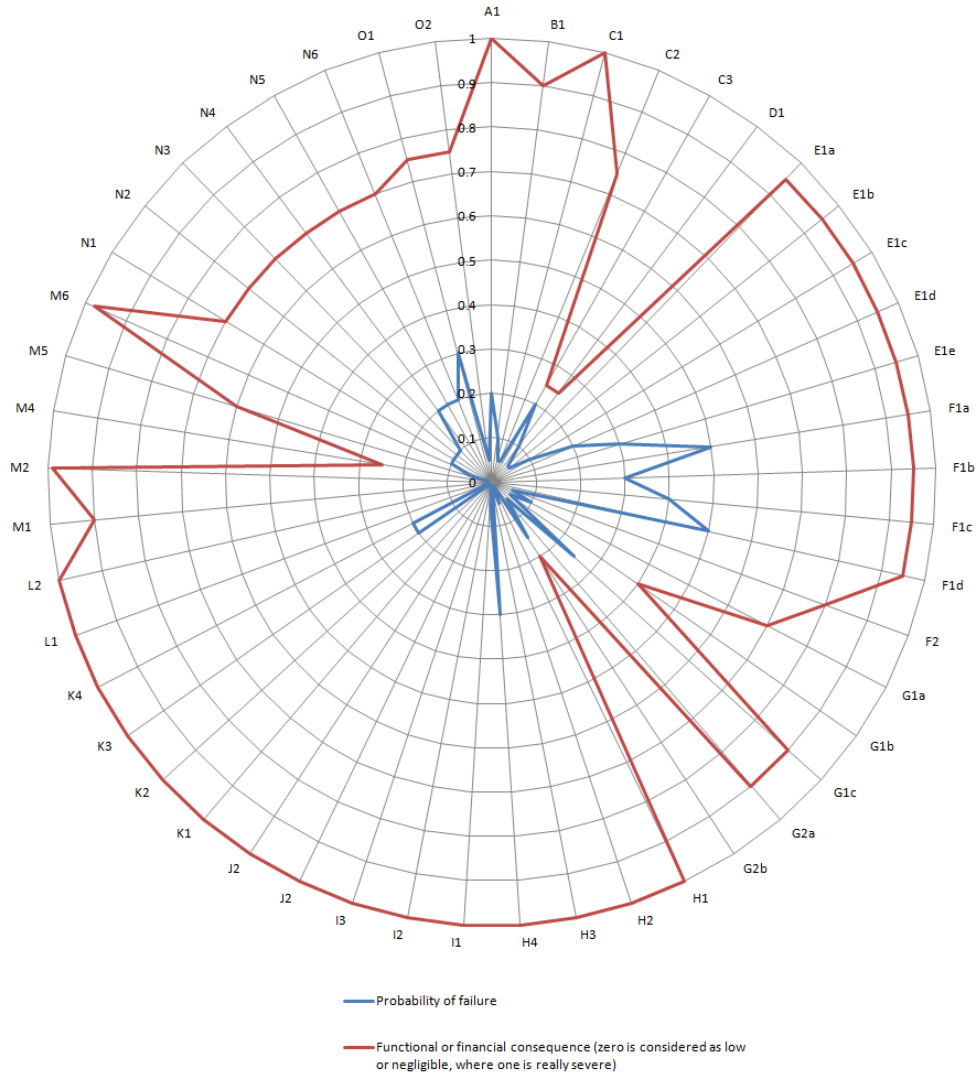


Figure 3.4: Technical Risk Map

Chapter 4

Design Options

In this chapter the design options are repeated from the baseline report. This is done so that the reader gets the whole picture from options to the design finally chosen. This is done for the ADCS, the telecommunications subsystem, the Electrical Power System (EPS), the orbits, the Optical Emitting Payload (OEP) and the Optical Receiving Payload (ORP), in subsections 4.1 to ?. The full text has not been included, and the diagrams have been moved to appendix A.

4.1 Attitude Determination and Control Subsystem

The design of the ADCS is twofold: on one side there is the attitude determination, on the other the attitude control. If the state of the satellite is not as it should be the attitude control part adapts the attitude.

A design option tree for the ADCS can be found in figure A.1 on page 83. The chart displays a few properties of each design option for a quick comparison.

4.1.1 Attitude Determination

For attitude determination a number of different techniques can be used. First of all there are inertial measurement units like gyroscopes and accelerometers. Then there are Sun sensors, Earth scanners and star trackers to determine the attitude of the satellite. A recent technique to determine the attitude is using accurate relative Global Positioning System (GPS) measurements with multiple antennas on the satellite body.

4.1.2 Attitude Control

The attitude control is able to change the attitude of the satellite. Thrusters exert gases and momentum wheels spin up to give a momentum to the satellite. In magnetic torquers a current through a coil produces a Lorentz force, using the magnetic field of the Earth. Control Moment Gyro (CMG)s have a constant speed, but the angle in which the force vector is directed is adapted by a single or double set of gimbals.

Passive means of attitude control include gravity gradient, spin stabilization and passive magnetic.

4.1.3 Note on Receiver Pointing

It is important to acknowledge the fact that the receiver payload does not necessarily need to be pointed with the use of ADCS. Also actuators and optics can be used for the pointing.

4.2 Optical Emitting Payload

4.2.1 Introduction

Satellite altimetry missions use active remote sensing techniques. For that reason the quality of the system is dependent on the emitted electromagnetic radiation and the analysis of the returned signal. Considering the orbit of a regular Earth observation satellite to be in the order of 500 to 800 kilometers (statement based on earlier altimetry missions) and the fact that the power of the emitted radiation decreases exponentially with distance, finding a proper optical emitting device is not a simple task. Next to the decrease in energy, atmospheric absorption or scattering at specific wavelengths are also another important issues to consider, since altimetry missions usually are designed to measure the actual Earth's surface, i.e. the emitted photons need to be able to reach the surface, have enough energy to scatter and reach the receiver.

To be able to select any optical emitting device, the important parameters for optimizing the altimetry results should be revised. Several problems occur if emitting radiation is chosen as the remote sensing technique.

- i First of all, general electromagnetic radiation will show isotropic behavior. This results in an effective energy loss, since most of the radiation is not pointed towards the desired position. Hence, a divergence limited source would be preferable.
- ii As mentioned before, the wavelength is an important parameter since it will influence the photons actually reaching Earth. Since the Earth's atmosphere is transparent for wavelengths in the visible spectrum, it would be better to have an electromagnetic radiation source with a wavelength in this interval. Next to that, a regular radiation source (like the Sun) emits radiation consisting of a whole spectrum of wavelengths. The less the number of discrete wavelengths (preferable in the visible spectrum), the higher the quality of the analysis can be.
- iii The total work done on the photons to reach the Earth's surface, scatter and return to the receiver, is generally very large. To cope with this large work, the energy of the specific energy pulses should be high.

All of these criteria are important when considering the optical emitting device. The most convenient mechanism for solving these preliminary problems can be solved by using a Light Amplification by Stimulated Emission of Radiation (laser) system. Optical emitting devices using laser technique have considerably low divergence (high energy density), discrete and known wavelength characteristics and a relative high pulse energy.

4.2.2 Laser Characteristics

The characteristics of laser systems are determined by the quantum mechanical interaction of electrons (and holes) between the conduction and valence band. Quantum mechanics predicts that electron energy levels are discrete and quantized, hence, predicting the existences of energy gaps. The electron configuration in a given chemical element, will be distributed according to the Boltzmann distribution, assuming the element is in thermal equilibrium. Generally, the electrons will exhibit the lowest energy state. Electron excitation

can take place by energy addition to an n -level energy system, where n denotes the number of quantised energy levels. This energy can be thermal, electric or photonic.

Photonic excitation, i.e. electron excitation by an induced photon, can lead to stimulated emission, which is the starting point for the working principle of the laser technique. To achieve photonic excitation, the energy of the incoming photon should be equal to the the difference in electron energy level from ground state to excited state. Since this energy is dependent on wavelength, the resulting wavelength of the laser radiation is known as well (incoming wavelength equals wavelength laser radiation). Every chemical composition has its characteristic discrete energy levels and bandgaps, allowing different bandgap energies and hence, different wavelength characteristics.

The laser is an optical emitting device consisting of a certain aperture value. For this reason, diffraction will occur. However, due to the low divergence, the diffraction will be lower relative to isotropic radiating sources.

Radiation from the laser can be continuous or pulsed. The input power, also known as the pump power, is the power needed to ensure the right amount of stimulated electron emission in the laser cavity. This power is then redirected towards the radiation. Since many lasers are pulsed, with pulses in the order of pico- to nanoseconds with relatively high frequency, the pulse power, i.e. the power divided per unit pulse, is in the order of 0.001 to 1 Watt. Peak powers in that case can exceed 1 gigawatt [Xu(2000)].

4.2.3 Laser Types

There are actually many types of lasers. The main types are considered below:

1. Gas. A variety of lasers is based on gases as gain media. The laser-active entities are either single atoms or molecules, and are often used in a mixture with other substances having auxiliary functions. Most gas lasers emit with a high beam quality, often close to diffraction-limit, since the gas introduces only weak optical distortions.
2. Semiconductor lasers, also known as diode lasers, are lasers based on semiconductor gain media, where the optical gain is usually achieved by stimulated emission at an interband transition under conditions of a high carrier density in the conduction band.
3. Solid-State lasers are lasers based on solid-state gain media such as crystals or glasses doped with rare Earth or transition metal ions. They are mainly optically pumped with flash lamps or arc lamps, which will lead to high powers and low costs but also to relative low power efficiencies and moderate lifetime. [Paschotta(2008)]

Figure A.10 on page 91 gives the final design option tree of the laser emitter.

4.3 Electrical Power System

The electrical power system (EPS) is divided in to four parts: the power source, the energy storage, the power regulation and control and the power distribution. These are also the four main branches in the EPS design options structure. Each of these will be considered individually in this section. Figures A.3, A.4 and A.9 (pp. 85-90) show the complete design option tree for the EPS.

4.3.1 The Power Source

Launch vehicles primarily use batteries as power source, because launch durations are quite short and thus batteries can be kept fairly small. For missions lasting from weeks to years however, batteries would be too large for the mission to be useful.

Typically, there are four types of power sources for longer missions: static power sources, dynamic power sources, fuel cells and photovoltaic solar cells.

Static power sources use a heat source for thermal-to-electric conversion. This conversion can be done by either a thermoelectric or a thermionic concept. The thermoelectric converter uses the fact that the radioactive source (typically plutonium-238 or uranium-235) has a slow rate of decay. Because of this, there exists a temperature gradient between the p-n junction of individual cells which is used to provide the desired direct current electrical output. The efficiency of such a system is about 5-8%. Thermionic energy conversion, on the other hand, uses a hot electrode facing a cooler electrode to convert thermal energy to electrical. These electrodes are sealed in a chamber containing an ionized gas. The hotter electrode can be seen as the emitter: it emits electrons that flow across the inter-electrode gap towards the receiver (the cooler electrode). Once arrived, these electrons condense and return to the emitter through an electrical load connected externally between the two electrodes. Typical system efficiency is about 10 - 20%.

Dynamic power sources function somewhat differently. They also use a heat source (typically concentrated solar radiation, radio isotopes or a nuclear-fission reaction) to produce thermal energy but the conversion method to electrical power is different. The generated heat is used to heat up a fluid to drive an energy-conversion heat engine. This is done using a Stirling cycle (efficiency of 25-30%), a Rankine cycle (efficiency of 15-20%) or a Brayton cycle (efficiency of 20-35%).

Fuel cells are self-contained generators that convert the chemical energy of an oxidation into electrical power. They consist of two half-cells, each with an electrode and an electrolyte. The two half-cells may use the same electrolyte or they may use different ones. In the fuel cell, one half-cell gets oxidized, it loses electrons, and the other is reduced, it gains electrons. As the electrons flow from one half-cell to the other a difference in charge and thus an electric current is created. Fuel cells can be regenerative or not, unfortunately regenerative types have not been space-proven yet [Rees(2001)]. The efficiency of fuel cells can be as high as 80%, but will drop significantly at higher currents.

Photovoltaic solar cells are most common. They convert incident solar radiation directly into electrical power. They consist of a semiconductor with metal plates on the top and bottom. Part of the incident solar radiation gets absorbed and is transferred to the semiconductor. The energy excites electrons who are then free to move around. The metal plates move the electrons, which creates a current, to power different subsystems. An efficiency of 29% has been achieved in the lab [Doody(2001)], but production efficiencies are around 22% [Wertz(2006)]. Several options are available for the placing of the solar cells. The biggest difference is between solar panels and body-fixed solar cells. Body-fixed solar cells require a spinning satellite to be able to make optimal use of the cells. Solar panels, however, can be pointed towards the sun to have minimum cosine loss. The panels can be rigid or flexible, flexible panels being easier to transport but less strong than rigid panels.

A comparative table for the different power sources can be found in table 11-35 on page 410 of [Wertz(2006)].

4.3.2 Power Storage

Power storage is the second subdivision of the EPS. They can either provide all the power for short missions (primary batteries), during eclipse or they provide back-up power for longer mission (secondary batteries).

Batteries can be both a power source and a power storage system. The following design options apply

for both uses.

Primary batteries usually are used for short-term missions, up to about one day. Sometimes they are also used for long-term mission for tasks that require small power usage like memory back-up for example. They have a high specific energy density, which makes them a good choice for short missions. The number of batteries and their corresponding weight and size required for longer mission makes them a bad candidate. The most typical battery type use silver zinc, lithium thionyl chloride, lithium sulfur dioxide, lithium monofluoride and thermal cells.

Secondary batteries are mostly used on missions which use photovoltaics as a power source. Here they provide power when the solar panels are eclipsed and at moments when power requirement peaks. To keep the secondary batteries from becoming too large, they are required to be rechargeable. Some common secondary batteries are: Nickel-Cadmium, Nickel-Hydrogen (both space qualified), Lithium-Ion and Sodium-Sulfur (both under development). The nickel-hydrogen batteries have three space-qualified design variants: individual, common and single pressure vessel.

The individual pressure vessel contains only one electrochemical cell within. Usually they are connected in series to obtain the desired voltage. The internal electrode stacks are connected in parallel. The only difference between the individual and common pressure vessel is that the common pressure vessel has two electrode stacks, connected in series. This means that there are only half as much pressure vessel and less pieces, resulting in a higher specific energy density. Finally, the single pressure vessel has multiple cells connected in series that share a common supply of hydrogen. The cell stacks are each contained in a container with its own electrolyte supply [Wertz(2006)].

Lithium-Ion batteries offer a significant advantage over nickel based ones. According to [Wertz(2006)], these types of batteries should be space qualified in the near future. At the moment, the effect of temperature on the performance is being researched. At present there are no components that are expected to be critically effected by temperature, resulting in a wide temperature range. Thus lithium-ion batteries may be a very interesting candidate for space applications in the near future [Jusef Hassoun and Scrosati(2009)].

4.3.3 Power Regulation and Control

The power regulation mainly concerns the bus regulation. The bus is the connection between power source and the different loads. It can be unregulated, quasi-regulated or fully regulated. The unregulated bus has its converters at the individual loads (see section 4.3.4). A quasi-regulated bus has a battery charge regulator and a fully regulated bus also has a battery discharge regulator. Batteries can be charged individually or in parallel. Batteries that are charged in parallel degrade faster. Because the current is not controlled, one battery could receive all the charge current. Eventually the batteries will balance out, but the battery life will be limited to about five years. To ensure a longer lifetime, they should be charged individually (for example by using a linear, charge-current-control design). A parallel charging system, however, is simpler and smaller than an individually charging system.

Because the optimum power source output and the bus input are different, a system has to be put in place to deal with this. An example of two possibilities will be given and explained for solar panels. There are two ways of doing this: with a peak-power tracker (PPT) and with direct-energy-transfer (DET). A PPT is a non-dissipative system: it exacts the exact power the satellite requires (up to the arrays peak power). Every solar panel has a peak power point, which can be seen from the panels IV-curve. So the panel produces the most power at a certain current and voltage. But when a battery is charging, it is charged at its own current and voltage. The result of this is that the battery will change the panel's current and voltage to its own, forcing the solar panel to under perform. A PPT uses a DC/DC converter to change the solar panel's output to the required battery input, thus letting the panel perform at its peak power point, increasing the efficiency. However, because the PPT is connected in series to the solar array, it uses about 4-7% of the total power.

A DET system uses a shunt regulator to shunt away the excess power from the subsystem, usually at the array, to avoid internal energy dissipation. Shunt regulators can keep the bus voltage at a predetermined voltage. These systems are extremely efficient and have a lot of advantages over a PPT system: lower mass, less parts and a higher total efficiency at End-of-Life (EOL).

4.3.4 Power Distribution

A Power Distribution System (PDS) consists of the electrical load profile, the control options and fault protection. After the load profile has been determined, the first choice to make is the type of current of the distribution system. Mostly direct current is used because spacecraft generate direct current. An AC/DC converter would need more electronics, resulting in more parts and a higher mass. But systems working with alternating current can be single phase or multiple phases [Kuphaldt()]. The main difference is that, in a single phase system all voltages from the source vary in unison, whereas the different currents of the multi-phase system reach their peak value at different times. Each mode has its advantages and disadvantages. Single phase systems are simpler and thus cheaper but when higher loads are required multi-phase system are more useful. They can help to reduce vibrations, for example.

The PDS can either be centralized or decentralized. The decentralized option requires a converter at each individual load, resulting in an unregulated bus. The centralized option regulates power to all loads from the main bus. The advantage here is that the EPS does not have to be tailor-designed.

The fault protection mainly is about isolating failed loads. If it is not isolated, a short circuit can occur. This will draw excess power and stress the cables. The isolation is usually done with fuses. The different design options here are the fuse types and location. The short circuit can also be dealt with by using cables that have extra current carrying capabilities. These come in varying types and sizes. A last option is to foresee extra power storage capabilities to cope with a short circuit. Of course, the fault protection options are not limited to the use of just one of these. In practice, the three are used simultaneously.

4.4 Communications

For the communications subsystem 5 different topics were investigated:

- Tracking
- Swarm satellites crosslink frequency
- D/L and U/L frequency
- Antenna configuration
- Communications architecture

4.4.1 Tracking

For tracking there are the following design options:

- Microcosm Autonomous Navigation System (MANS)
- GPS
- Tracking and Data Relay Satellite (TDRS)

- Satellite crosslinks
- Ground tracking

MANS uses observations of the Earth, Sun and Moon from a single sensor to provide real-time position and attitude data. These objects can be unambiguously identified with high reliability and low cost. Observations can be done with minor modifications to attitude sensors which are already on most spacecraft. The MANS flight software can also make use of data from a GPS receiver, star sensors, gyros and accelerometers to increase the accuracy. MANS can provide ground point look and sun directional information, which also works at any altitude in between LEO and GEO.

GPS is a system of navigation satellites which allows position determination with an accuracy of 50-100 m for non-military use. GPS can also be used to determine attitude by using multiple GPS antennas attached to a rigid element of the spacecraft which allows accuracies between 0.3 and 0.5 degrees. There must always be four GPS satellites in sight in order for the system to work, but which can not be guaranteed that this number of satellites is in sight continuously.

TDRS is a system of two satellites operated by NASA, which can provide tracking data coverage of 85% to 100% of most low-Earth orbits. The system collects mostly range and range-data from the TDRS satellite to the satellite being tracked. Angular information is available, but which is much less accurate than the range and range-rate data. If atmospheric drag effects on a satellite are small, TDRS can achieve 3σ accuracies of 50 m, which is considerably better than most ground-tracking systems.

Satellite crosslinks allow relative position determinations by using of cross link equipments. If absolute position determination is required, a separate tracking system is required. Which can also allow relative position determination, making the satellite crosslinks technique redundant.

Finally ground tracking allows determination of range and range rate. Angular measurements are also available at times but which are typically far less accurate. Several passes over a ground station are required for orbit determination. 3σ accuracies typically are about several kilometers for LEO.

4.4.2 Swarm Satellites Crosslink Frequency

The frequency band normally used for inter satellite communications are the V-band frequency. This band lies around 60 GHz and has no limit on the power flux density.

4.4.3 D/L and U/L Frequency

Frequency bands available for upload and download of scientific data are:

- C-Band
- X-Band
- Ku-Band
- Ka-Band
- SHF/EHF-band

Details for all frequency bands can be found in [Wertz(2006)], p. 566.

4.4.4 Antenna Configuration

The following antennas, suitable for beamwidths of less than 20 degrees, producing gains above 15dB, are considered:

- Parabolic reflector center-feed
- Parabolic reflector cassegrain
- Parabolic reflector off-set feed
- Phased array
- Lens with switched-feed array
- Parabolic reflector off-set shaped subreflector with feed array for scanning

Drawings and descriptions of these antennas can be found in [Wertz(2006)], p. 573.

4.4.5 Data Storage

Today Dynamic RAM is almost exclusively used by satellites for mass data storage because they allow very large capacities of 1000 Gbits and more. Typically, they do not have external addressing to each RAM location but operate on a block or file basis. The block may be of the order of 1000 bytes or sometimes it will correspond to one source packet. Dynamic RAM has a simple structure: only one transistor and a capacitor are required per bit, compared to six transistors in Static RAM. This allows Dynamic RAM to reach a very high density [et al.(2007)].

Since this technology has recommended itself as the best around, there is no logical reason to design or trade-off other options. For this reason it is not included in the design option tree.

4.4.6 Communications Architecture

In this subsection we will discuss the possible communications architectures and the transmission power and bandwidth required for the communication subsystem in each satellite:

- Centralized architecture
- Decentralized architecture
- Extremely decentralized architecture

In centralized architecture there is one central satellite which handles all communication between the swarm and the Earth. Which means the communication subsystem of the central satellite requires a broad bandwidth and high transmission power both for the communication between itself and the swarm and the Earth. All data can be stored, organized and compressed efficiently on this central satellite. Data can also be stored on each satellite as a backup in case there is no continuous communication.

A decentralized architecture gives all satellites the bandwidth and transmission power to communicate with the ground, but communication within the swarm is also still possible. In this architecture each satellite has to store its own data itself.

In an extremely decentralized architecture all satellites communicate independently to the ground and also communication between the swarm goes through ground stations. Also for this architecture all satellites need to store their own data.

The design option tree for communications subsystem is shown in figure A.2 on page 84.

4.5 Orbit Architecture

In this section the design options in the orbit architecture tree as seen in figures A.6, A.7 and A.8 (pp. 88-88), are described.

The orbits are divided in four categories: LEO, Medium Earth Orbit (MEO), Geosynchronous Earth Orbit (GEO) and High Earth Orbit (HEO). Some orbits like hyperbolic and parabolic trajectories are not included as they are not relevant for the mission.

After the main categories there are subdivisions, which can in turn have subdivisions as well. These subdivisions list the special orbits types that are possible, sometimes there is also a block called “other”. This is because special orbit types have special constraints, as will be detailed in later sections; whereas the “other” block is there to represent all the other possible orbits. It is not possible at this point to determine exact values as the orbit depends on the payload, the power subsystem and the communications subsystem.

All orbits are assumed to be Keplerian orbits. As such the orbit can be described as a plane located in 3D space. Therefore six elements will define the position of the satellite - the classical orbital elements. The elements are: the semimajor axis (a), the eccentricity (e), the inclination (i), the right ascension of the ascending node (Ω), the argument of perigee (ω) and finally the true anomaly (ν). As a reference for the last four terms, figure A.5 may be used.

The most important of the four Keplerian elements during this part of the design are: the semimajor axis, the eccentricity and the inclination. The remaining elements are not considered until detailed design.

The following sections will each describe one of the four main categories. They are described in the order listed in the first paragraph of this section. However, first the most common orbits are discussed in the following paragraphs.

4.5.1 Common Orbits

Some special orbits are repeated multiple times in the orbit architecture trees as shown in figures A.6 to A.8 (pp. 88-88). These common orbits are the polar orbit, the sun synchronous orbit, the sun synchronous polar orbit, the frozen orbit and the repeat orbit.

1. Polar orbit: This orbit is unique in the sense that the satellite will pass over or closely pass over both poles during a single revolution. As such the angle of incidence i is close to ± 90 degrees. This setup allows for near global coverage, and is useful for polar ice sheet research.
2. Sun Synchronous orbit: An orbit where the satellite passes over the same ground area at the same local time each revolution. At increasing altitude the inclination increases as well, so above approximately 5000 km this orbit tends to lose its usefulness [Wertz(2006)].
3. Sun Synchronous Polar orbit: A combination of the previous two items. For this orbit to keep the same local time the altitude should be as low as possible.
4. Transfer orbit: Used to transfer the payload from one orbit to another
5. Frozen orbit: An orbit where there are no long-term changes in argument of perigee and eccentricity. The eccentricity is determined based on a given semimajor axis and inclination.
6. Repeat orbit: An orbit where the satellite comes across the same point on the ground after a integral number of revolutions. A combination of a repeat orbit and a frozen orbit also a possibility.

4.5.2 Low Earth Orbit

The altitude of a satellite in LEO ranges from approximately 80 to 2000 km [nas(2008)]. The lower limit arises due to the fact of the presence of atmospheric aerodynamic drag, which reduces the velocity and places it in a different orbit. Placing a satellite in a too low orbit means many attitude corrections have to be made (to prevent de-orbit), which is undesirable. The upper limit arises from the inner Van Allen radiation belts, because at 2 to 5 km the radiation is the most intense [et al.(2007)]. Figure A.6 shows the design option tree for the LEOs.

4.5.3 Medium Earth Orbit

The altitudes for these orbits have the range from 2000 to 35700 km, which is in between the LEO and the GEO. These are the last orbits where sun synchronous orbits are typically used. This is because of the increase in inclination angle, as mentioned in 4.5.1. Figure A.6 shows the design option tree for the MEO.

4.5.4 Geosynchronous Orbit

Figure A.7 shows the design options for the geosynchronous orbits. This type of orbit is characterized by the satellite completing its orbit in exactly one day. This is not to be confused with a Geostationary orbit, which is a special case of geosynchronous orbit where the eccentricity is 0 and the altitude 35786 km. For the reason mentioned in section 4.5.1 sun synchronous orbits are not used at this altitude. GEO has two special types of orbits, the supersynchronous and the subsynchronous orbits. The apogee of supersynchronous orbits is located located at significantly higher altitude than that of a GEO orbit, and both orbits are placed under the GEO category due to the relation with the GEO. The supersynchronous orbit is also known as a graveyard orbit (or other similar synonyms). As the last name suggests this orbit is used to store dead satellites. Recently another application is used, namely to send the satellite to supersynchronous orbit and change the inclination here and then place the satellite in GEO. This is a more efficient maneuver than changing the inclination at GEO [jer()]. Sometimes a payload is placed in a subsynchronous orbit by the rocket after which the payload has to use its own propulsion to get into GEO.

4.5.5 High Earth Orbit

Continuing the trend indicated in previous sections these orbits are located above the GEO orbits. Sun synchronous orbits are usually not used for this orbit as well. Figure A.8 shows the design options for the HEO, meanwhile the HELLO discussed in the next subsection is part of this figure.

4.5.5.1 Highly Elliptical Orbit

The Highly Elliptical Orbit (HEllo) is defined as a subcategory of the HEO, because a satellite in one of these orbits spends most of its time at its apogee. Other than their high eccentricity, the other orbital elements can take any value. Some special orbits are the Molniya orbit and the Tundra orbit. The Molniya orbit has a period of half a sidereal day and the Tundra orbit has a period of a whole sidereal day. For both orbits the inclination often used is 63.4 degrees, this inclination ensures there is no shift or perigee along the orbit. When designing an orbit with a different incidence angle, the oblates of the Earth has to be accounted for to negate this effect.

Chapter 5

N^2 Chart

The N^2 chart shows the interfaces between the different functions of the system. The chart can be found in figure 5.1 on page 34. The functions are in the dark grey boxes, while the interactions are shown by the dotted boxes and move clockwise. The system is split up in the emitter satellite, a receiver satellite and the ground segment, denoted by the large bold boxes. Outside of these boxes the outside world is, composed of e.g. the Sun and customers. The starred interactions depend on the level of communication centralisation.

The basic workings of the system is that the laser sends down a laser pulse, which is reflected by the Earth and received by receivers in the receiver satellites and the main satellite. Combined with the time from the navigation subsystem the photon counts are stored in the data storage. The communication subsystem sends down the data to be received by the ground station. Before a laser pulse can be sent or received the satellites need to be pointed by the Attitude Determination and Control Subsystem and the pointing mechanism. The current attitude is determined by the attitude determination subsystem. The EPS subsystem provides power to all other subsystems.

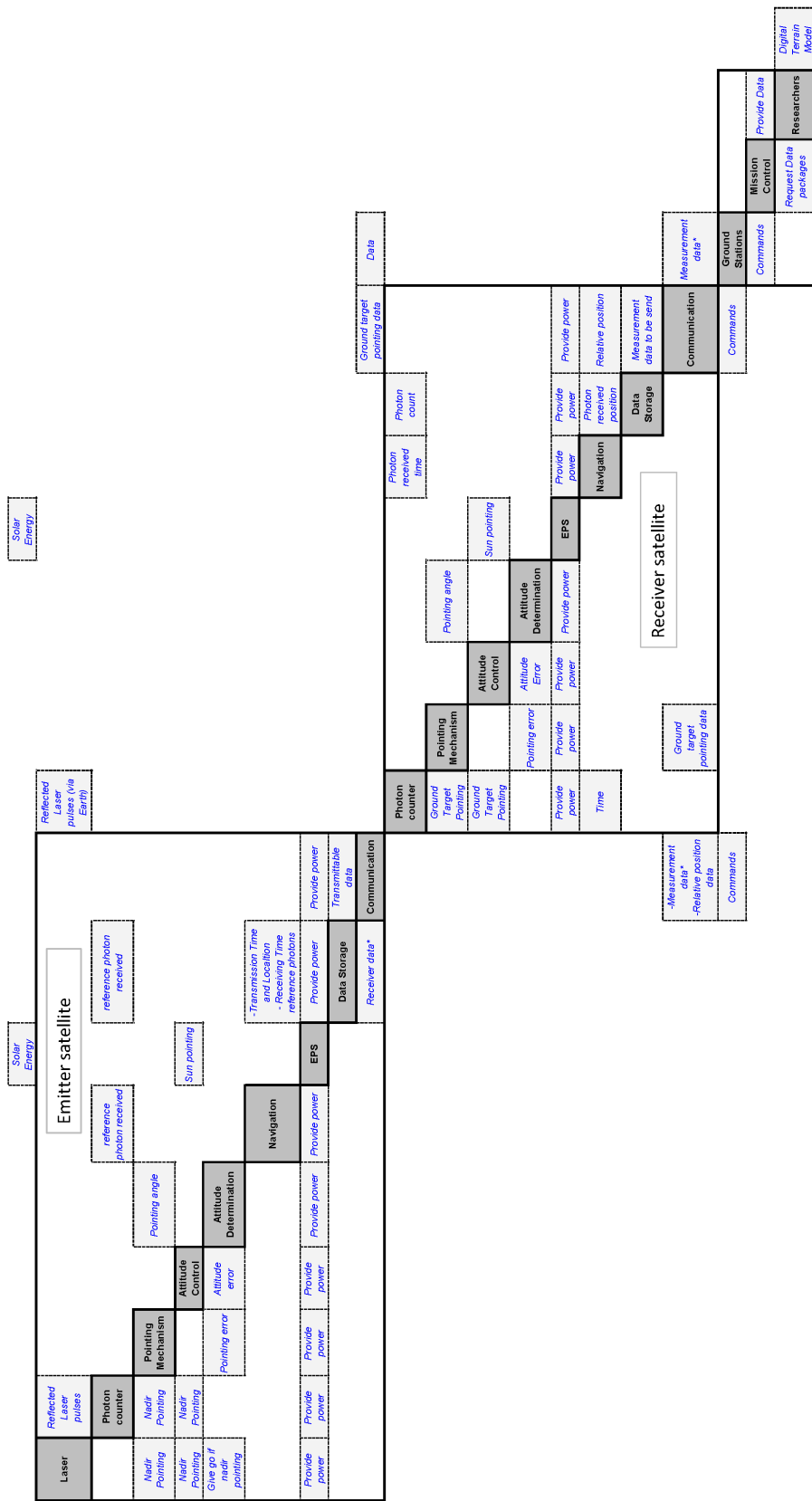


Figure 5.1: N^2 chart of the Laser Swarm mission

Chapter 6

Tradeoff

6.1 AODCS

The AODCS is used for determining and controlling the attitude and orbit of the satellites. In this section first the ADCS design option tree is pruned in section 6.1.1. The subsystem can be split up into four smaller parts; attitude determination (discussed in section 6.1.2), attitude control (section 6.1.3), orbit determination (section 6.1.4) and orbit control (section 6.1.5).

6.1.1 Pruning the ADCS design option tree

The gravity-gradient stabilisation and passive magnetic options are eliminated because they provide insufficient accuracy and do not allow pointing to an any target other than the mass or magnetic centre of the Earth. The spin stabilisation option is pruned because the satellite needs to be able to make measurements continuously. Double gimbal CMGs are also not a viable option, because they are too complex and heavy compared to the other systems. For the attitude determination the initial measurements and magnetometers options are eliminated because of their deteriorating accuracy over time. The pruned design option tree can be found in figure 6.1.1 on page 36.

6.1.2 ADS

The ADS consists for a collection of sensors to determine the roll, pitch and yaw angles and rates of the satellites. The design options left after the pruning in section 6.1.1 are GPS, Sun sensors, Star trackers and Horizon sensors.

GPS uses one receiver and multiple antennas, by measuring the relative positions of the different antennas the attitude of the satellite can be calculated. Most modern LEO satellites are already carrying a GPS receiver, but a long baseline between antennas is needed for a high accuracy. Sun sensors use the angle towards the Sun for making their attitude measurements. The technology behind Sun sensors has been around for a long time and several micro Sun sensors are available on the market, the Field Of View (FOV) of a typical Sun sensor is about 120° . Star trackers look at a portion of the sky and uses familiar stars to determine the attitude of the satellites the system can work autonomously, but the optics required are usually quite bulky. Horizon sensors use the limb of the Earth, i.e. the transition of the solid Earth to cold space, to determine the attitude of the satellite. The system only works on the roll and pitch axis.

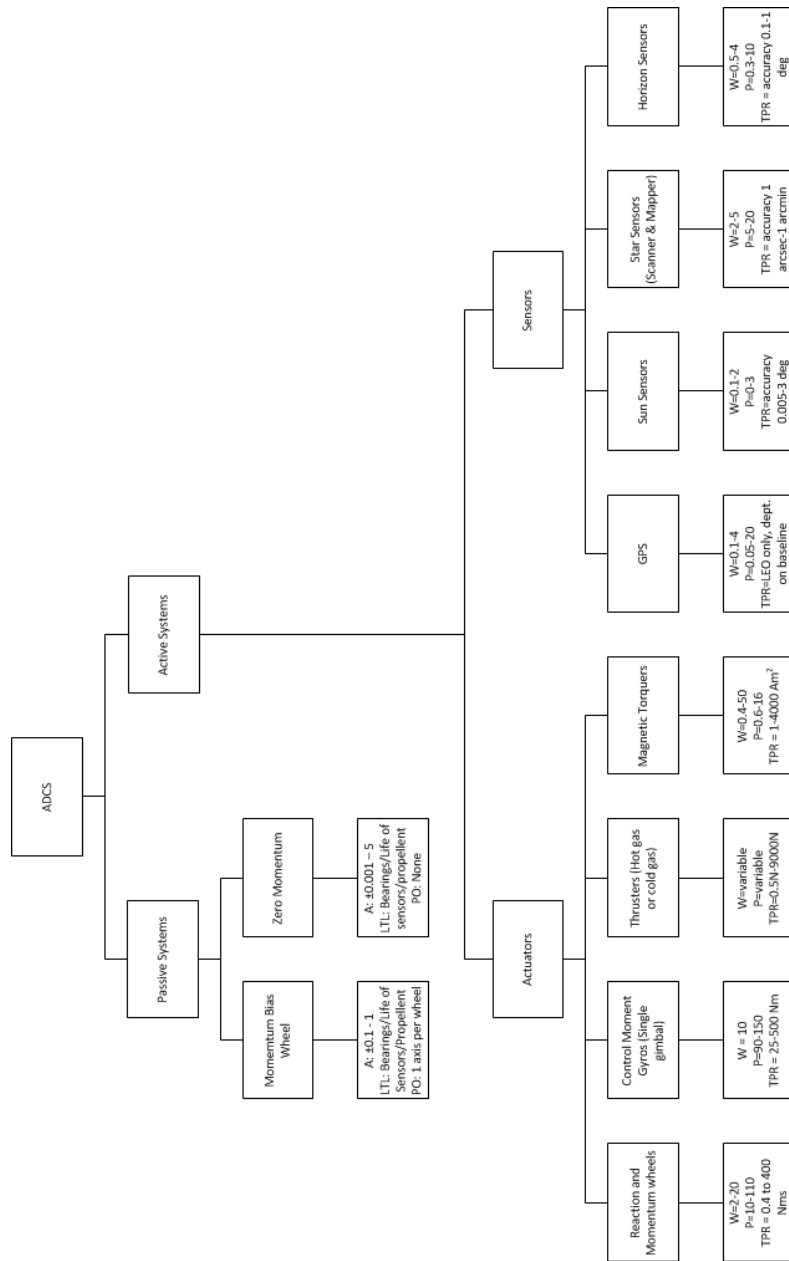


Figure 6.1: Pruned design option tree for the ADCS

Another option is to use a complete Components Of The Shelf (COTS) ADCS system like the one from Maryland Aerospace Inc. [mar(2010)]. Their IMI-100 ADACS contains everything needed for complete ADCS with an accuracy of 1° . For attitude determination it uses 3 magnetometers, by adding additional sensors e.g. a ring laser gyro and a miniaturised star sensor the accuracy can reach 1-3 arcsec [imi(2010)].

6.1.2.1 Trade method

The trade-off is made by comparing three concepts for attitude determination. The first concept uses the Maryland Aerospace IMI-100, the second concept uses Sun sensors by day and a star tracker by night, the third concept uses GPS for attitude determination (see figure 6.2 on page 37). Scores are awarded to the performance on a number of criteria. The best weighted overall score wins the trade-off.

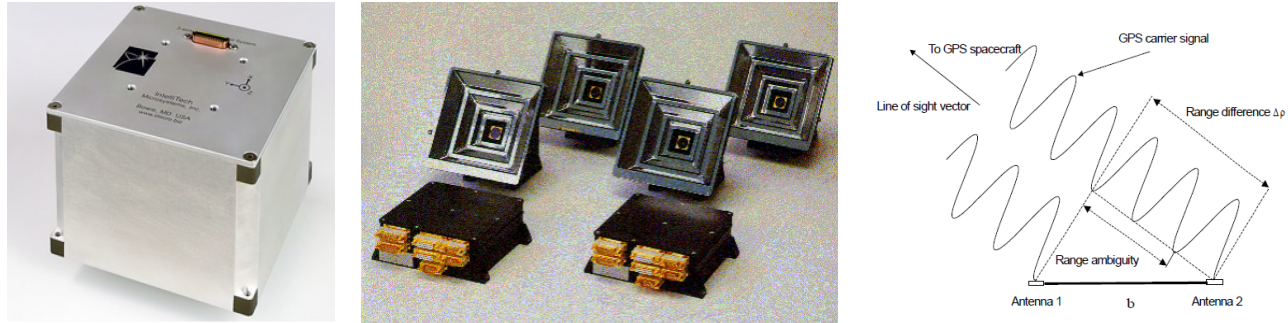


Figure 6.2: The three concepts for the design of the ADS. From left to right: Concept 1 uses the IMI-100 system from Maryland Inc. [imi(2010)], Concept 2 uses Sun sensors and star trackers [Chu(2009b)], Concept 3 uses GPS for attitude determination [Chu(2009b)]

6.1.2.2 Trade criteria

The concepts for ADS are traded in terms of attitude determination accuracy, purchasing price, power required, size and the amount of additional development required for implementing the concept.

6.1.2.3 Weight factors

The accuracy of the ADS is the main driver for the choice of the system so it is given a weight factor of 9. Because the volume and power for satellites are limited they are also important with a given weight factor of 7. Although the total cost of the system is relevant, if a better performance can be achieved at a higher cost can be acceptable, weight factor 3. If a lot of work still is required to implement the system in the satellite the mission can be delayed, development gets a weight factor of 5.

6.1.2.4 Trade-off

The results of the trade-off can be found in table 6.1 on page 38. The attitude determination accuracy of concept 1 and concept 3 are both around 1° for micro satellites, the performance of concept 2 is much better with an estimated accuracy of 0.01° . In the Innovative Solutions In Space (ISIS)' webshop [cub(2010)] concept 1 costs about EUR 45000, the development costs of concept 2 are estimated to be about EUR 15000, a space qualified GPS receiver will cost about EUR 25000 [spa(2010)]. The first concept will use about 1.5 W

on attitude determination, concept 2 uses a power of about 2 W, a GPS receiver takes about 1 W. The size of the IMI-100 is 100x100x79 mm, the Sun sensors can be as small as 30x30x14.5 mm [tno(2010)] and ISIS is currently developing a star sensor with a size of 50x50x100 mm, a space qualified GPS receiver is about 100x70x25 mm. The IMI-100 system is completely developed and can just be build in, for a system with Sun sensors and a star tracker still some design needs to be done in for example locations on the satellite, for a GPS system the antenna positions need to be chosen for optimal accuracy.

Criteria	Weight Factor	Concept 1	Concept 2	Concept 3
Accuracy	9	4	8	4
Size	7	2	6	4
Power	7	6	5	7
Price	3	3	5	4
Development	5	8	4	5
Weighted total		141	184	150

Table 6.1: Trade-off graph for the attitude determination system. The weight factor signifies the importance of the criterion. Grades are given on a scale of 1 to 10, 1 being the worst, 10 the best

After the trade-off the best solution for the ADS is to use Sun sensors and a star tracker. Although the most design work is needed, it is able to give the best accuracy for the lowest price.

6.1.3 ACS

The satellites in the constellation all need to point accurately to the Earth, a passive ACS will therefore not be sufficient for the control of the attitude of the satellites. For active attitude control actuators are needed. After the pruning, four options remain for the attitude control. Reaction and momentum wheels, CMGs, Thrusters and Magnetic torquers.

Reaction wheels are basically torque rotors with a high-inertia wheel attached to it; they can provide single axis control to a spacecraft. Momentum wheels are reaction wheels with a nominal spin rate, adding gyroscopic stiffness to two axis of the spacecraft. Changing the spin rate gives control over the third axis. CMGs consist of a wheel with a constant rotation speed and one or two gimbals to rotate the wheel, determining the direction of the momentum. This way very accurate attitude manoeuvres can be made, but complex control algorithms are needed. Usually the weight and cost of CMGs are quite high. Thrusters expel mass to induce velocity or a momentum to the satellite. The velocity can be used for keeping the orbit and will be discussed in section 6.1.5. To be able to induce a momentum to a satellite multiple thrusters with an offset to the center of mass of the satellite. Thrusters are split up into hot gas types, which require a chemical reaction of the propellant, and cold gas types that rely on latent heat and phase change in the propellant. The power which can be generated by thrusters is high, but the fuel required will limit the lifetime of the satellite. Magnetic torquers are magnetic coils or electromagnets generating dipole moments on the satellite. They can be used for both manoeuvring and desaturation of e.g. reaction wheels. Because they rely on the magnetic field of the Earth they are less useful in higher orbits.

The IMI-100 ADACS contains three miniature reaction wheels and three magnetic coils for desaturating the wheels. For a 2 kg, 2U cubesat it can provide a slew rate of $8.4^\circ/s$ [imi(2010)].

6.1.3.1 Trade method

In the trade-off three concepts for attitude control are compared to each other on a number of criteria. The first concept is using thrusters for attitude control, the second option is using reaction wheels with magneto torquers for desaturation, the third option is using Maryland Aerospace's IMI-100. The concept with the highest weighted score wins the trade-off. The options are shown in figure 6.3 on page 39.

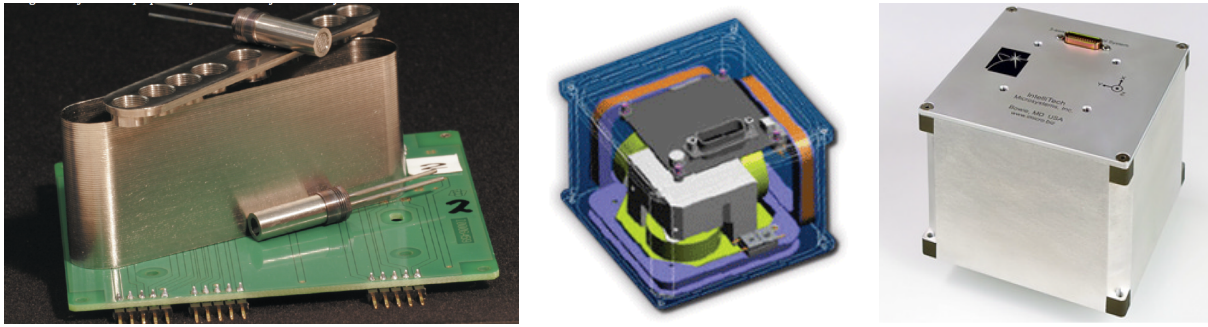


Figure 6.3: The three concepts for the design of the ADS. From left to right: Concept 1 uses thrusters [tno(2010)], Concept 2 uses reaction wheels and magneto torquers [cub(2010)], Concept 3 uses IMI-100 system from Maryland Inc. [imi(2010)].

6.1.3.2 Trade criteria

The concepts for ACS are traded in terms of the rate the concepts are able to adjust the attitude, attitude control accuracy, purchasing price, power required, size and the amount of additional development required for implementing the concept.

6.1.3.3 Weight factors

A high rate in which the satellite can be controlled is convenient, but not driving, weight factor 5. Since attitude control will be used for the pointing of the instrument the accuracy is very important for the choice so it is given a weight factor of 8. Because the volume and power for satellites are limited they are also important with a given weight factor of 7. Although the total cost of the system is relevant, if a better performance can be achieved at a higher cost can be acceptable, weight factor 3. If a lot of work still is required to implement the system in the satellite the mission can be delayed, development gets a weight factor of 5.

6.1.3.4 Trade-off

The results of the trade-off can be found in table 6.2 on page 40. Thrusters are able to make attitude adjustments with a high rate, both concept 2 and concept 3 use reaction wheels for attitude adjustments, so they will have comparable performance. Attitude adjustments done by thrusters are really coarse, so they have a low accuracy. With a custom designed system the accuracy of concept 2 the performance will be better than a COTS system. For the use of thrusters also other components are required like e.g. fuel tanks, fuel lines and pumps. Reaction wheels and magneto torquers all take up space in the satellite, but can be made relatively small. The IMI-100 system is encased in a separate box, so it will take more room. For its power the thruster system needs fuel, which all has to be taken along for the entire mission. The reaction

wheels in concept 2 and 3 require only power when the motors are running, as do the magneto torquers. Combined with the fuel, tanks and other extra material the thruster system needs to bring it will be a very expensive option. Especially for the small kind of satellites being considered for the mission. Not many micro propulsion systems are yet on the market. Developing the system with reaction wheels can be a much cheaper option. Buying the system as COTS will save working costs, but in the end be a little more expensive than a in house development. Thruster systems for small satellites are rare, so a lot of development is still required. Some research has already been done on an active ACS for the student satellite Delfi-n3Xt [del(2010)], this research can be extended for the Laser Swarm mission. The IMI-100 system is already build and just has to be integrated.

Criteria	Weight Factor	Concept 1	Concept 2	Concept 3
Rate	5	8	6	6
Accuracy	8	4	8	7
Size	7	2	6	5
Power	7	3	6	6
Price	3	2	8	7
Development	5	4	6	8
Weighted total		133	232	224

Table 6.2: Trade-off graph for the attitude control system. The weight factor signifies the importance of the criterion. Grades are given on a scale of 1 to 10, 1 being the worst, 10 the best

After the trade-off the best solution for the ACS is to use reaction wheels and magneto torquers. Although the scores are close to concept 3, the more dedicated design improves the performance of the COTS system.

6.1.4 ODS

The determination of the orbit will be discussed in section ??.

6.1.5 OCS

The orbit considered for the satellites is very low (for satellite orbits), therefore the drag of the atmosphere has to be taken into account. The equation for acceleration due to drag on the satellite is

$$a_D = -\frac{1}{2}\rho(C_D A/m) V^2 \quad (6.1)$$

where ρ is the density of the atmosphere, C_D is the drag coefficient for the satellite (typically between 2-4), m is the mass of the satellite and V is the satellite's velocity with respect to the atmosphere. The orbital velocity of a circular orbit is

$$V_c = \sqrt{\frac{\mu}{a}} \quad (6.2)$$

where μ is the standard gravitational parameter of the Earth, $398,600.4 \text{ km}^3/\text{s}^2$. For circular orbits the equation for ΔV per revolution can be simplified to

$$\Delta V_{rev} = \pi (C_D A/m) \rho a V \quad (6.3)$$

where a is the orbit semi-major axis [Wertz(2006)].

Station keeping for an orbit between 400 and 500 kilometers requires a maximum ΔV of 100 m/s or on average 25 m/s [Zandbergen(2009)].

The ΔV a propulsion system can produce is quantified by Tsiolkovsky's rocket equation

$$\Delta V = gI_{sp} \ln \left(\frac{m_0}{m_0 - m_p} \right) \equiv gI_{sp} \ln \left(\frac{m_0}{m_f} \right) \equiv gI_{sp} \ln (R) \quad (6.4)$$

where g is the Earth's gravity constant, I_{sp} is the specific impulse of the engine, m_0 is the starting mass, m_p is the mass of the fuel used, $m_f = m_0 - m_p$ and the mass ratio R is $m_0 / (m_0 - m_p)$. From this the ratio of fuel to the total mass can be derived to be

$$\frac{m_p}{m_0} = 1 - e^{-(\Delta V / I_{sp} g)} \quad (6.5)$$

Depending on the altitude of the satellite orbit a thruster for attitude keeping can be selected in a later stage of the design.

6.2 Trade-off for the electrical power system

This section will be about the trade-off for the electrical power system (EPS). First the design option structure will be pruned with the obvious non-candidates eliminated so only the viable options remain for the trade-off. When this is done, the preparation of the trade-off can be done. First the method and rationale will be discussed. Afterwards the different criteria of the trade-off will be discussed. The important characteristics of the candidates are going to be determined and these will be the base on which the trade-off will be performed. In section 6.2.2.3 the importance of each criteria will be determined. The last section will give a summary of the whole trade-off with the corresponding results.

6.2.1 Pruning of the EPS design option structure

In the next section the design option tree for the EPS will be pruned. The design option trees for the power source, storage, distribution and regulation and control will be dealt with individually in sections 6.2.1.1, 6.2.1.2 and 6.2.1.3 respectively.

6.2.1.1 Power Source

Fuel cells have a high specific energy density but were not taken into account as a feasible power source because the amount of reactant they would have to bring for long term mission is too large for microsatellites. Primary batteries were equally unfeasible because of their limited lifetime, which is in the order of minutes to months. Radio isotopes and nuclear fission reactors were discarded because of their high cost and low specific power, as were thermionic and thermoelectric conversion for static power sources. This leaves photovoltaics and concentrated solar radiation together with an engine in a thermodynamic power cycle.

The pruned design option tree for the powersource can be seen in figure 6.4

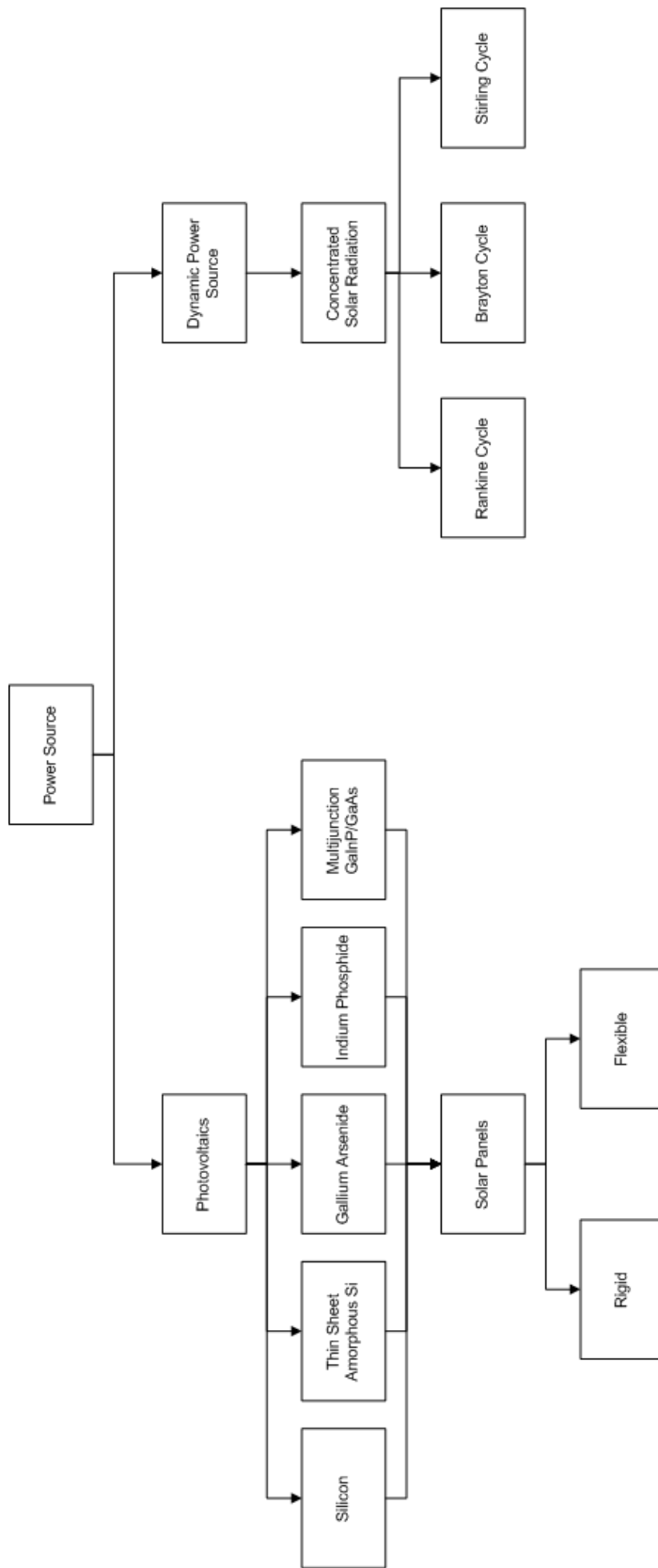


Figure 6.4: The pruned design option tree for the power source

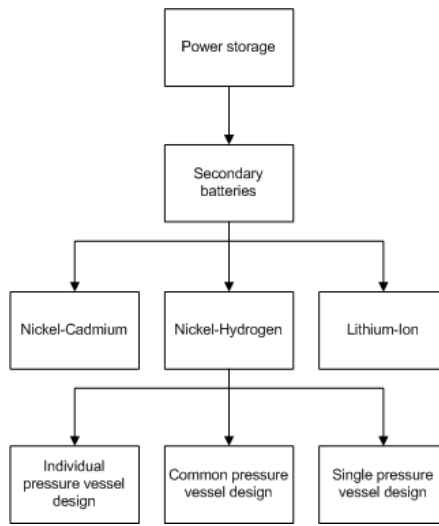


Figure 6.5: The pruned design option tree for the power storage

6.2.1.2 Power Storage

The only obvious candidate for power storage was secondary batteries because, as mentioned before, the lifetime of primary batteries is too short. Of the most common secondary batteries, sodium-sulfur batteries are not an option for us because their operating temperature at 350 degrees Celsius is too high.

The pruned design option tree for the powersource can be seen in figure 6.5

6.2.1.3 Power Distribution, Regulation and Control

For the power distribution, regulation and control there were no obvious non-candidates. Because the power distribution, regulation and control depend on the type of power source, which depends on the payload power requirements, pruning will be done later on after these subsystems have been chosen — this is done in the tradeoff.

The design option tree for the powersource can be seen in figure 6.6

6.2.2 Trade method rationale and organization

In this section the question of how the trade-off is done will be answered. First some additional information of the two options for the trade-off are given and afterwards the method and organization itself will be discussed. After the pruning of the design option structure the only candidates left were photovoltaics and concentrated solar radiation together with an engine in a thermodynamic power cycle. After some further research the option of using concentrated solar radiation was also discarded. Almost no information was found about that kind of powersource for use in space. Therefore it was decided to abandon this kind of power source because without any data or information it will not be possible to determine if that option is feasible. So that leaves only photovoltaics. Solar cells come in a lot of different types. The most common are crystalline solar cells, multijunction cells and thin film solar cells but with lower efficiency. Soon it was clear that crystalline would not be a good option. Multijunction cells have a higher efficiency while thin film cells have a lower mass and production cost. Because the efficiency, mass and production cost are the most important characteristics and

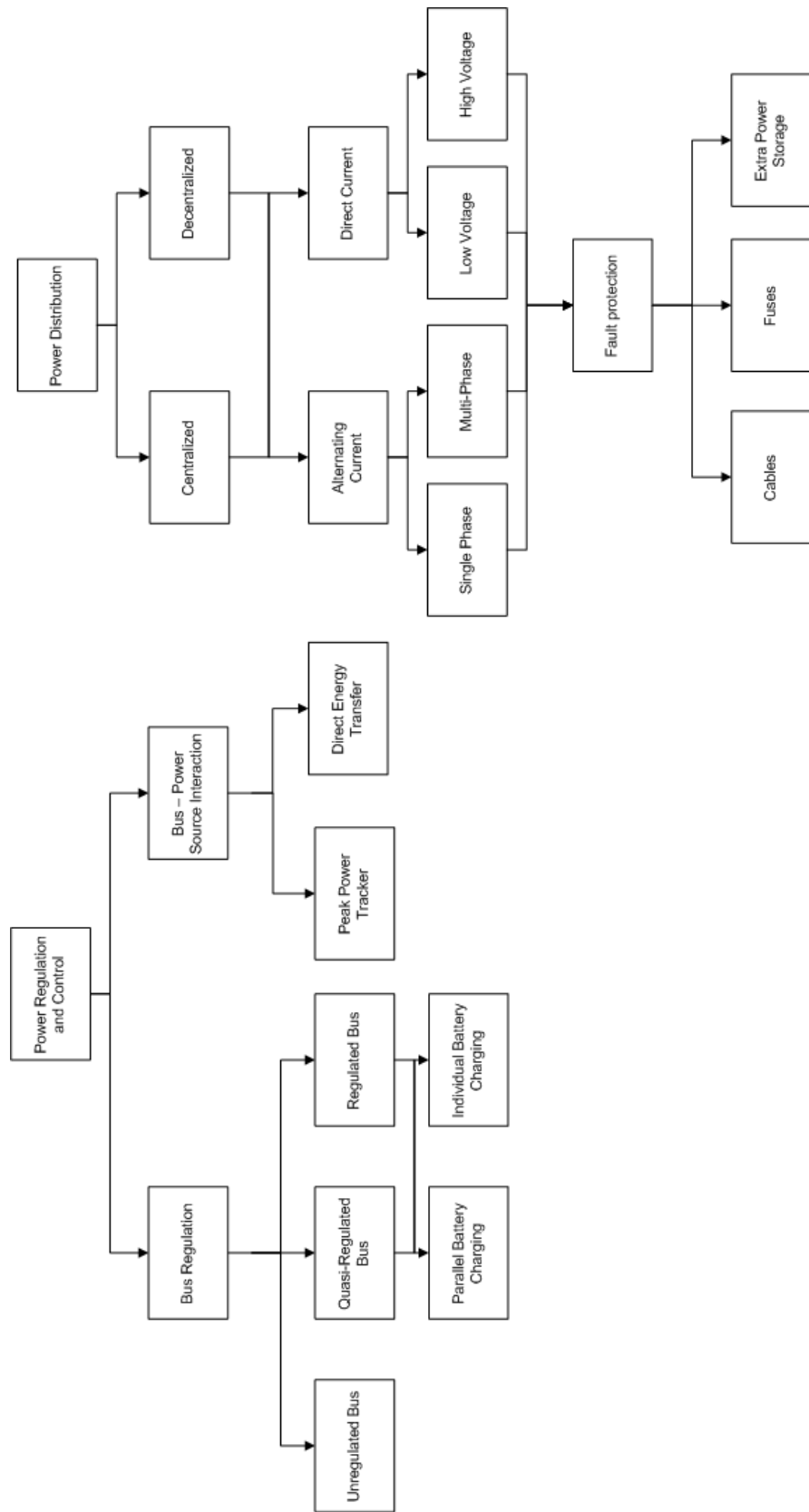


Figure 6.6: The design option tree for the power distribution and regulation and control

crystalline solar cells do not excell in any of these areas (compared to multijunction and thin film cells), they will not be considered as an option for the power source.

6.2.2.1 Multijunction solar cells

A solar cell converts solar energy to electrical energy. When a photon hits the surface of a solar cell it is either reflected or transmitted. If it is transmitted the energy it contains will excite an electron from the valence band to the conduction band. In the conduction band they have a higher energy than in the valence band, which allows them to move around. This happens in a so called pn-junction. Single crystalline solar cells have only one pn-junction whereas multijunction ones have more than one. Each pn-junction has a certain bandgap, depending on the material of the junction. The bandgap is the difference between the valence band and the conduction band.

This means that if a certain material has a bandgap of one electronvolt, one electronvolt of power needs to be given to an electron for it to be able to go from the valance band to the conduction band. From this it follows that one pn-junction will only be able to use part of the solar spectrum. Multijunction cells use several pn-junctions connected in series so that a larger part of the solar spectrum can be used.

Figure 6.7 gives a schematic representation of a triple-junction solar cell [SPECTROLAB()]. The (metallic contacts) in aluminium are low resistivity electrodes that transfer the current from the solar panel to the power grid. They are disposed on the two sides of the structure but mainly on the backwards face so that the shadowing on the lightning surface is reduced.

The anti-reflective coatings are primarily used to increase the transmission of the photons and correspondingly decrease the reflectance at the wavelengths that will be used.

Tunnel junctions provide a low electrical resistance and optically low-loss connection between two subcells. Without them, the p-doped region of the top cell would be directly connected with the n-doped region of the middle cell. Hence, a pn junction with opposite direction to the others would appear between the top cell and the middle cell. Consequently, the photovoltage will be lower. Tunnel junctions decrease this negative effect.

In figure 6.7, the three materials for the pn-junctions that were used are Gallium-Indium-Diphosphor, Gallium-Arsenide and Germanium. These three pn-junctions cover a larger part of the solar spectrum than single junction solar cells, making them more efficient.

Figure 6.8 [N.V.Yastrebova(2007)] shows the range of wavelengths that each junction of a triple-junction cell absorbs. From this picture it is clear that multiple pn-junctions cover a far larger part of the solar spectrum than one single pn-junction.

6.2.2.2 Thin film solar cells

Thin film solar cells are created by depositing one or more thin layers of photovoltaic material on a substrate. The thickness range of such a layer is wide and varies from a few nanometers to tens of micrometers. An example of a thin film solar cell shown in figure 6.9. Here the CIGS cell is shown. Glass is commonly used as a substrate. A molybdenum layer is deposited which serves as the back contact and to reflect most unabsorbed light back into the absorber. The absorberlayer is a p-type layer. The most efficient absorber is a so called CIGS absorber. It is a direct bandgap semiconductor with the highest absorptance coefficient of all solar cells. CIGS stands for Copper-Indium-Gallium-Selenide and these are the materials of the four thin layers of which it consists. A thin n-type buffer layer is added on top of the absorber. The buffer is overlaid with a thin, intrinsic Zinc-Oxide layer which is capped by a thicker, Aluminum doped Zinc-Oxide layer. Despite increasing the series resistance, the Zinc-Oxide layer is beneficial to cell performance. The

Aluminum doped Zinc-Oxide serves as a transparent conducting oxide to collect and move electrons out of the cell while absorbing as little light as possible [?].

6.2.2.3 Trade off method and rationale

Now that the two candidates are known, the preparation of the trade-off can begin. Thin film CIGS cells and triple-junction cells will be compared with each other with respect to certain criteria (i.e. cost, mass,...). For every criterium each candidate will receive points on a scale from one to ten, with ten being the highest. Each criterium will get a weight factor, depending on how important it is. To determine which solar cell type is the best, their points for each criterium will be multiplied with that criterium's weight factor. All these results will be added and the candidate with the highest total of points will be the best candidate for the mission. The first thing to do is to determine which criteria will be used. Efficiency, mass and cost are the three most important characteristics for the solar cells. They are also the ones that can deviate the most between different types of solar cells. Furthermore also the packing factor, degradation, solar cell height and resistance to vibrational noise during launch are trade-off criteria.

The three most important characteristics, mass, cost and efficiency, are all given a weight factor of ten. The degradation of the cells is also an important criterium. A large degradation factor will increase the solar array area dramatically, especially for missions lasting a couple of years. Therefore its weight factor will be eight. The height of the cells influences the space each satellite needs when being launched. It could mean the difference of having an extra satellite per launcher, so it also is important. It received a 7 as weight factor. When considering a solar panel, not the whole panel is filled with solar cells. Part of it is taken up by wiring, the metal contacts of the cells, the loss in area because of the shape of the cells,... All these factors are bundled in the packing factor. The higher the packing factor, the less solar array area is needed. Its weight is 7. During take-off, the launcher and its payload experience large vibrational loads. The solar panels of the satellites need to be able to resist these loads. If they are affected too much by it some cells might be damaged, resulting in less power generation. The weight factor in this case is five. This is on the low side, because these vibrational loads will not be really destructive.

6.2.3 Trade-off summary

In this section the summary of the trade-off process and the results will be discussed. For all the trade-off criteria, except for the resistance to vibrational loads, the marks each option receives are based on hard numbers. The candidate with the best characteristics will receive a ten and the other candidates marks are a fraction of that ten, based on the actual data. For example, if option 1 has a cost of 100 euros per watt, and option 2 costs 250 euros per watt, example 1 will receive a 10 for the criteria cost and example 2 will receive a four.

Table ?? lists the marks both candidates received and also their totals. From this it is obvious that the thin film CIGS is the better candidate for our mission.

The chosen thin film CIGS solar cells were ones developed by Dutchspace. They are some of the best available and have been proven in flight with the Delfi-C3 satellite. For the triple-junction cells those developed by AzurSpace were chosen. They are also one of the most efficient multijunction cells currently on the market and have been proven in flight. The data gathered for use of the exact numbers was taken from those two sources.

The efficiency of the CIGS cells is about 12% and that of the triple-junction cells is 28%. This gives scores of ten and four respectively. The mass of the cells are 240g/m² and 850g/m², resulting in a ten and a three for the thin film CIGS and the multijunction respectively. Degradation is low for both options, but the thin film CIGS has almost no open current and open voltage degradation, giving it a ten and the

	Weight Factor	Candidates	
		Thin film CIGS	Triple-junction
Efficiency	10	4	10
Mass	10	10	3
Cost	10	10	4
Degradation	8	10	9
Packing Factor	7	8	8.5
Resistance to vibrational loads	5	8	6
Cell Height	7	10	2
Total		486	345.5

Table 6.3: Trade-off table for the power source

multiplication a nine. Average values of the packing factor found in the literature were used for the trade-off. The found values were 80% and 85%, resulting in grades of eight and eight and a half. The height of the thin film CIGS cells is about $20\mu m$ giving it a ten. The triple-junction cells have a thickness of about $150\mu m$, giving it a two. The grading of the resistance to vibrational loads was not done by comparing values because there are none available. It is known that stiffer panels have less resistance to vibrational loads than flexible panels, giving the thin film CIGS an advantage. This results in an eight for that type of cells and a six for the multiplication cells. The data in the above paragraph was taken from [?], [?], [?], [SPECTROLAB()], [cub(2010)] and [?].

For the power storage in the form of secondary batteries no real trade-off was needed. Nickel-Hydrogen batteries have been used extensively over the past years, but recently lithium-ion batteries have been tested for space application. Their specific energy can be up to three times as high as Nickel-Hydrogen batteries. It has been proven that, when kept within a certain temperature range, they have the same performance in space as on Earth. This is why our team has opted for these Lithium-Ion batteries as power storage [?].

6.3 Orbit Altitude

During the design of the orbit, very careful attention has to be given to the choice of the mission altitude for the entire formation. This parameter is vital for the lifetime requirement.

Initially it was apparent that the choice of the emitting payload would give a hard altitude constraint, however as described in section (ADD REF TO OPTICAL EMITTING PAYLOAD TRADEOFF HERE), with the use of complex optical instruments it was possible to open a wider range of altitudes for selection. The governing properties of the orbit for altitude selection have now become the orbit perturbations.

This section details the considerations in regards to these properties. A separate radiation exposure analysis is also done. Finally a suitable altitude is chosen based on this analysis.

6.3.1 Earth Oblateness

ADD J2 PARAGRAPH

6.3.2 Perturbations due to Other Celestial Bodies

ADD MOON PARAGRAPH HERE

6.3.3 Solar Radiation Pressure

All orbiting bodies are affected by solar radiation pressure. The acceleration due to this phenomenon can potentially affect stationkeeping of the swarm if all satellites have different cross-sectional areas normal to the sun. This perturbation is not directly related to orbit altitude, however it is an important step in orbit analysis. In figure 6.3.3 on page 55, the relationship between the acceleration and the normal area to the sun for different satellite masses is shown. Similarly, a graph relating the mass to the acceleration for different cross-sectional areas is shown in figure 6.3.3 on page 56.

These figures present design boundary overviews and a general feeling of behavior due to solar radiation pressure is shown. The inverse relationship is obvious. In order to minimize this perturbation it is required to have high mass while retaining the smallest possible area normal to the sun.

What is important to note is that if the ratio of area to mass could be maintained constant between the emitting and the receiving satellites, then they would experience the same perturbation, which is a favorable condition. Acceleration with respect to this area/mass ratio can be seen in figure 6.3.3 on page 57.

	Total Mass	Max. Area
Emitter	250	10
Receiver	50	2

Table 6.4: Mass and area estimates(REVISE)

Based on preliminary mass and area estimates shown in table 6.4 on page 48, it is estimated that the both the emitter and the receiver platforms will experience a deceleration in the order between 10^{-9} and 10^{-10} (CHECK THIS!!). While these values might not seem significant at first, especially relative to atmospheric drag (see section 6.3.4), they will become relevant for stationkeeping as explained earlier.

6.3.4 Atmospheric Drag

Atmospheric drag is by far the most relevant perturbation for LEO satellites. It directly relates to mass as it influences the amount of fuel required to maintain the orbit, where as the mass influences the rate at which the orbit decays. Altitude selection relies heavily on estimation and analysis of drag data as for longer mission times, higher altitudes are preferred, while optical instruments prefer lower altitudes for increased accuracy.

The drag that the satellite experiences due to atmospheric density is described by the following formula:

$$D = -\frac{1}{2}C_D \rho V^2 A \quad (6.6)$$

It follows that orbital parameter changes (semi-major axis, period and velocity respectively) per orbit are calculated using the following equations (assuming negligible eccentricity):

$$\Delta a = -2\pi \left(C_D \frac{A}{m} \right) \rho a^2 \quad (6.7)$$

$$\Delta P = -6\pi \left(C_D \frac{A}{m} \right) \rho \frac{a^2}{V} \quad (6.8)$$

$$\Delta V = \pi \left(C_D \frac{A}{m} \right) \rho a V \quad (6.9)$$

The fundamental problem with accurately predicting effects due to atmospheric drag is twofold: firstly it is very hard to predict the satellite's ballistic coefficient:

$$\frac{m}{AC_D} \quad (6.10)$$

Even with a well known mass to area ratio, the coefficient of drag can be highly variable, highly dependent on the shape of the satellite and its orientation with respect to the velocity vector. Throughout the following analysis a C_D of 4 has been used as a worst-case scenario. This value is representative of a flat plate traveling with its normal vector pointing in the direction of velocity. In reality this drag coefficient changes. The cross-sectional area normal to the velocity vector can also vary for the swarm satellites if the whole platform is reoriented for instrument pointing. The whole ballistic coefficient ranges from about 25 kgm^{-2} to 100 kgm^{-2} . The satellites being considered in this document are at the lower range of these values.

The second reason drag calculations are so unreliable, is because air density at any altitude is highly variable. Raising air density is primarily connected with solar activity. As solar activity increases every 11 years (see figure 6.3.4 for recorded and predicted solar activity), the atmosphere heats up. Contrary to conventional gas laws that would dictate a fall in density as the gas expands, the atmosphere simply rises, increasing density at higher altitudes.

The density difference during maxima and minima for different altitudes is shown in figure 6.3.4. Depending on the altitude, the density could vary for up to a whole order of magnitude between the minimum and maximum.

Orbit decay periods for the emitter and receiver satellites are shown in figures 6.3.4 and 6.3.4 respectively. The Orbit decay is calculated using equations 6.7 - 6.9. Orbit maintenance is not taken into account. The time range considered is a 5 year mission lifetime. The basis for the receiving satellite sizing was taken to be the frontal area of a Delfi-C3 satellite ($10 \times 10 \text{ cm}$) plus an initial estimated solar array area of 0.2 m^2 . The mass of the said satellite was the same as in table 6.4 on page 48. The emitter satellite is sized to be about 0.1 m^2 frontal area and an additional $6 \text{ m} \times 2$ of solar array area. The mass is again taken from table 6.4 (REVISE!).

From the analysis of the orbit decay it is strikingly obvious how important the solar activity is during mission lifetime. Even at an altitude of 500 km neither satellite would be able to maintain its orbit for more than a 100 days (REVISE WITH AREA NUMBERS). From this analysis it is clear that substantial orbit maintenance is required as the satellites will most probably not have refocusing equipment for the optical instruments. A more comprehensive idea of the orbit maintenance can be gathered from total ΔV estimations shown in figures 6.3.4 and 6.3.4 (pages 62 and 63) and tabulated in table 6.5 on page 50(CHECK TABLE). This is the total velocity change required to keep the satellites in a certain circular orbit. The calculations are based on equation 6.9.

It can be clearly seen that ΔV budget is almost five times (CHECK) larger at low altitude at solar maximum when compared to the solar minimum. Overall the values for ΔV at high altitudes, at solar minimum and time average look very favorable.

Three important conclusions can be drawn from the preceding analysis:

- In order to avoid fast orbit degradation, and in turn greater mass due to propellant necessary to maintain orbit, the satellites should be placed as high as it is allowable by optical instruments. Based

Altitude	SOLAR MIN			TIME AVERAGE			SOLAR MAX		
	300	400	500	300	400	500	300	400	500
EMITTER	771.35	67.92	8.21	1836.54	252.39	44.72	3729.59	700.58	164.60
RECEIVER	0.56	0.05	0.01	1.33	0.19	0.03	2.70	0.52	0.12

Table 6.5: Required ΔV for various orbit altitudes. In m/s .

on drag analysis it is recommended to inject at 500 ± 25 km.

- The launch timeframe should be designed in such a way that the mission halftime falls under the solar minimum to reduce drag. This will also allow for a reduction in mass.
- The area/mass ratio for the emitter and receiver satellites should be designed as equivalent as possible. This will allow for slower constellation decay and for generally better stationkeeping.

6.3.5 Exposure to Particle Radiation

In space, satellites are exposed to streams of highly energetic charged particles coming from the sun. Radiation from these particles can cause severe damage to satellite subsystems, including the payload. The main particle radiation source encountered by the swarm in the LEO comes from the Van Allen Belts. These are regions around the Earth where charged particles (protons, electrons and ions) are trapped inside the magnetic field of the planet.

The total radiation dose consists of three components: proton dose, electron dose and the so-called Bremsstrahlung X-Ray dose produced by the interaction between the electrons and the shielding material of the satellite. In LEO, energetic protons in the inner radiation belt contribute most to the total radiation dose. This total is also strongly linked to the orbital altitude and below 1000 km will increase at approximately by the 5th power of the altitude. Furthermore, just like with atmospheric drag, the solar activity plays a major role, thus all cases will be examined.

The number of particles trapped in the Van Allen belts in the vicinity of the orbit under question can be modeled using The Space Environment Information System (SPENVIS) that can be located at the following address: <http://www.spenvis.oma.be/>. SPENVIS contains a large array of NASA and ESA (as well as other) tools and models for complex orbit analysis. For the purposes of this evaluation two models are used: AP-8 and AE-8. The first model predicts proton flux with energy levels above 100 MeV. The latter estimates the flux of electrons with energy of 0.5 MeV or above.

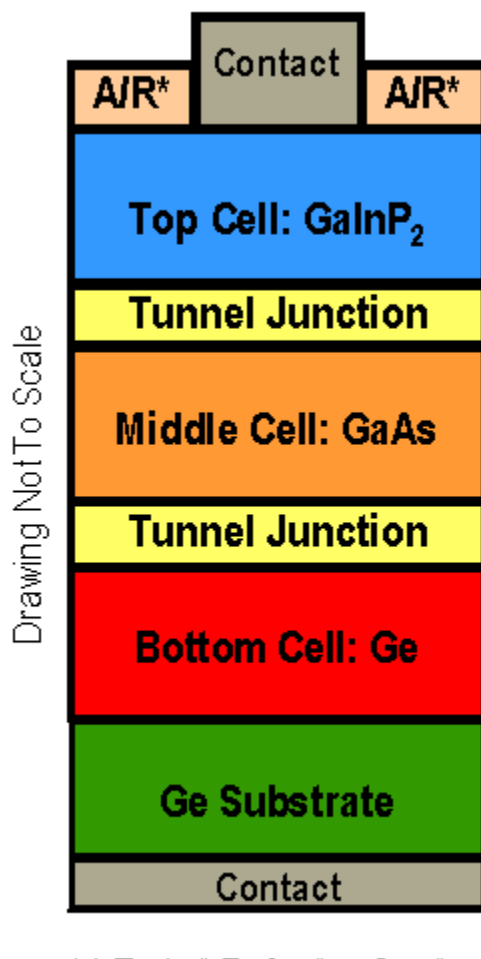
Figure 6.19 on page 64 illustrates the trapped proton flux for solar minimum and maximum as a function of distance from Earth Center. It is evident that in LEO, the proton flux stays relatively static w.r.t. solar activity. For the considered altitudes of 300 to 500 km (1.047 to 1.078 Earth radii) the satellites would encounter relatively the same order of magnitude of proton radiation. It is also evident that any higher altitude would mean a substantial increase in bombardment and hence reduction in the reliability of the subsystems.

Figure 6.20 on page 65 illustrates the trapped electron flux for solar minimum and maximum as a function of distance from Earth Center. It is evident from this figure that lower altitudes would considerably reduce the radiation flux (up to one order of magnitude).

Based on this data, the following conclusion emerges: while altitudes of around 500 km remain relatively safe, a lower orbit will result in a lower particle radiation flux, increasing reliability. Altitudes above 500 km become more and more dangerous for the mission.

6.3.6 Conclusion

ADD ALTITUDE CONCLUSION



*A/R: Anti-Reflective Coating

Figure 6.7: Schematic representation of a triple-junction solar cell

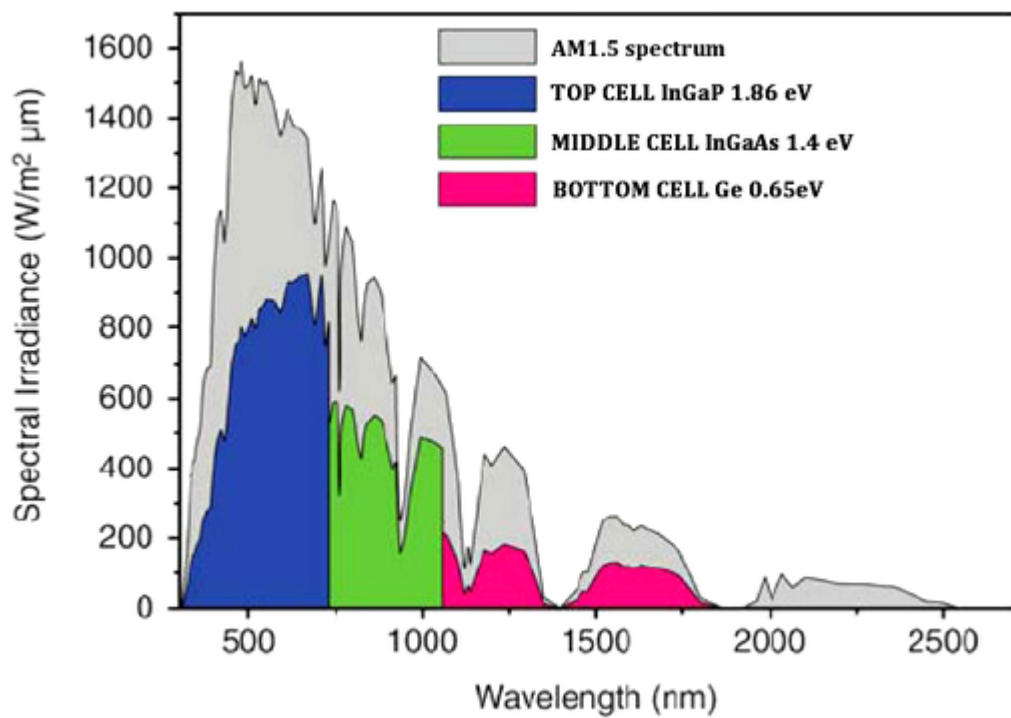


Figure 6.8: Spectral irradiance of a triple-junction solar cell in function of the wavelength

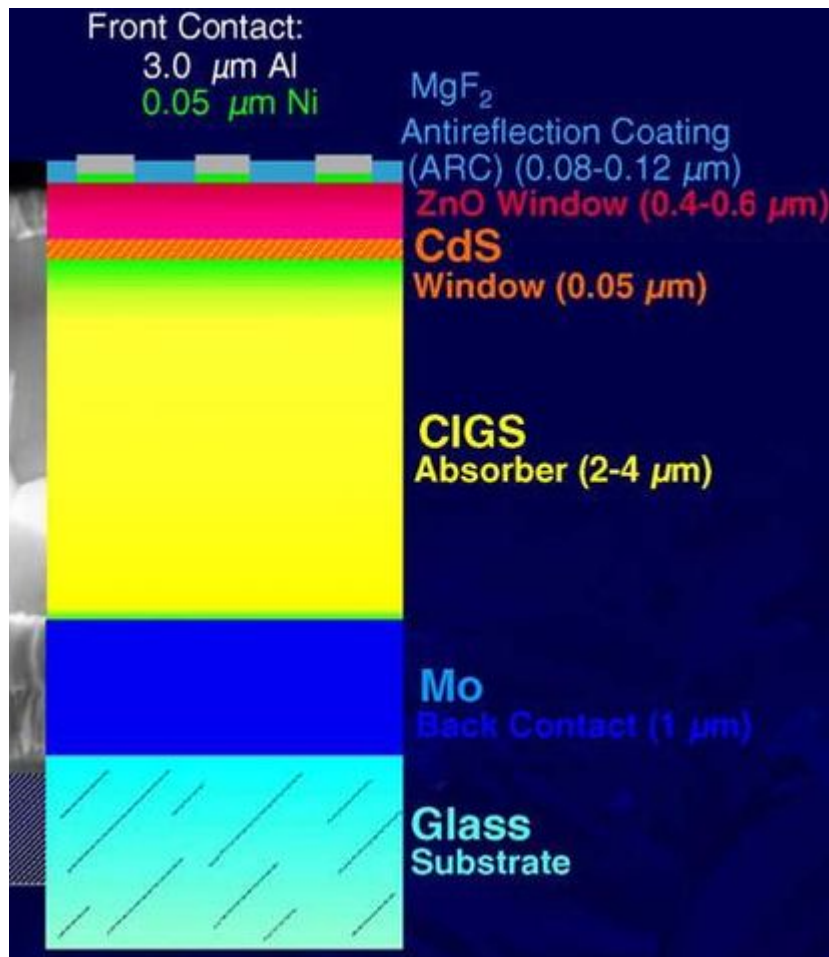


Figure 6.9: Schematic layout of a thinfilm CIGS solar cell

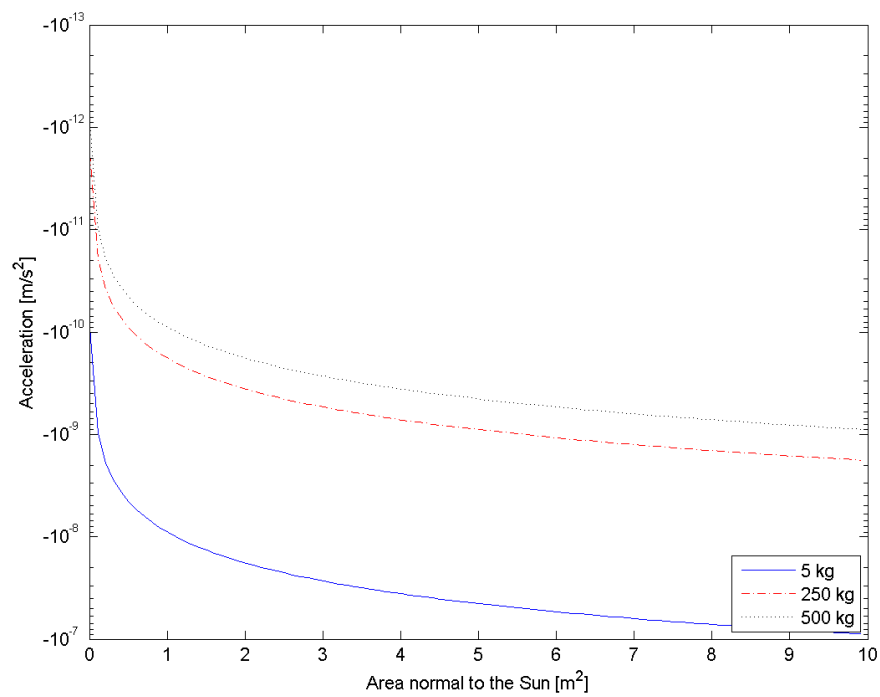


Figure 6.10: Acceleration due to solar radiation pressure vs. area normal to the sun, for different satellite masses.

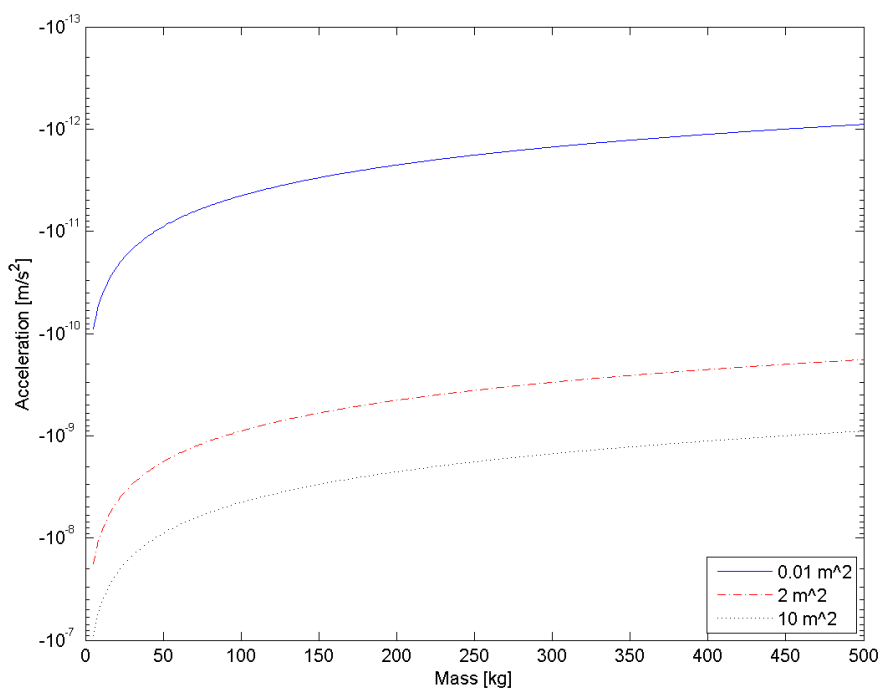


Figure 6.11: Acceleration due to solar radiation pressure vs. mass, for different areas.

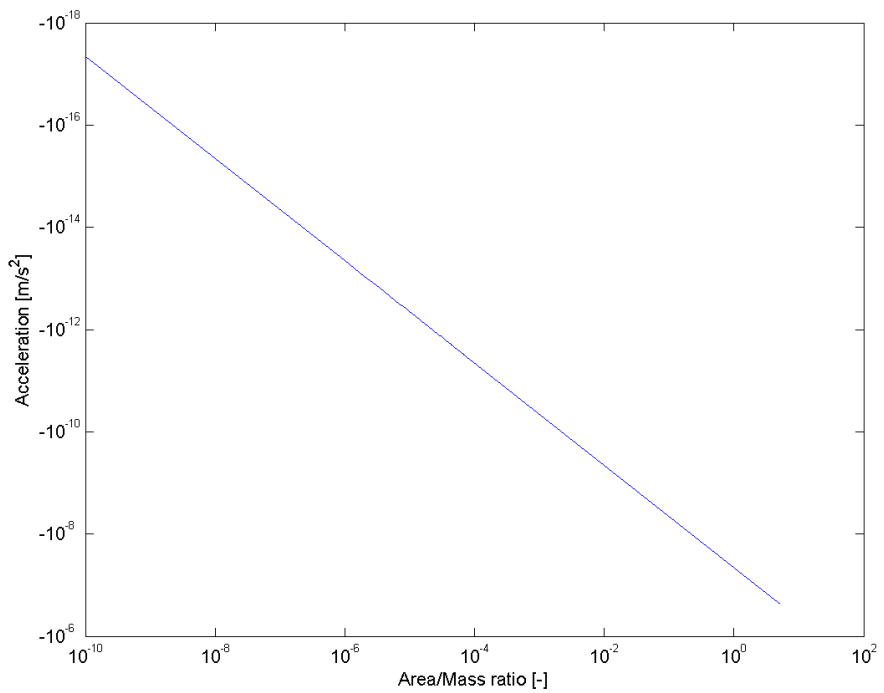


Figure 6.12: Acceleration due to solar radiation pressure vs. Area/Mass ratio.

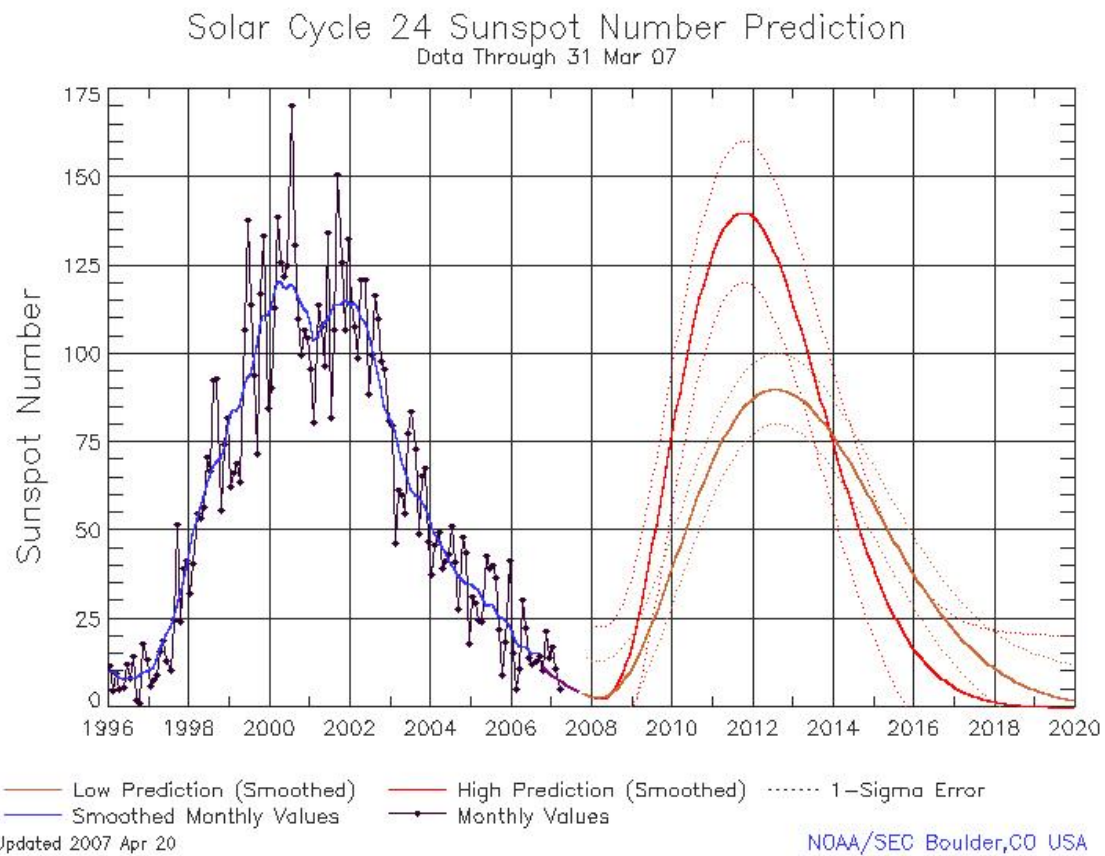


Figure 6.13: The solar cycle, clearly showing the solar maxima at 11 year intervals. Data after 2007 is projected. *Source: NASA*

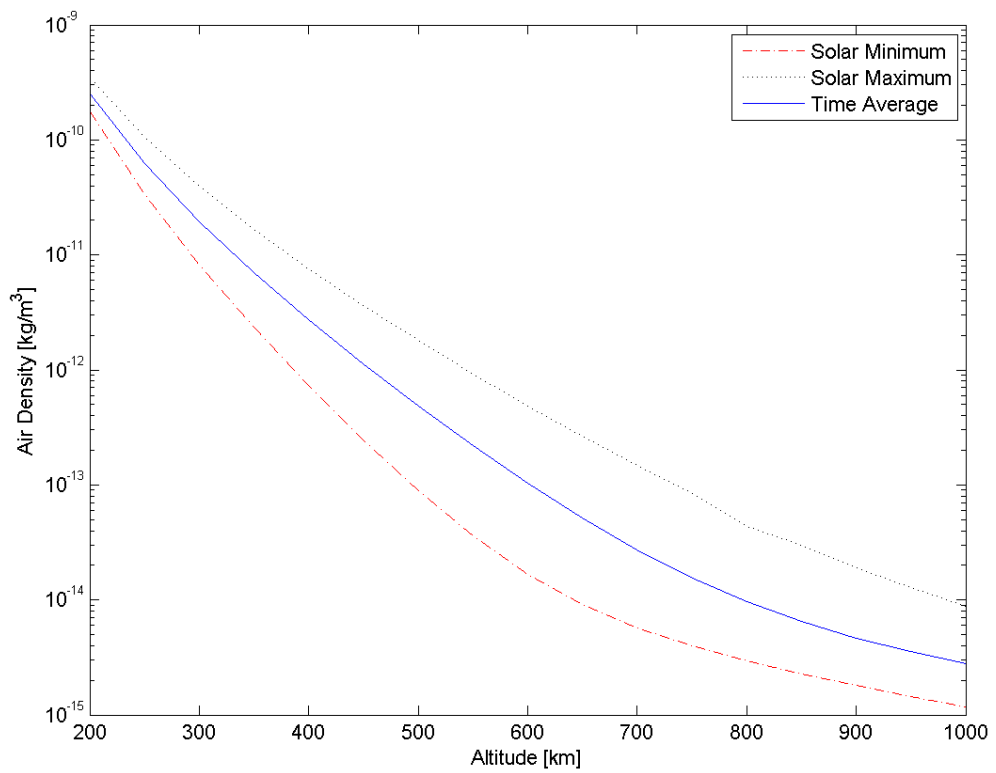


Figure 6.14: Air density vs. orbit altitude for different solar cycle stages.

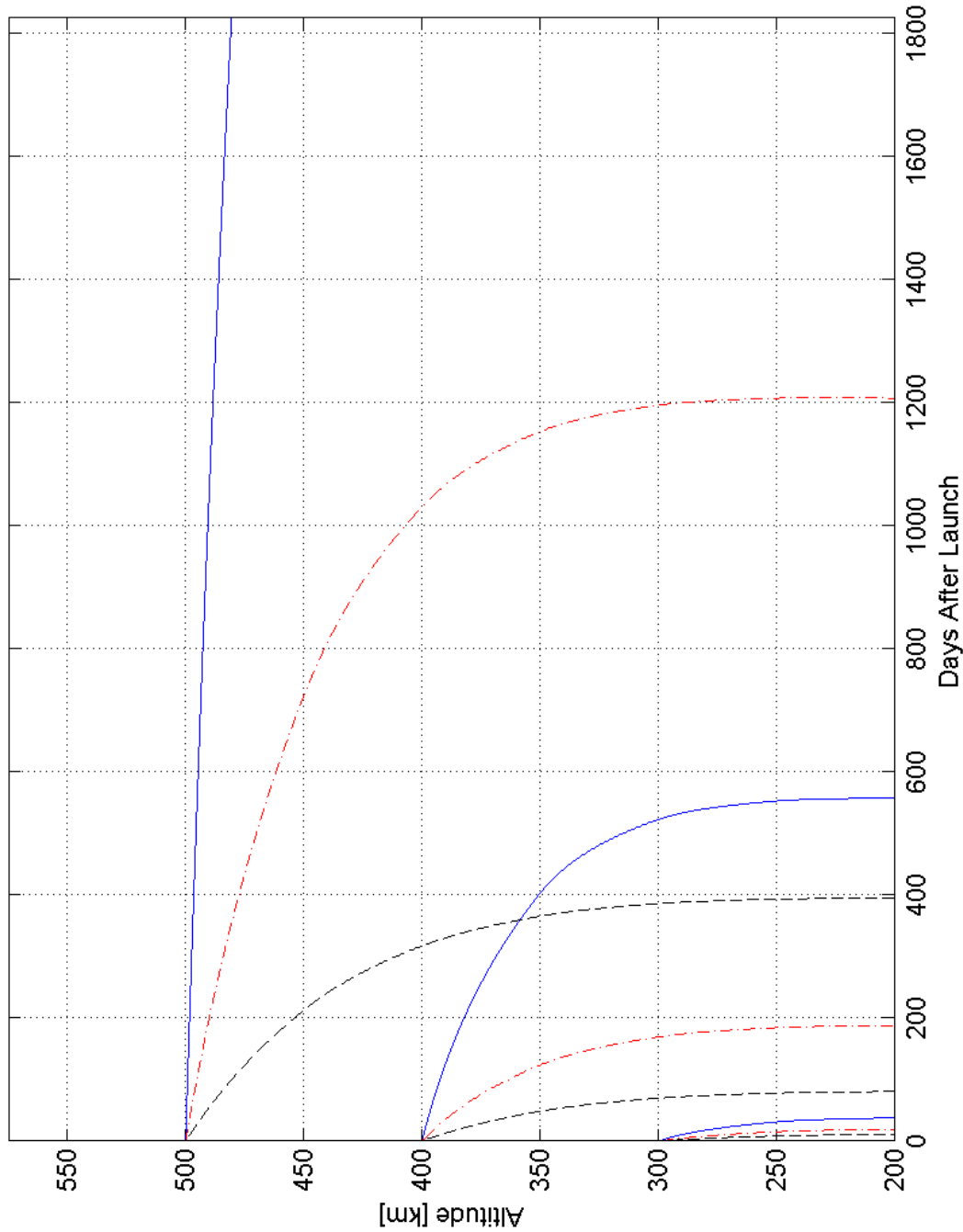


Figure 6.15: Orbit decay for a satellite with $C_D = 4$, $A = 6.1 \text{ m}^2$ and $m = 200 \text{ kg}$. Estimates for initial orbital altitudes of 300, 400 and 500 km at solar maximum (---), solar minimum (—) and time average (---) (CHECK MASS AND AREA).

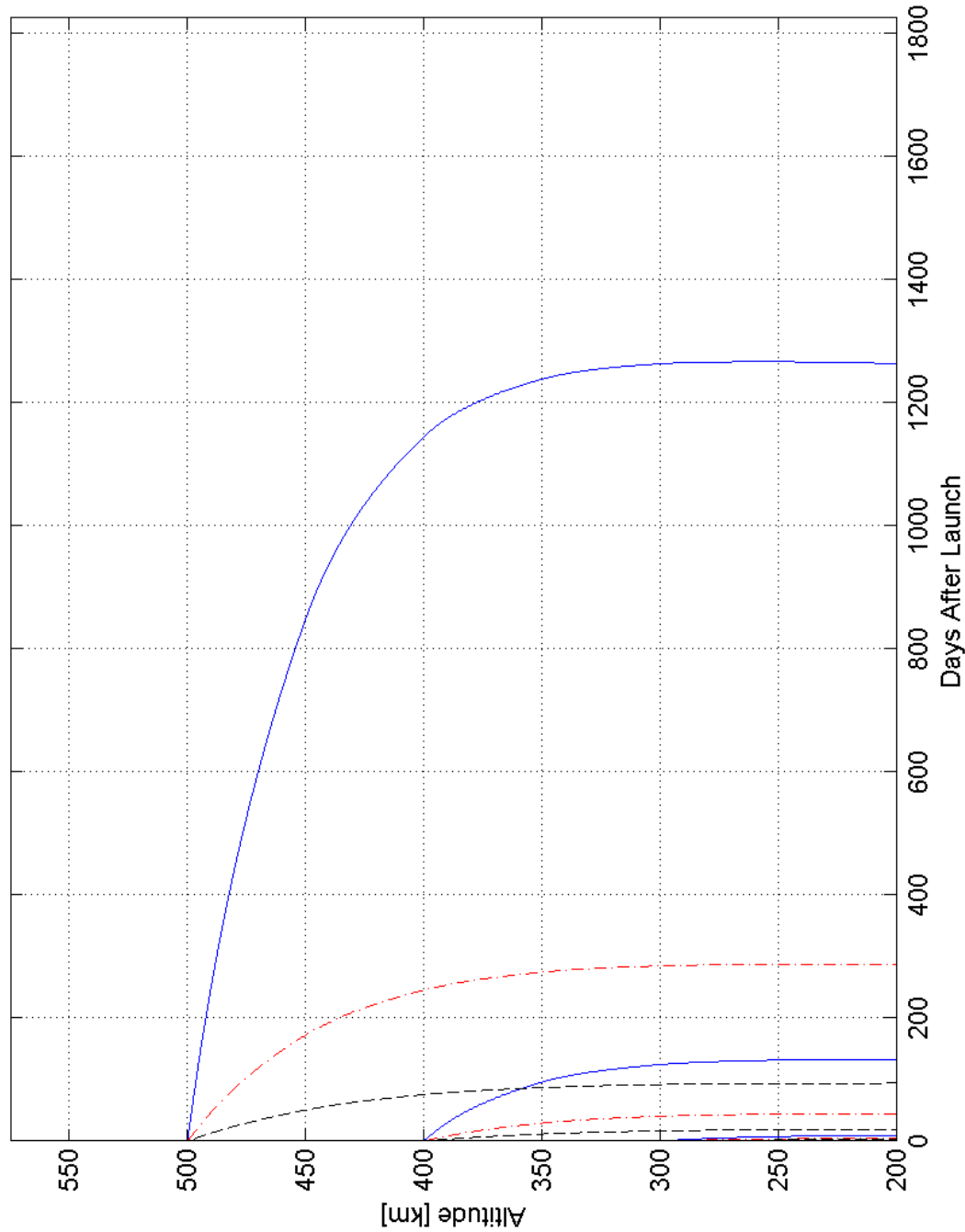


Figure 6.16: Orbit decay for a satellite with $C_D = 4$, $A = 0.21 \text{ m}^2$ and $m = 10 \text{ kg}$. Estimates for initial orbital altitudes of 300, 400 and 500 km at solar maximum (---), solar minimum (—) and time average (---) (CHECK MASS AND AREA).

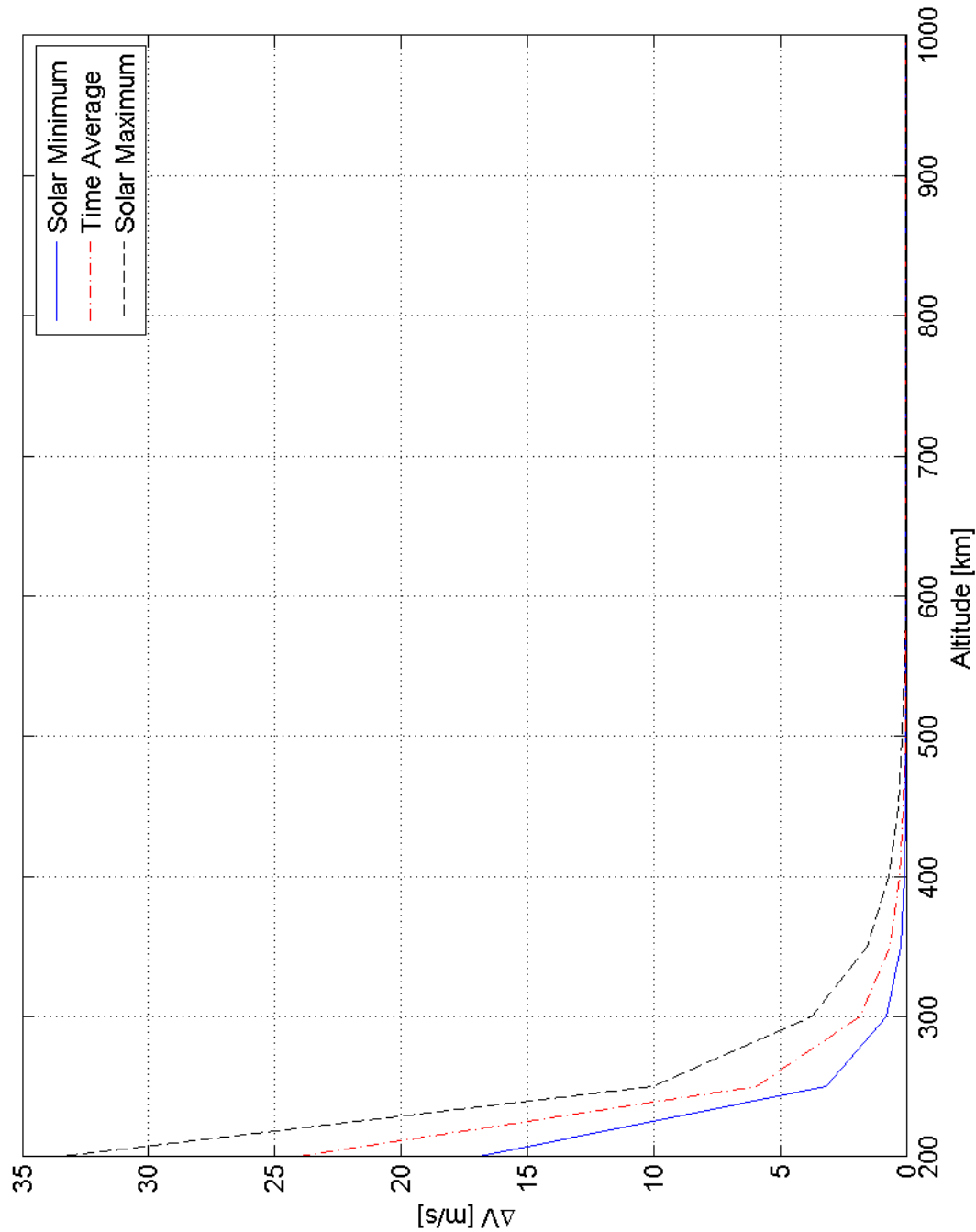


Figure 6.17: Total ΔV for a satellite with $C_D = 4$, $A = 6.1 \text{ m}^2$ and $m = 200 \text{ kg}$. Estimates for a range of orbit altitudes and different solar cycle stages. (CHECK MASS AND AREA).

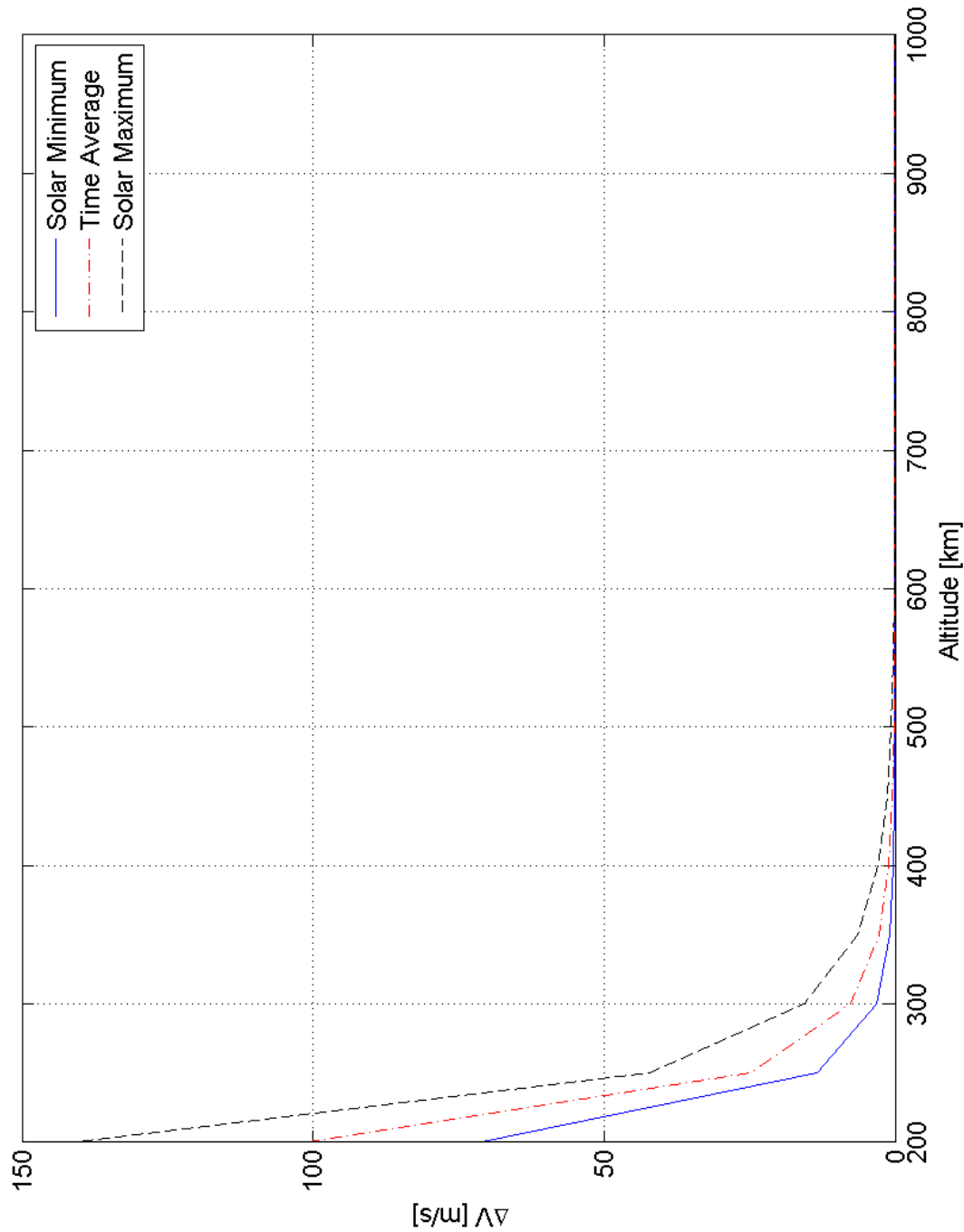


Figure 6.18: Total ΔV for a satellite with $C_D = 4$, $A = 0.21 \text{ m}^2$ and $m = 10 \text{ kg}$. Estimates for a range of orbit altitudes and different solar cycle stages. (CHECK MASS AND AREA).

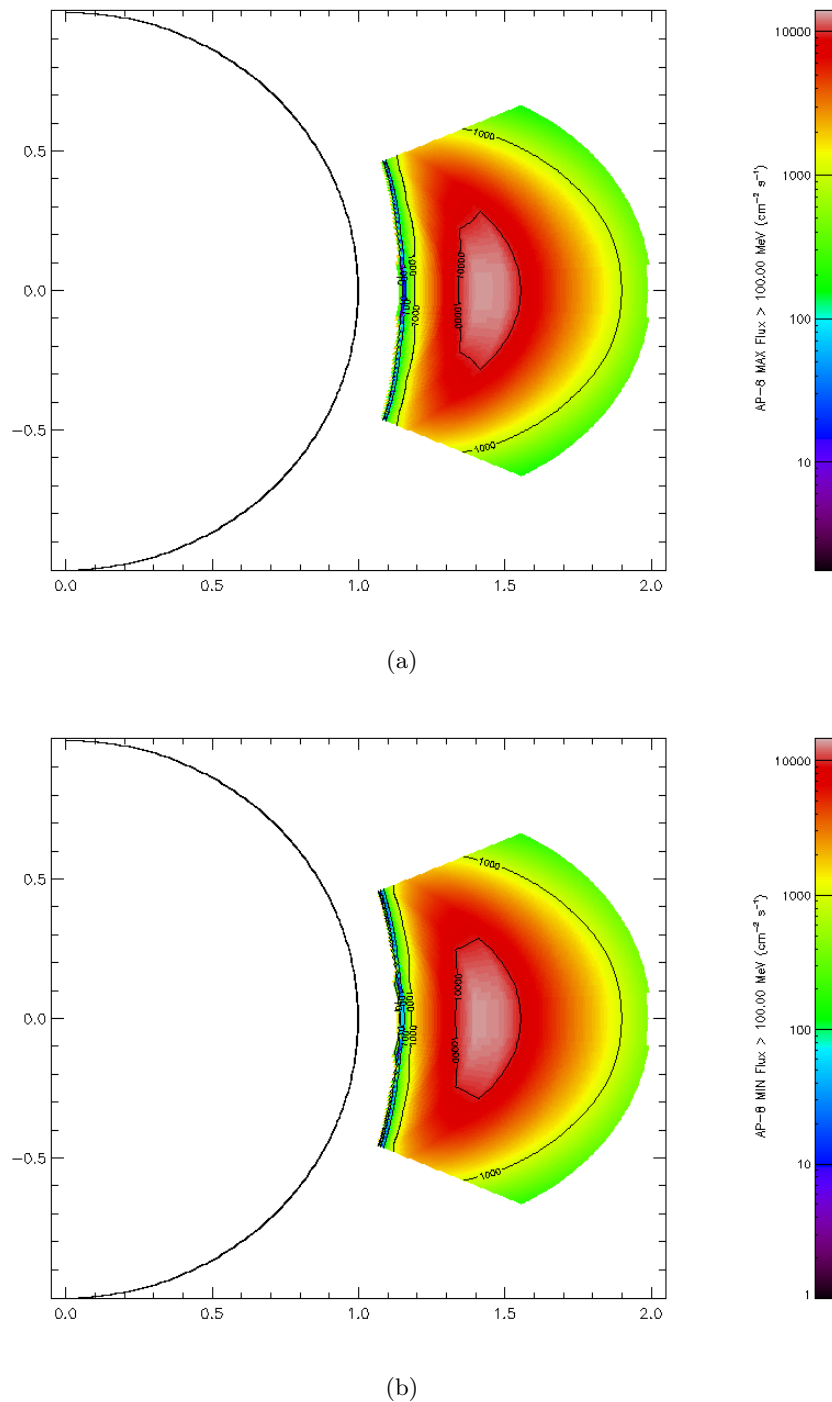


Figure 6.19: AP-8 Proton Flux Model (energy > 100 MeV) at solar maximum (a) and solar minimum (b) as a function of distance in mean Earth radii.

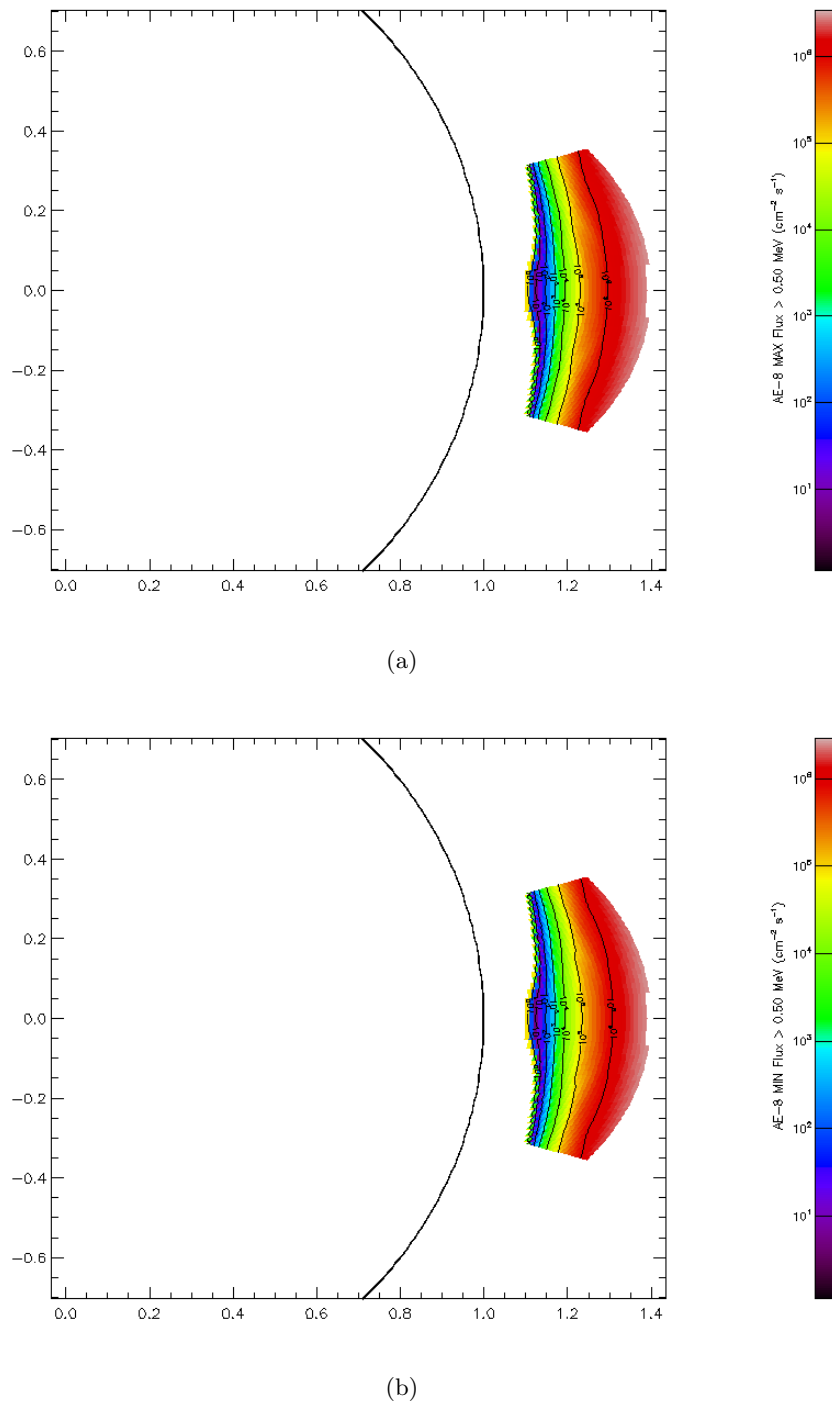


Figure 6.20: AE-8 Electron Flux Model (energy > 0.5 MeV) at solar maximum (a) and solar minimum (b) as a function of distance in mean Earth radii.

Chapter 7

Operations and Logistics

In order for the laser swarm to be successful it has to operate efficiently and effectively, so that the obtained surface model and other data can be sold on the market. This chapter will consider some of these operations and their required logistics. Note that only operations after successful orbit injection and deployment, and before the EOL are considered. A graphical representation of the hierarchy of the options considered here can be found in figure 7.

Navigation and orbital control is an important operation for the laser swarm mission. All satellites have to be aware of where there are, and the position of the formation as a whole has to be known as well. Though most of this system can be automated it is important there are people on the ground who check for any anomalies and give corrections whenever necessary.

Mission control entails the real time control of the satellites, the amount of people required for mission control is very low due to the predictable nature of this mission, because of this nature most of the mission is automated. The only active inputs by humans should be inputs that correct some sort of anomaly. This being dependent on other operations like navigation and orbital control and various supporting operations.

The measurements will be performed completely automatically, with human inputs only being used to correct an error in the automation or to change the routine. The measuring operation includes the both the emitter and the receivers, for a greater detail of the functions that have to be performed the function flow diagram may be consulted.

Payload support is comprised of one or more people who monitor the condition and performance of the payload of the emitter, and a separate group of people who monitor the receivers. In case of an anomaly they determine the severity and change the satellite or payload operations if necessary.

Spacecraft operations is similar to payload support, except that the person or people who work on this operation monitor the rest of the satellite.

Computer and communications support is staffed several people who monitor and the automated systems, and one or two persons who monitor the communications between satellites and satellites to the ground. Their main job is to make sure the system remains operational if an anomaly occurs.

Data services entails everything that happens with all data both on ground and aboard the satellites. The data can be anything from measurement data to navigational data. This operation support all the other ones. While largely automated some human interaction is needed to ensure the data is decoded, debugged, archived and generally handled properly. Minimal human interaction will be required to reduce the mission costs.

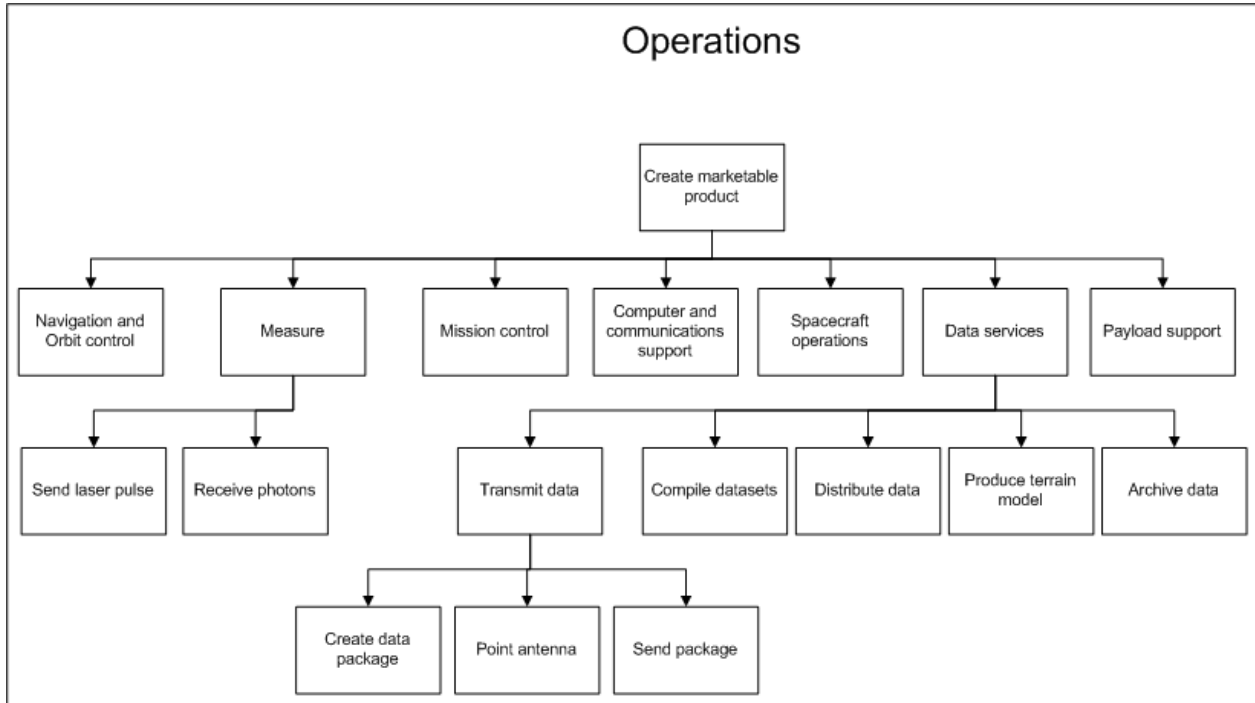


Figure 7.1: Hierarchy of the operations for the laser swarm mission.

Data transmission involves the sending of data between satellites and from the satellites to a ground station. It is a fully automated process as the orbits of the swarm have been simulated before the launch.

Chapter 8

Stability & Control

In this chapter the requirements for stability and a short general introduction to the control of the satellites. Conditions for stability are derived in section 8.1, the control of the satellite is discussed in section 8.2.

8.1 Stability

A satellite is considered in a nadir pointing, circular orbit around the Earth. When small rotations are assumed the equations of motion can be linearised. The linearised combined dynamic and kinematic equations are

$$J_{11}\ddot{\theta}_1 - n(J_{11} - J_{22} + J_{33})\dot{\theta}_3 + 4n^2(J_{22} - J_{33})\theta_1 = 0 \quad (8.1)$$

$$J_{22}\ddot{\theta}_2 + 3n^2(J_{11} - J_{33})\theta_2 = 0 \quad (8.2)$$

$$J_{33}\ddot{\theta}_3 + n(J_{11} - J_{22} + J_{33})\dot{\theta}_1 + n^2(J_{22} - J_{11})\theta_3 = 0 \quad (8.3)$$

where J_{nn} is the inertia tensor, θ_n are the rotation axis (roll, pitch and yaw) and n is the orbital rate defined as

$$n = \sqrt{\frac{\mu}{|R_c|^3}} \quad (8.4)$$

where μ is the Earth's gravitational constant and R_c the radius of the orbit of the satellite center of mass. As can be seen in equation 8.2 the rotation around the pitch axis is independent of the rotation rates about the other two axis. By taking the Laplace transform of this equation the characteristic equation is found to be

$$s^2 + \frac{3n^2(J_{11} - J_{33})}{J_{22}} = 0 \quad (8.5)$$

Stability requires that the characteristic roots are purely imaginary. This is only true if

$$J_{11} > J_{33} \quad (8.6)$$

For simplification of equations 8.1 and 8.3 the parameters $k_1 = (J_{22} - J_{33})/J_{11}$ and $k_3 = (J_{22} - J_{11})/J_{33}$ are defined. The linearised equations of motion for roll and yaw then become

$$\ddot{\theta}_1 + (k_1 - 1)n\dot{\theta}_3 + 4n^2k_1\theta_1 = 0 \quad (8.7)$$

$$\ddot{\theta}_3 + (1 - k_3)n\dot{\theta}_1 + n^2k_1\theta_1 = 0 \quad (8.8)$$

Laplace transforming equations 8.7 and 8.8 gives

$$\begin{bmatrix} s^2 + 4n^2k_1 & (k_1 - 1)ns \\ (1 - k_3)ns & s^2 + n^2k_3 \end{bmatrix} \begin{bmatrix} \theta_1 \\ \theta_3 \end{bmatrix} = \begin{bmatrix} 0 \\ 0 \end{bmatrix} \quad (8.9)$$

To find the non-trivial solution the determinant of the matrix in 8.9 needs to be zero.

$$s^4 + (1 + 3k_1 + k_1k_3)n^2s^2 + 4k_1k_3n^4 = 0 \quad (8.10)$$

This equation is true when

$$\frac{s^2}{n^2} = \frac{-(1 + 3k_1 + k_1k_3) \pm \sqrt{(1 - 3k_1 + k_1k_3)^2 - 4^2k_1k_3}}{2} \quad (8.11)$$

For the roots to be imaginary the following equations should hold

$$1 + 3k_1 + k_1k_3 > 0 \quad (8.12)$$

$$1 + 3k_1 + k_1k_3 > 4\sqrt{k_1k_3} \quad (8.13)$$

$$k_1k_3 > 0 \quad (8.14)$$

The satellite is stable around all three axis when conditions 8.6, 8.12, 8.13 and 8.14 are all met [Chu(2009a)].

8.2 Control

The fact that there is no or little friction in space is both an advantage as a disadvantage for spacecraft. The advantage is that less power is required for the spacecraft to move, the disadvantage is that there is nothing to stop the spacecraft from moving when it does. Every torque which is imposed on the satellite, both by external and internal sources, has to be countered to stop the spacecraft from rotating. The simplified control equations of motion for the satellite are

$$M_{c1} = J_{11}\ddot{\theta}_1 \quad (8.15)$$

$$M_{c2} = J_{22}\ddot{\theta}_2 \quad (8.16)$$

$$M_{c3} = J_{33}\ddot{\theta}_3 \quad (8.17)$$

If the satellite needs to make a manoeuvre with an angle of θ_{man} two torques need to be exerted on the satellite with a magnitude of

$$M_c = 4\theta_{man}J/(t^2) \quad (8.18)$$

where t is half the time required for making the total manoeuvre. The torques first need to be in one direction for half the time, then in the opposite direction for the other half of the time [Chu(2009c)].

Chapter 9

Sustainable Development Strategy

In this chapter a Sustainable Development Strategy is discussed in the order of production (section 9.1, page 71), operations (section 9.2, page 71) and end of life (section 9.3, page 72).

9.1 Production and Logistics

The design is aimed at a swarm of mostly identical satellites. This may allow for series production which is more efficient in terms of resources than a one-of large satellite with a lot of unique components. This also implies that the number of different spare parts could be reduced. Smaller satellites could also use smaller facilities for production and testing.

Transportation can be split up into two parts: transportation to the launch site and the launch from the surface to the final orbit in space. On both occasions the system can again profit from its small size. If the satellites are not launched all together, they can “piggyback” on another satellite’s launcher.

Spreading the swarm, i.e. piggybacking using different launchers, has several advantages. First of all, the emissions are lower than in case of a dedicated launcher. Also, if the first satellite fails before the launch of the rest of the swarm, the others can be repaired and thus less resources are wasted.

9.2 Operations

Once in orbit, the satellite’s influence on the Earth is very limited. The only real concern is the debris it leaves behind during launch and deployment, which can be dangerous to other satellites orbiting the Earth. However, the deployment mechanism , which is responsible for most of the debris, is not included in this technical feasibility study. Later studies developing the ideas from this feasibility study should take it into account, since more satellites could mean more deployment mechanisms and hence more waste. One aspect that can be dealt with is the efficient use of resources. The swarm can be designed in such a way that if one of the satellites fails a replacement satellite can be sent, whilst any remaining satellites can be reused.

9.3 End of Life

Each satellite will be at the end of its life if it cannot perform its function anymore. It is important that after the mission is over all satellites are removed from their orbit and burn up in the atmosphere so that they do not pose any danger to other satellites. Final decommissioning of the swarm will be more complex than for a regular satellite, since every individual satellite has to be decommissioned separately.

Chapter 10

Simulation

10.1 Introduction

This report preliminarily discusses the design and workings of a software tool developed with the purpose of guiding and validating the results of the tradeoff done in the main laser swarm project, as well as demonstrating the feasibility of the concept of the laser swarm.

Generally speaking, the simulator program is divided into two parts. The first part is the simulation of the physical path of the photons in the laser pulse up to the point where they are received by the receiving satellites. This part has been documented in section ??.

The second part is the analysis of the received photon data, to determine terrain height and the terrain Bidirectional Reflection Density Function (BRDF). Obtaining this data is what the software and in general this feasibility study is about. This part is described in section 10.3.

10.2 Simulation

In this section the simulation of the satellites, moving through space and sending and receiving laser pulses, is discussed. In subsection 10.2.1 the emitter and receiver satellite orbits are considered. In subsection 10.2.2 the way the Earth's surface was modeled is explained. In subsection 10.2.3 the path of the signal is examined, whereas in subsection 10.2.4 the introduction of noise into the signal is disclosed.

10.2.1 Orbit

The orbit of each satellite in the constellation is defined by means of six Keplerian elements. These define the shape of the orbit, the orientation of the orbit with respect to the center of the Earth and the position of the satellite on the orbit.

As there are a number of rotating bodies, three reference frames are used in order to facilitate the process of locating the satellites in space. The three reference frames used in the simulation are described below.

The first is True Of Date (TOD). Its X-axis points towards the direction of the vernal equinox and its Z-axis coincides with the axis of rotation of the earth. TOD takes into account nutation and precession of

the earth. For practical reasons, it does not rotate with respect to the Sun.

In the second place there is Earth-Centered, Earth-Fixed (ECEF). Its X-axis points towards 0° latitude and 0° longitude. The XY plane lies in the plane of the equator. Its origin is in the center of mass of the Earth.

Thirdly there is the PQW. The P-axis points towards the perigee of the orbit, the PQ plane lies in the plane of the orbit and the W-axis is perpendicular to the plain of the orbit. The origin of the frame is at the focal point.

The program converts between the before-mentioned reference frames for the user's convenience.

The position of the satellite is defined with respect to the TOD reference frame. Kepler's equations are solved for a certain time to determine the position. The orbit is determined for every satellite in the constellation. The orbit is assumed to be perfect, meaning that its orientation and shape do not change: perturbations are not considered.

The Earth's rotation about its own axis and around the Sun is simulated in order to provide a more realistic simulation environment. From the rotation of the Earth around the Sun, the sun vector is deduced; this is used in noise calculations.

Most of the functions are adapted to the simulator from the Java Astrodynamics Toolkit (JAT) library.

10.2.2 Earth Model

The Earth model is the digital representation of the Earth surface. It stores a Digital Elevation Model (DEM), and the scattering characteristics of the local terrain. In section 10.2.2.1, the DEM implementation will be elaborated and section 10.2.2.2 describes the way incoming radiation is scattered.

10.2.2.1 Digital Elevation Model

A Digital Elevation Model is a digital representation of a topographic surface. For the ground representation in the simulator a few tiles of the Advanced Spaceborne Thermal Emission and Reflection Radiometer (ASTER) Global Digital Elevation Model (GDEM) were used. This DEM was created using the complete history of the ASTER instrument launched on the Terra satellite. This DEM has a spatial resolution of one arc-second and a vertical accuracy of 7 – 14 meters. The elevations of the intermediate points were obtained using nearest-neighbor interpolation.

The ASTER GDEM elevations are expressed with respect to the World Geodetic System 1984 (WGS84) ellipsoid. To simplify the internal simulator, the DEM tiles were projected to the EPSG:3857 spheroid. The projection is done using the GeoTools Java toolkit [geo(2010)].

The digital elevation is used to compute the total distance (and thus the time) that the laser pulse travels. Because scattering is dependent on the terrain normal, this normal is derived from the DEM, using the two perpendicular surface gradients that can be extracted from the DEM.

10.2.2.2 Scattering Model

Scatter is the physical process where incident radiation is absorbed and reflected back towards the atmosphere. To this end a scattering model is used. This scattering model is a way to construct a BRDF. A BRDF is a distribution of the incident light over the hemisphere [Rees(2001), pages 47-49]. An example is

shown in figure 10.2.2.2, page 75.

The most basic example of a BRDF is the Lambertian model [Rees(2001), pages 49-50]. This model assumes a homogeneous perfectly rough surface, causing a homogeneous scattering distribution. Apart from the index of refraction of the air, the incident radiation vector and the exitant radiation vector (which are all known), use of Snell's law is needed to find Fresnel's coefficients, thereby requiring the index of refraction of the ground.

A modification that can be made to take into account the tendency of surfaces to scatter more in the direction of the surface normal, is called the Minnaert model [Rees(2001), page 50]. It causes a more elliptical BRDF. It depends on the Minnaert parameter κ .

Another important modification is the Henyey-Greenstein term. It accounts for the tendency of surfaces to back- or forwardscatter [Rees(2001), page 51]. This rotates and deforms the elliptical BRDF obtained from the Minnaert model. The Henyey-Greenstein term is parameterized by Θ . The final result is shown in figure 10.2.2.2, page 75.

This is the scattering model used in the program. Because there is no data from which all three parameters can be accurately determined, a coefficient map was made up. It does not matter much what the precise form of the BRDF used in the simulation is, so long as it can be retrieved.

With the help of the formulae from [Rees(2001), pages 43-51], the incidence vector can be taken and the number of photons radiated in a specific direction can be calculated. Note that the program does not integrate over part of the sphere: because the angle of the cone is very small, the BRDF is assumed to be constant over the cone. The error induced here is worth avoiding the computationally expensive integration.

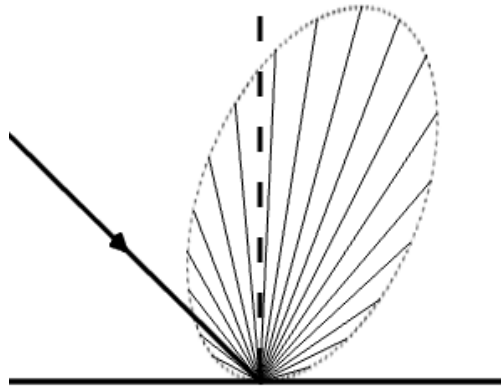


Figure 10.1: Example of a BRDF

10.2.3 Signal Path

The simulated path that the laser signal follows is visualized in figure 10.2.3 on page 75. There are three distinct phases. The first one is the travel of the signal down through the atmosphere. This is followed by the scattering on the Earth's surface. Finally the pulse has to travel back up through the atmosphere. This sequence is elaborated on in more detail below.

The signal originates from the emitter. For each pulse, the emitter position is determined from a set of Kepler elements. The energy in the pulse is found by distributing the emitter power over a constant number of pulses of a given duration.

The signal then starts to propagate through the atmosphere. The atmosphere affects the signal in several manners, but the most important one is the attenuation of the signal. Attenuation is the only disturbance by the atmosphere taken into account. The pulse energy exponentially decays with travel distance through the atmosphere. Furthermore also the optical thickness of the atmosphere is taken into account.

Then the intersection of the pulse with the DEM is computed. As a simplification in this process, the intersection of the pulse (i.e., the ray) with a sphere is computed. The sphere has a radius of the average terrain height of the DEM tile plus the Earth radius. Then the ray-sphere intersection point coordinates are converted into latitude and longitude. These are then used to find the actual terrain elevation from the DEM and the three-dimensional position.

Then the scattering characteristics are constructed. For this, the terrain normal and the inbound laser pulse vector are used. The power of the emitted pulse is now distributed over the entire footprint area of the emitter and then scattered back using the scattering technique described in section 10.2.2.2. The backscattered energy is computed separately for every receiver satellite.

The reflected pulse now travels back through the atmosphere. More attenuation takes place along this path. The energy received by the receivers now depends on the receiver aperture. The received energy can then be converted into photons by dividing the energy received by the energy per photon.

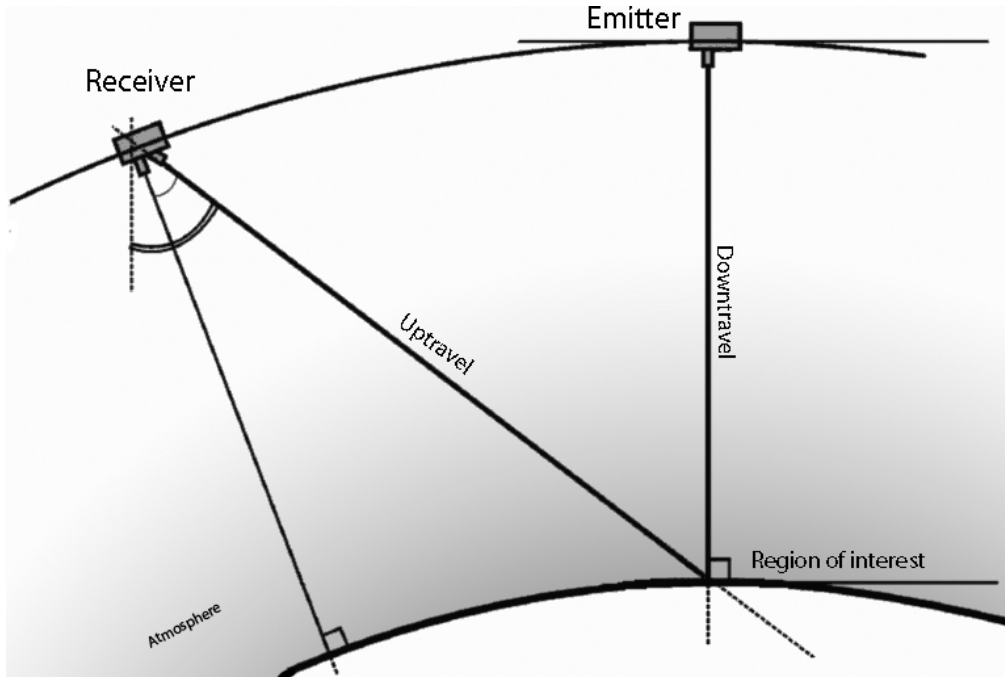


Figure 10.2: Signal path representation

10.2.4 Noise

The main source of noise in the system comes from the Earth's surface. This includes sources on the Earth such as lights along highways and reflected radiation, i.e. the Earth's albedo. The amount of radiation that is received by the receivers depends on the footprint of the receivers. This is an ellipse created by the intersection of the cone originating from the receiver with the terrain. A simplification is made in that the DEM is assumed to be a flat area with the elevation of the center point.

The amount of power emitted per square meter is dependent on the illumination of the Earth by the Sun. If the Sun illuminates the footprint, the emitted power is the scattered power of the Sun in the receiver detection wavelength bandwidth. This power can be found by integrating Planck's law over the detection spectrum and the solid angle the Sun subtends to the receiver footprint on Earth. If the Sun does not illuminate the receiver footprint, the only contribution to noise is the Earth's greybody radiation, which is also taken into account.

While noise propagates through the atmosphere it is also attenuated. This attenuation is computed in the same way the signal attenuation is; see section 10.2.3.

10.3 Data Analysis

In this section the analysis of the received photon data taken care of in the software tool is elaborated on. The analysis consists of two parts: the terrain altitude determination and the BRDF determination. The first is expounded in subsection 10.3.1, the second in 10.3.2.

10.3.1 Altitude Determination

In order to tackle the problem of decrypting the raw data and converting it into a coherent terrain model, various statistical techniques need to be employed. The basic principle behind the altitude determination of the terrain is as following. First the time difference between generation and reception of the pulse is registered. As the position of the emitter at the time when the pulse was sent is known, just like the position of the receiver at the time the pulse was received is, the distance to ground can be determined. In theory only one emitter and one receiver are necessary to determine the altitude, but due to various uncertainties in position and noise characteristics of the received data, more receiving satellites are necessary to obtain a reliable and complete terrain representation.

In the simulator the emitter is modelled such that it records the time when the pulse was sent. The receivers are modelled such that they register the time and intensity (in photons) of the received pulse. The problem is that not all emitted pulses are registered, and sometimes noise, which does not correspond to any emitted pulse, is registered.

One of the ways to solve this problem is to use multiple receivers. The noise could be identified and removed by means of looking for a spike in the received photons for the whole swarm within a certain time range (usually twice the time it takes for a light beam to travel the orbit altitude). This data could be filtered by means of correlating the distance of the receiver to the Earth center and the time of the received pulse. Usually, the larger the distance, the larger the time difference. This method helps to eliminate outliers. Since the footprints overlap, the measured altitudes could be further smoothed out by means of a running average.

10.3.2 Bidirectional Reflection Density Function Determination

The BRDF returns the ratio of the radiance to irradiance for a given angle perpendicular to the surface. In theory, it is possible to measure it by means of the received photons of all of the receivers for a given pulse, where each received photon indicates the relative intensity. From the position of the receivers the direction of the irradiance vector can be calculated. Having the direction and intensity of the reflected radiation a segment of the BRDF for a specific incident angle could be reconstructed. By making a multiple passes over the same region, a partial BRDF for different incidence angles can be recorded. If the data is interpolated, a complete BRDF can be determined.

10.4 Simulations

In order to determine the correct sizing of various subsystems, the behavior of the swarm needs to be known. To this purpose several simulations have been ran. The first and most important one is to determine the variation of the photon count with increasing altitude. This simulation is described in section 10.4.1 on page 78. In section 10.4.2 on page 79, second simulation is discussed. This simulation determines the amount of noise photons received from the sun with respect to the number of photons from the laser emitter.

10.4.1 Variation of Photon Density with Altitude

To determine the number of photons with increasing altitude, a simulation was ran with several constellations. These constellations differ only on the constellation altitude. Each constellation exists of a single transmitter and receiver, on the same orbit. Furthermore, to reduce errors not due to the altitude effect, the scattering coefficients and elevation remain constant over the entire DEM area.

The scattering coefficients values used were 1.5 for the index of refraction, 1.3 for the Minnaert correction and -0.5 for the Henyey-Greenstein correction. The area over which the simulation ran is a rectangle stretching from (48° lat; 8° long) to (54° lat; 9° long). The laser (500 nm) that was used has 10W of laser power, spread over 5000 pulses per second, each with a length of 1ns. The receiver satellite has an aperture of 8x8 cm (0.0064 m²) with a perfect receiver. The constellation orbital parameters are as follows:

- Semi-major axis: Earth radius + altitude (variable),
- Eccentricity: 0,
- Inclination: 90°,
- Right ascension of ascending node: 8.5°,
- Argument of perigee: 0°,
- True anomaly: 0°.

1

The results are shown in table 10.1 and visualized in figure 10.4.1. The datapoints show a clear exponential decaying trend. This trend can be approximated with the mathematical function $y = e^{-0.0052 \cdot x + 0.6558}$. This function shows a high decay rate with increasing altitude. For example moving from altitude of 500km to 350km halves the number of received photons. To compensate for this effect, one would have to design the laser to have double the power, or the receiver double the aperture. This is because both of these parameters directly effect the number of received photons.

Altitude [km]	300	325	350	375	400	425	450	475	500
Average # photons	0.4249	0.3613	0.2991	0.2692	0.2483	0.2054	0.1843	0.1641	0.1483

Table 10.1: Simulation results for varying altitude

From this simulation, one can conclude that purely on the bases of received photons, a lower altitude is better. This is in direct contradiction to the drag analysis. However higher altitudes are possible, with increased laser power and/or receiver aperture area.

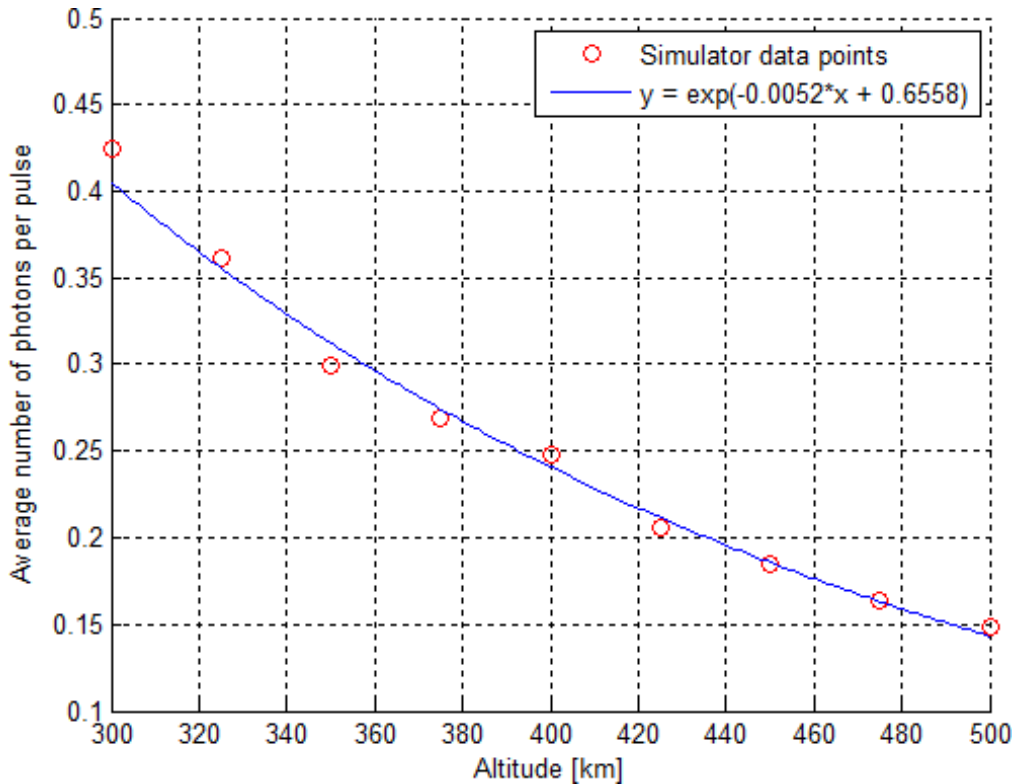


Figure 10.3: Height variation effect in the # received photons

10.4.2 Solar Photons Fraction

The goal of this simulation is to get an idea of the number of photons received due to radiation noise from the sun. This is required to get an idea of what fraction of photons is actually from the laser emitter and what fraction is noise. A single pass over an again flat area with constant scattering coefficients was simulated.

The scattering coefficients remain the same as for the previous simulation. Also the same orbit characteristics were used, only at a fixed altitude of 450 km. The emitting laser now has 33 W of lasing power. The other characteristics of the emitter remain the same. The receiver satellites have an aperture are of 20x20 cm (0.04 m^2) and are sensitive in a band of 1 nm around the center laser wavelength (500 nm). Furthermore the receiver has an optical efficiency of 90% and quantum efficiency of 40%. The results are summarized below:

- Pulses sent: 24989 (about 5s)
- Photons from pulses received: 12289 (86.5%)
- Sun noise photons received: 1930 (13.5%)
- Total photons received: 14219

From these results, one can conclude that the majority of the photons received are indeed from the transmitted laser pulses, and not from the sun. Furthermore, about every second pulse is detected by the receiver. Coupled with the swarm concept, that means that per pulse, a couple of photons are detected. This knowledge can be used to filter out the lower random sun noise photons. This means that this orbit altitude combined with the given laser power is sufficient to filter out the noise.

Bibliography

- [Mar(2008)] Ocean surface topography from space, Jul 2008. URL <http://sealevel.jpl.nasa.gov/overview/benefits.html>.
- [cub(2010)] Cubesatshop.com. online, 2010. <http://www.cubesatshop.com>.
- [del(2010)] DelfiSpace, the nanosatellite programme of the Delft University of Technology, 2010. <http://www.delfispace.nl>.
- [geo(2010)] Geotools, May 2010. URL <http://www.geotools.org/>.
- [imi(2010)] Miniature 3-axis reaction wheel & attitude determination and control system for cubesat kittm nanosatellites, April 2010. http://www.cubesatkit.com/docs/datasheet/DS_CSK_ADACS_634-00412-A.pdf.
- [jer()] Lecture 6: Orbits. URL <http://jersey.uoregon.edu/~js/space/lectures/lec06.html>.
- [mar(2010)] Maryland aerospace inc., April 2010. <http://www.miniadacs.com>.
- [nas(2008)] Ancillary description writer's guide. global change master directory., 2008. URL <http://gcmd.nasa.gov/User/suppguide/platforms/orbit.html>.
- [spa(2010)] Spacequest, ltd., 2010. <http://www.spacequest.com/>.
- [tno(2010)] TNO. website, 2010. <http://www.tno.nl>.
- [Chu(2009a)] Dr. Q.P. Chu. Spacecraft attitude dynamics and control, course notes no. 1 part 3, 2009a.
- [Chu(2009b)] Dr. Q.P. Chu. Spacecraft attitude dynamics and control, course notes no. 2 part 1, 2009b.
- [Chu(2009c)] Dr. Q.P. Chu. Spacecraft attitude dynamics and control, course notes no. 2 part 2, 2009c.
- [David Stoppa and Charbon(2009)] Justin Richardson Richard Walker Lindsay Grant Robert K. Henderson Marek Gersbach David Stoppa, Fausto Borghetti and Edoardo Charbon. A 32x32-pixel array with in-pixel photon counting and arrival time measurement in the analog domain. 2009.
- [Doody(2001)] Dave Doody. The basics of space flight., February 2001. URL <http://www2.jpl.nasa.gov/basics/bsf11-3.php>.
- [et al.(2007)] Peter Fortescue et al., editor. *Spacecraft Systems Engineering*. John Wiley & Sons Ltd., Chichester, West Sussex, England, 3 edition, January 2007.
- [Jusef Hassoun and Scrosati(2009)] Priscilla Reale Jusef Hassoun, Stefania Panero and Bruno Scrosati. A new, safe, high-rate and high-energy polymer lithium-ion battery. *Advanced Materials*, 21:4807 – 4810, 2009.
- [Kuphaldt()] Tony R. Kuphaldt. All about circuits.
- [M. Gersbach and Charbon(2009)] E. Labonne J. Richardson R. Walker L. Grant R Henderson F. Borghetti D. Stoppa M. Gersbach, Y. Maruyama and E. Charbon. A parallel 32x32 time-to-digital converter array fabricated in a 130 nm imaging cmos technology. 2009.

- [Niclass(2008)] Cristiano L. Niclass. *Single-Photon Image Sensors in CMOS: Picosecond Resolution for Three-Dimensional Imaging*. PhD thesis, cole Polytechnique Fdrale de Lausanne, 2008.
- [N.V.Yastrebova(2007)] N.V.Yastrebova. High-efficiency multi-junction solar cells: current status and future potential. *Solar Energy*, 2007.
- [Paschotta(2008)] Dr. Rdiger Paschotta. Photonics: Laser and optical physics, 2008. URL <http://www.rp-photonics.com/lasers.html>.
- [Rees(2001)] W. G. Rees. *Physical Principles of Remote Sensing*. Cambridge University Press, Cambridge, second edition, sixth printing edition, 2001. ISBN 9780521669481.
- [SPECTROLAB()] INC SPECTROLAB. 28.3% ultra triple junction (utj) solar cells datasheet.
- [Wertz(2006)] Wiley J. Larson & James R. Wertz, editor. *Space Mission Analysis And Design*. Microcosm Press and Springer, El Segundo, CA (Microcosm Press) & New York, NY (Springer), 3 edition, 2006.
- [Xu(2000)] Zhizhan Xu. *Frontiers of laser physics and quantum optics*. Springer, 2000.
- [Zandbergen(2009)] B.T.C. Zandbergen. Delta-v (velocity increment) budget. online, November 2009. <http://www.lr.tudelft.nl/live/pagina.jsp?id=140fb8a8-0bfa-43dc-8ff9-02c923a2a8cb&lang=en>.

Appendix A

Design Option Diagrams

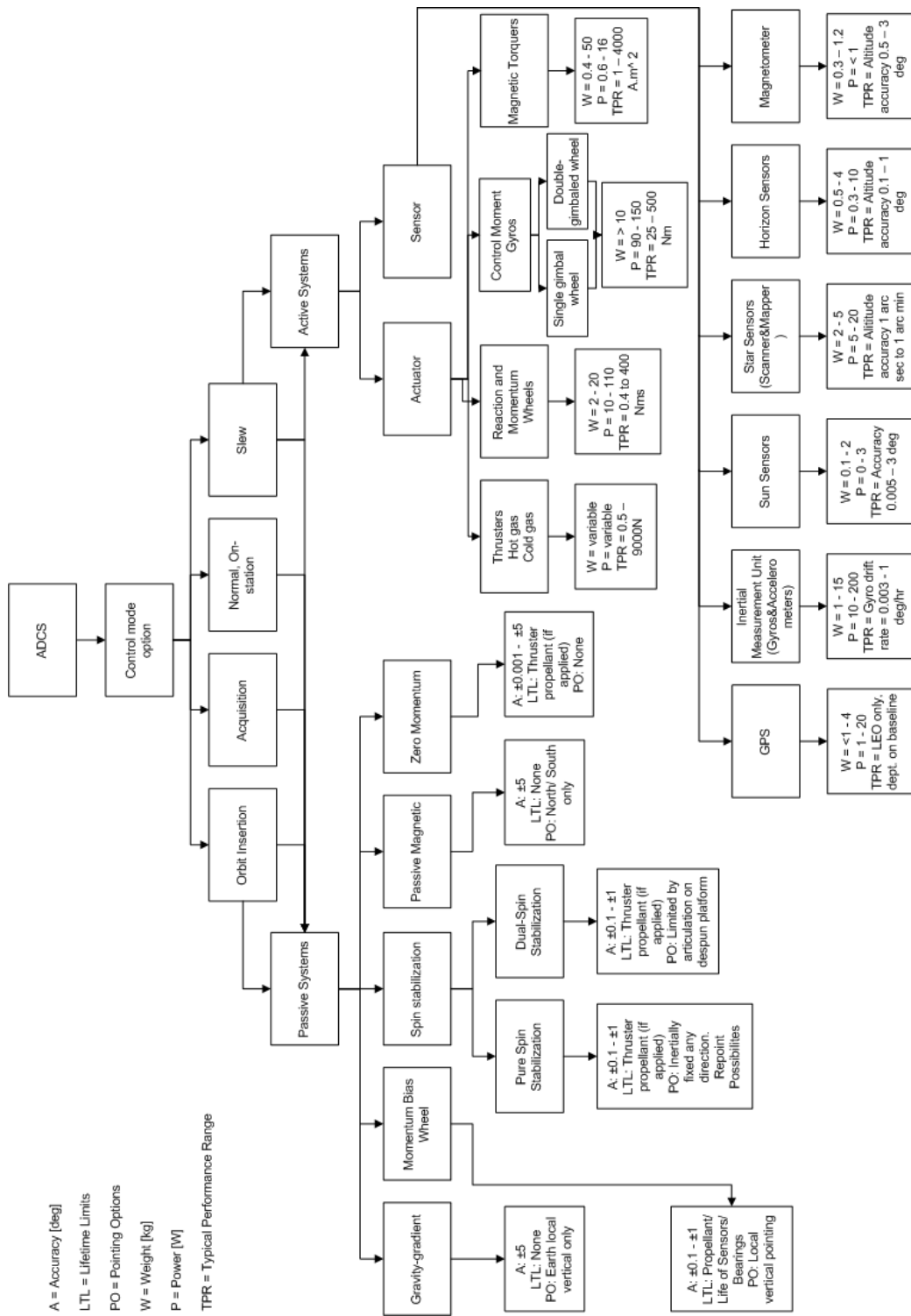


Figure A.1: Design option tree for the ADCS

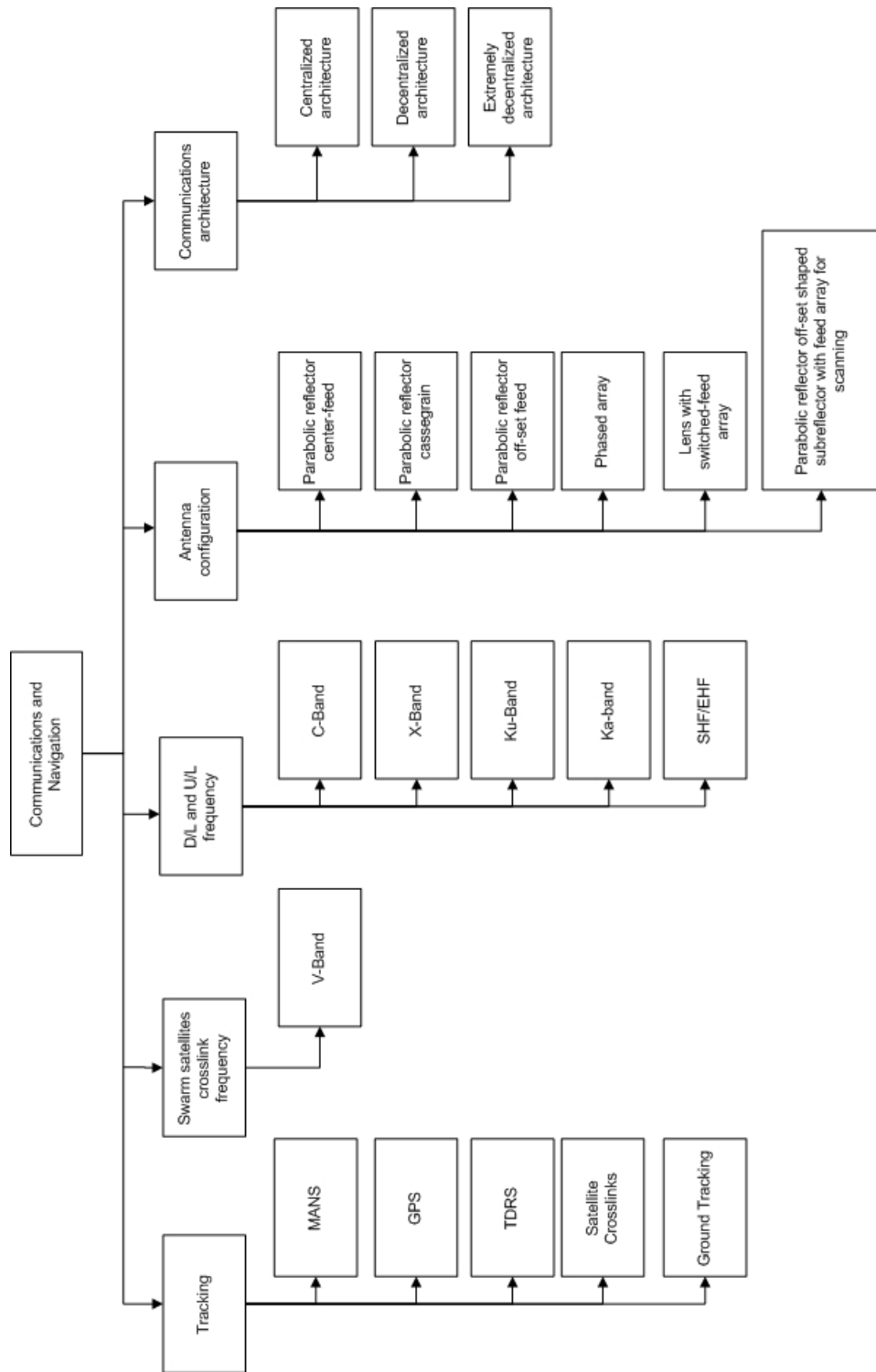


Figure A.2: Design option tree for the communication systems

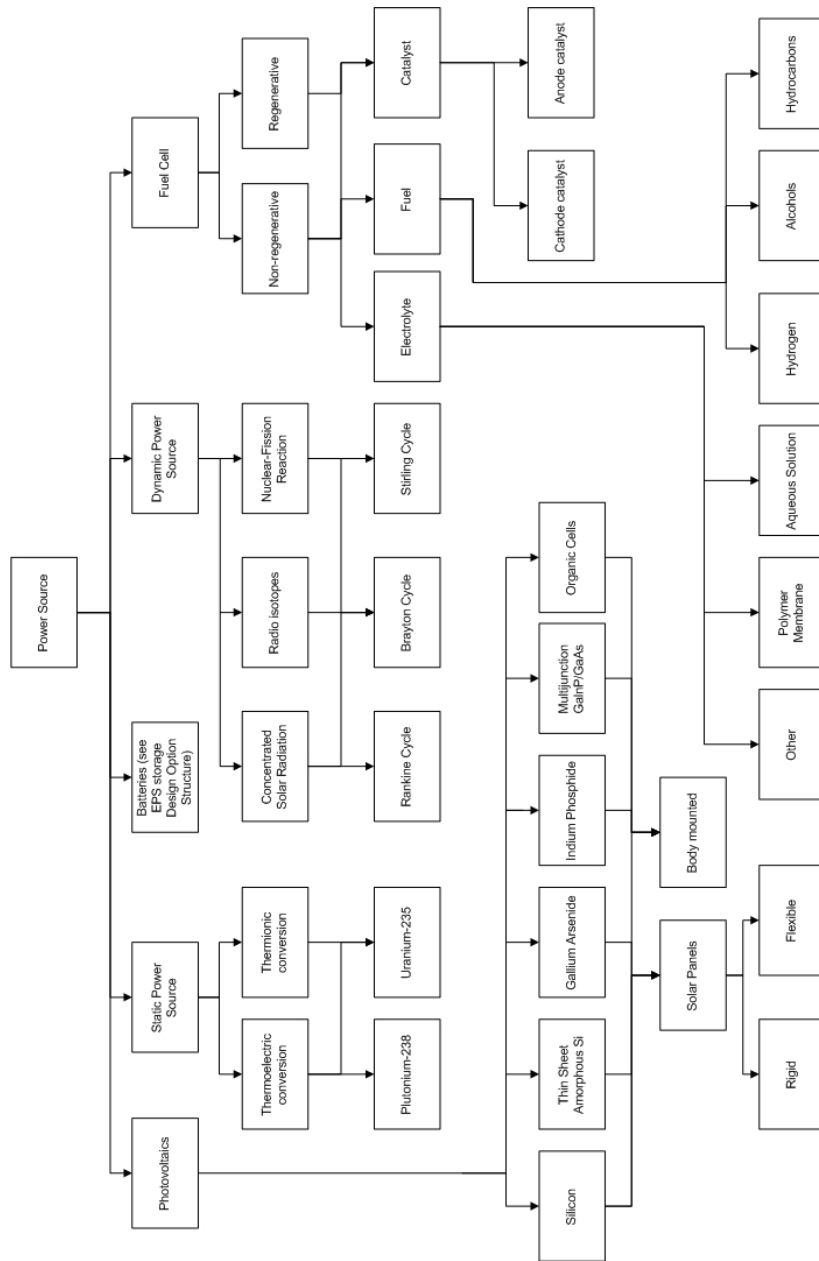


Figure A.3: Design option tree for the power source

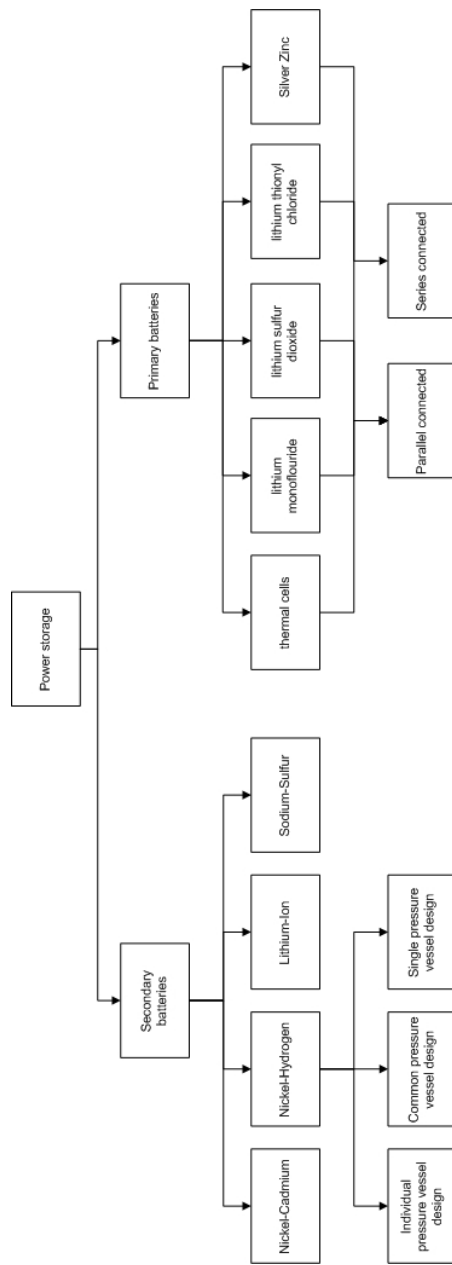


Figure A.4: Design option tree for the power storage

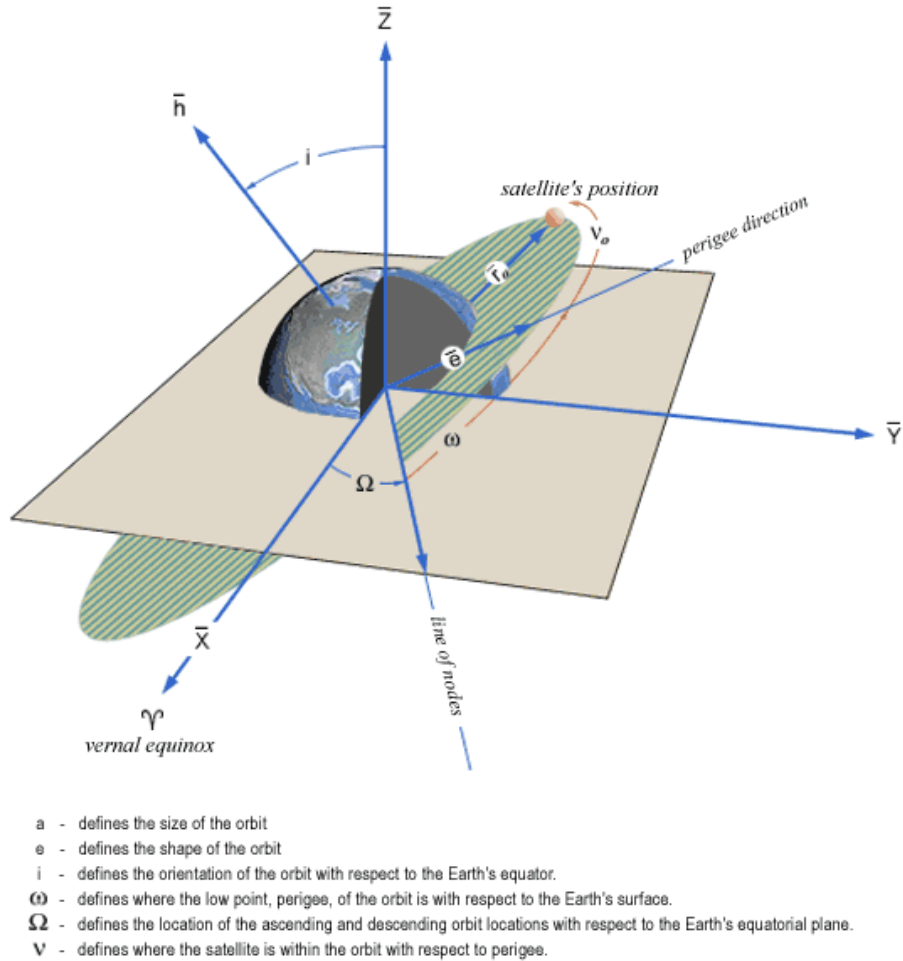


Figure A.5: Definitions of the inclination i , the right ascension of the ascending node Ω , the argument of perigee ω and the true anomaly ν . source: <http://reentrynews.aero.org>

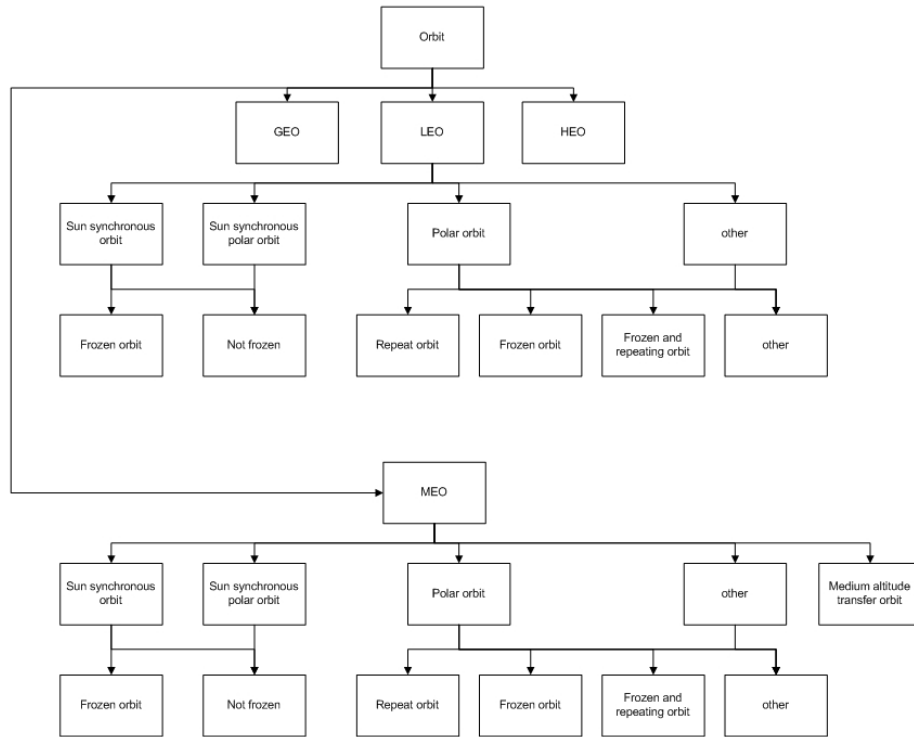


Figure A.6: Design option tree for the orbit architecture of LEO and MEO

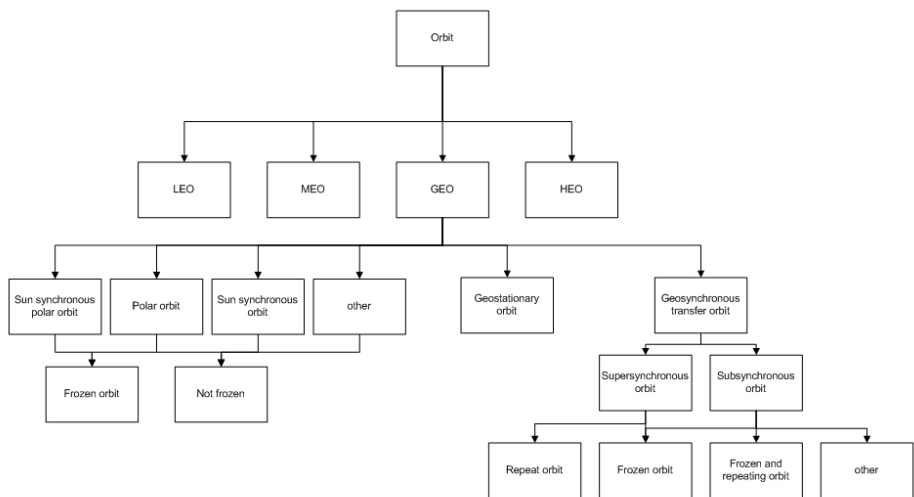


Figure A.7: Design option tree for the orbit architecture of GEO

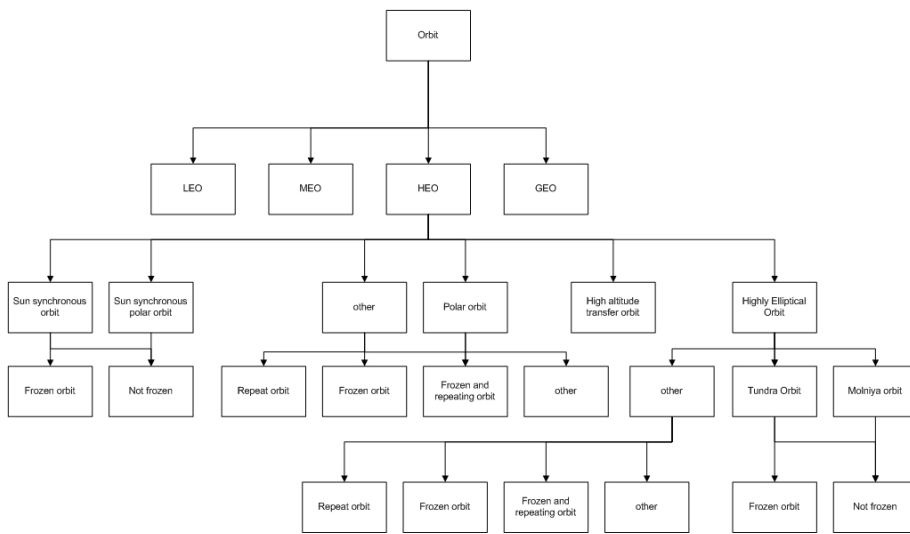


Figure A.8: Design option tree for the orbit architecture of HEO

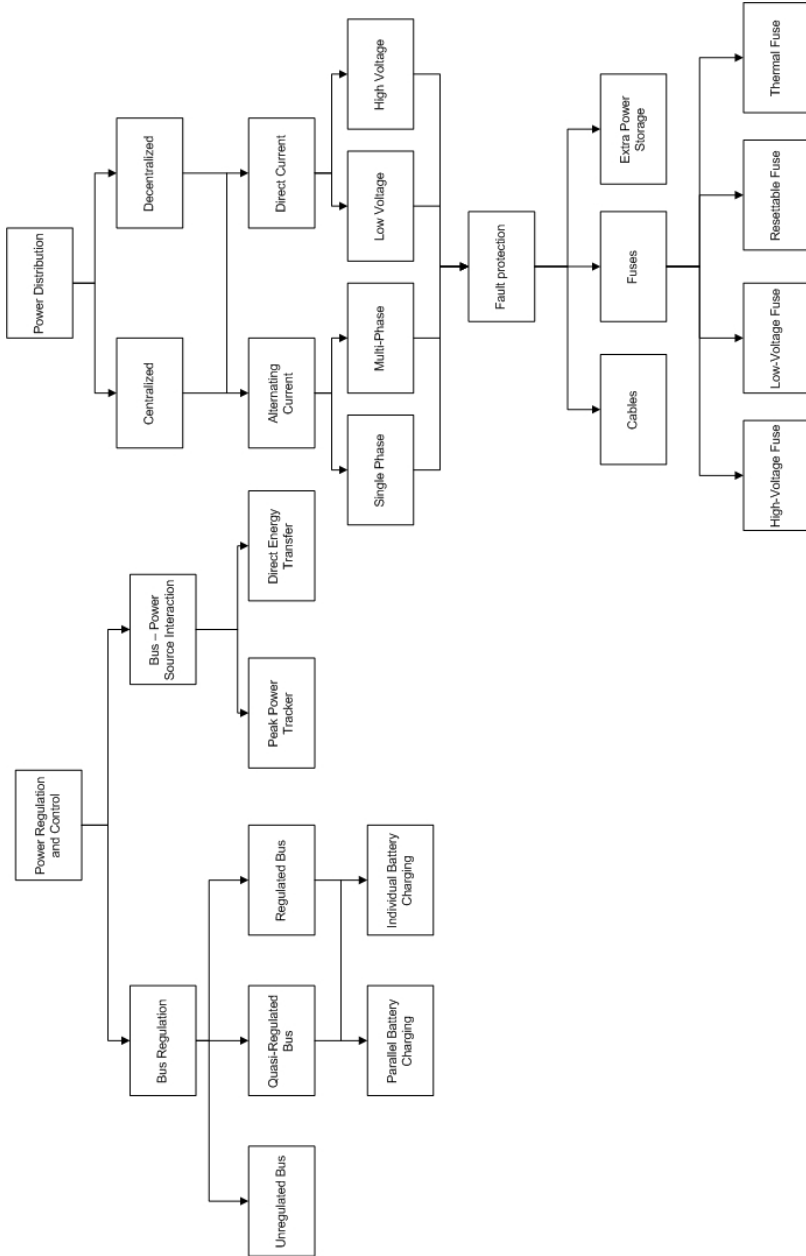
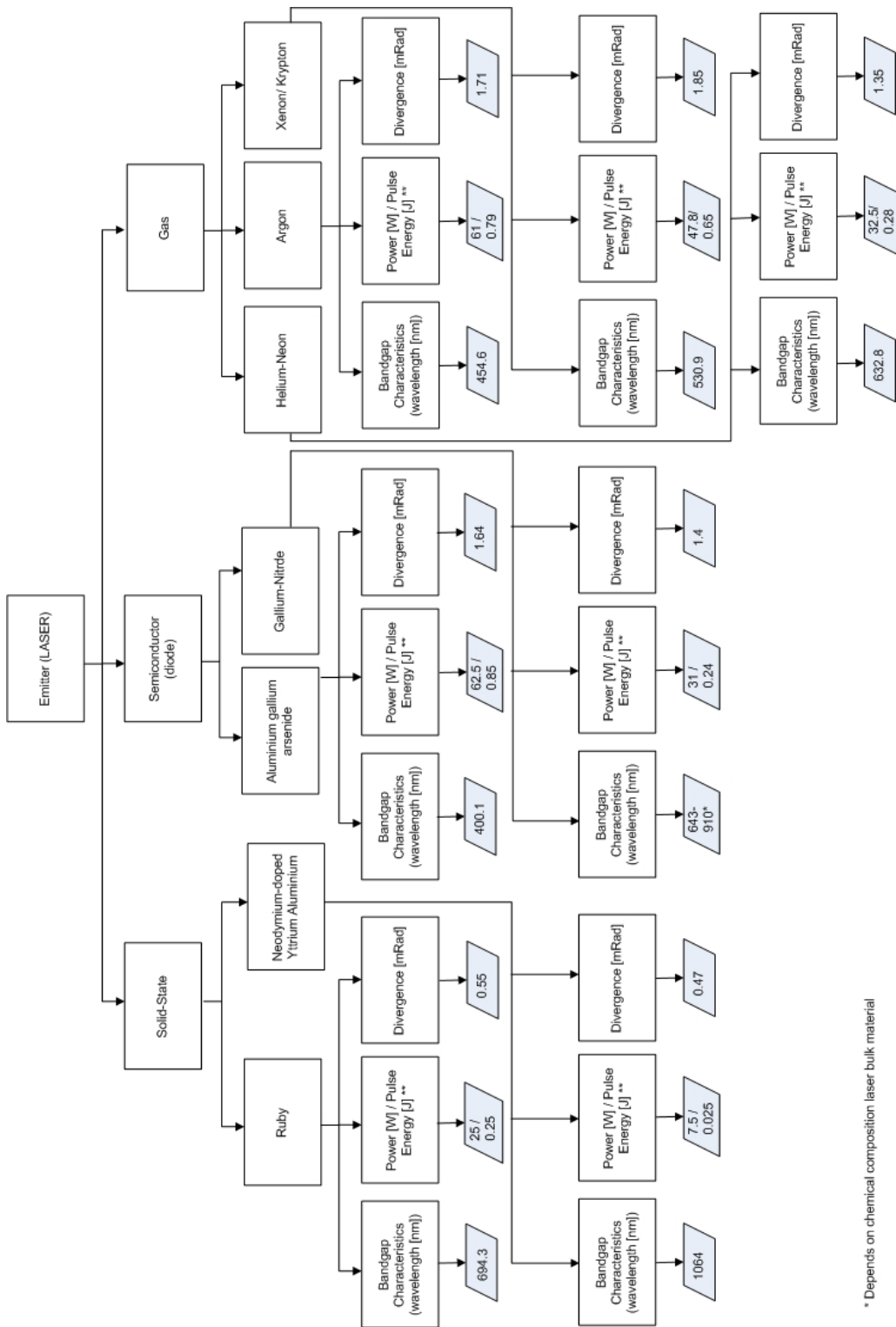


Figure A.9: Design option tree for the distribution and regulation and control of the EPS



* Depends on chemical composition laser bulk material

** Typical values; could be altered by varying repetition rate, external electron excitation or input power variation

Figure A.10: Design option tree of laser emitter. Numbers indicate typical values.

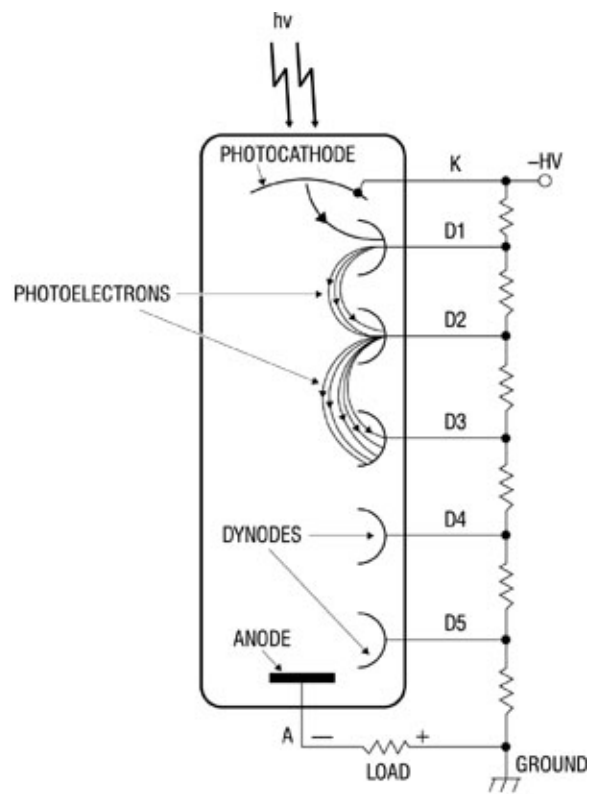


Figure A.11: Photomultiplier tube configuration and working mechanism

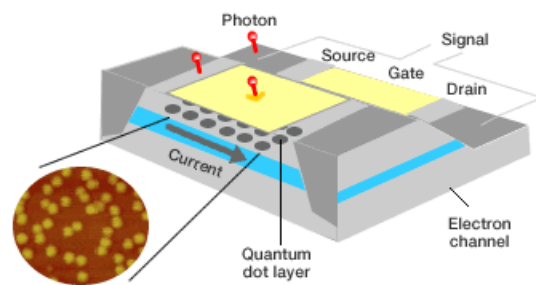


Figure A.12: Single photon detection using quantum dot configuration

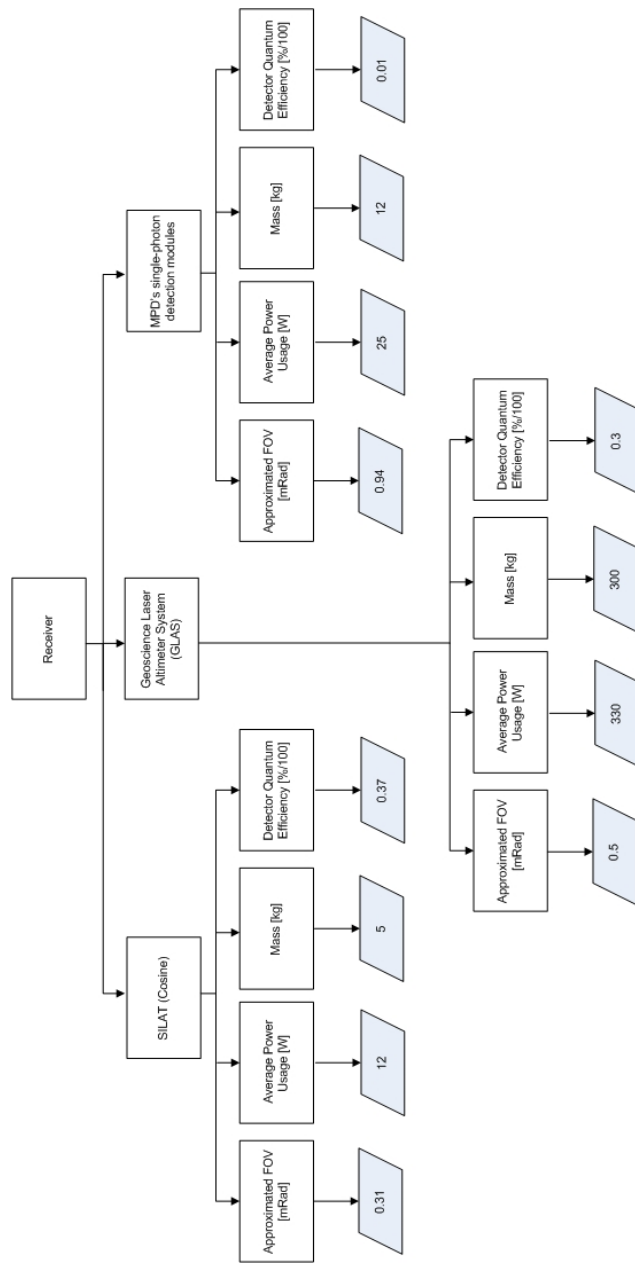


Figure A.13: Design option tree for laser receiver. Numbers represent typical values.

Appendix B

Gantt Chart